Molecular Genetic Analysis for Malignant Hyperthermia

A thesis presented to Massey University in partial fulfilment of the requirements for the degree of Master of Science in Biochemistry

Keisaku Sato

2004

ACKNOWLEDGEMENTS

I especially would like to thank my supervisor, Dr. Kathryn Stowell for her help, advise and patience during my project.

Ms. Robyn Marston helped me for some sample preparations and I obtained many ideas and protocols for experimental designs from Dr. Rosemary Brown, although I have never seen her yet...

I would also like to thank all members at the Twilight Zone. I have never had any difficulties or problems in the relationship with them. When I was having trouble and hard time, they were very kind and welcomed me warmly. I love the warm-hearted atmosphere in this laboratory.

Finally, I have to thank my mother who always understands and accepts me.

ABSTRACT

Malignant hyperthermia (MH) is a rare pharmacogenetic disorder in humans caused by inhalational general anaesthetics and depolarising muscle relaxants. An MH reaction shows abnormal calcium homeostasis in skeletal muscle leading to a hypermetabolic state and increased muscle contracture. A mutation within the calcium release channel ryanodine receptor of skeletal muscle (*RYR1*) is one of the causes of MH leading to the abnormally high release of calcium ions into the cytosol during MH reactions.

The MH reaction can also be triggered by excess exercise, heat and stress. A New Zealand male, identified as M818, showed a fulminant MH reaction which resulted in death. The reaction was caused by exercise, and he did not have a family history of MH. As this individual did not have any of the mutations within *RYR1* found to date in New Zealand families, the entire *RYR1* cDNA was screened for a novel mutation that may result in susceptibility to exercise-induced MH. This patient may have had a novel *RYR1* mutation because exercise-induced MH is quite rare. Screening of this gene, however did not identify any mutations within *RYR1*, suggesting that the M818 patient may have a mutation in another gene because MH is a heterogeneous disorder with 40-50% of families showing linkage to alternative loci.

Heterogeneity of MH can result in discordance between genotype and phenotype. Some MH susceptible patients do not have a *RYR1* mutation that is found in other individuals with the same kindred. One or more other genes could be associated with MH for these individuals although alternative loci have not been studied in New Zealand families. A genome-wide scan was performed to search for other candidate loci using a large MH kindred known as the CH family within which discordance has been observed. Non-parametric linkage analysis across all chromosomes identified five weak linkages from one branch, and two strong linkages from another branch of the CH family. Secondary linkage analysis was performed on one candidate locus identified in the genome-wide scan, and a weak linkage and recombination was observed within the shorter region. No candidate genes with obvious relevance to calcium homeostasis or signalling were identified within this region. The existence of alternative causative loci in this family cannot be ruled out however, because the loci identified from the genome-wide scan are very large and contain many genes of unknown function.

ABBREVIATIONS

A	absorbance
ATP	adenosine triphosphate
bp	base pair
CCD	central core disease
cDNA	complementary DNA
cM	centimorgan
4-CmC	4-chloro-m-cresol
C-terminal	carboxy terminal
DEPC	diethylpyrocarbonate
DHPR	dihydropyridine receptor
DNase	deoxyribonuclease
DMSO	dimethyl sulphoxide
dNTPs	dinucleotide triphosphates
EC	excitation-contraction
EDTA	ethylene diamine tetra-acetate
HEPES	N-[2-hydroxyethyl]piperazine-N'-[4-butanesulphonic acid]
IVCT	*in vitro* contracture test
kb	kilobase
MH	malignant hyperthermia
MHE	malignant hyperthermia equivocal (European protocol)
MHN	malignant hyperthermia negative (European protocol)
MHS	malignant hyperthermia susceptible (European protocol)
MH+	malignant hyperthermia positive (North American protocol)
MH-	malignant hyperthermia negative (North American protocol)
mRNA	messenger RNA

MOPS	3-[N-morpholino]propanesulphonic acid
NPL	non-parametric linkage
N-terminal	amino terminal
oligo(dT)	oligodeoxythymidine
pCO_2	carbon dioxide pressure
PCR	polymerase chain reaction
PCr	phosphocreatine
Pi	inorganic phosphorus
^{31}P NMR	phosphorus-31 nuclear magnetic resonance
RFLP	restriction fragment length polymorphism
RNase	ribonuclease
RT	reverse transcriptase
RT-PCR	reverse transcriptase-polymerase chain reaction
RYR	ryanodine receptor
SIDS	sudden infant death syndrome
SR	sarcoplasmic reticulum
SSCP	single stranded conformational polymorphism
TAE	Tris-acetate-EDTA buffer
Taq	*Thermus aquaticus*
TBE	Tris-borate-EDTA buffer
TE	Tris-EDTA buffer
Tm	melting temperature
Tris	tris (hydroxymethyl) aminomethane
T-tubule	transverse tubule
UV	ultraviolet light
VNTR	variable number of tandem repeat polymorphism

LIST OF FIGURES

LIST OF TABLES

TABLE OF CONTENTS

CHAPTER THREE : SCREENING OF MUTATIONS

CHAPTER FOUR : A GENOME-WIDE SCAN

CHAPTER ONE : INTRODUCTION

1.1 Overview of Malignant Hyperthermia

1.1.1 Introduction

Malignant Hyperthermia (MH) is an autosomal dominant inherited disorder of the skeletal muscle in humans as well as in different animals and is triggered by volatile anaesthetics and depolarising muscle relaxants used in general anaesthesia. MH leads to a hypermetabolic state and an abnormally high release of calcium ions from the sarcoplasmic reticulum of skeletal muscle (1). Palmerston North Hospital is the sole MH testing centre in New Zealand and also maintains a database of MH reactions and affected families. The incidence of MH is much higher in the lower North Island than other areas worldwide because there are some large families known to have the disorder. One patient will be diagnosed and treated as MH susceptible for every 100 patients in general surgery at Palmerston North Hospital (2). To date, about 40 families have been confirmed as MH susceptible in New Zealand from clinical reactions or *in vitro* contracture testing.

1.1.2 History

Inexplicable deaths and abnormal reactions during operations or in a postoperative stage were reported in the early 1900s. In 1960, it was reported that anaesthetics could cause hyperthermia and even death in several families (3). The disorder was found to be hereditary and the result of a dominant trait (4). Several years later, it was observed that individuals who had recovered from MH showed higher muscle contracture against halothane and caffeine in an *in vitro* test (5, 6). From these observations, the European MH Group developed a protocol of diagnostic testing using muscle specimens (7). The North American MH Group also developed a test protocol differing only in minor aspects (8). These protocols are still used today as the "gold standard" diagnostic tests for MH. The incidence of MH on a worldwide scale has been estimated to be 1:15,000 anaesthetics for children and 1:50,000 for adults (9). In the 1970s, two-thirds of affected patients died during or as a result of anaesthesia, usually from cardiac arrest. Dantrolene

sodium was introduced as an antidote for MH in 1979 (10) and as a result, mortality has dropped to less than 5 % today (11).

1.1.3 Clinical symptoms

Establishing the diagnosis of MH by clinical signs is difficult because none of the clinical symptoms can be regarded as specific signs of MH (12). MH reactions have variable intensity and time course. General signs observed from MH reactions include tachycardia, respiratory or metabolic acidosis, masseter spasm, generalised muscular rigidity, arrhythmias, rhabdomyolysis, skin mottling, and rapid temperature elevation (13, 14). Attempts have been made to predict MH susceptibility by observing these clinical indicators (15), however MH reactions can develop slowly, even in a postoperative onset without any clinical signs during the operation (16). Furthermore, some case reports have shown that MH susceptible individuals do not always show abnormal reactions against triggering drugs (17). These atypical forms of MH reactions may delay anaesthetists in establishing diagnoses and treatments of MH. Nevertheless, a clinical grading scale has been established to evaluate MH-like symptoms and is used to assess the relatively likelihood of clinical symptoms actually being MH (15).

1.1.4 Triggering agents

MH reactions can be triggered by anaesthetics widely used in general anaesthesia. These include non-halogenated anaesthetics such as ether and halogenated ones such as halothane, sevoflurane and desflurane (18). Halothane seems to be the most potent trigger. Depolarising muscle relaxants such as succinylcholine also induce MH although it has been reported that pure succinylcholine itself does not induce muscle contraction (19). Commercial succinylcholine solutions contain cresol derivatives such as 4-chloro-m-cresol (4-CmC) as a preservative, and it is thought that 4-CmC itself can be a trigger of MH reactions (20, 21). Chlorocresol derivatives are routinely added to commercial drugs as preservatives, and these drugs should not be used for MH susceptible patients. Some case reports have shown that psychotropic substances or tranquillisers like phenothiazines and tricyclic antidepressants may be triggers of MH although this is still controversial because of a low number of case reports (22, 23). These drugs should not be given to MH patients because they may induce symptoms

similar to MH and may hamper the establishment of a clinical diagnosis of MH.

Non-anaesthetic factors can also induce MH reactions. Exercise before the administration of a triggering agent increases the incidence and intensity of MH (24), and overheating alone can trigger MH reactions in swine (25). In fact, some case studies have reported MH reactions related to heat stroke in humans (26, 27). Some MH susceptible individuals show an abnormal response to graded exercise (28), and it has been confirmed that strenuous exercise can trigger MH in some individuals (29). Mental excitement may increase the intensity of reactions against drugs (30) and variance of intensity has been observed in an anxious patient (31). Hence, it has been suggested that MH may be a human stress syndrome (32). Overheating caused by viral infection has also been reported to induce MH (33).

1.1.5 Management and treatment

Any triggering anaesthetics should be avoided for MH susceptible individuals during anaesthesia. There are some suitable drugs for patients (34), and the non-triggering anaesthetic, propofol, is often used today for MH susceptible individuals. It is a non-water-soluble intravenous agent that does not trigger MH reactions (35). If MH reactions occur, it is critical to establish the diagnosis and terminate the administration of triggering drugs immediately. Dantrolene sodium is very effective in an MH reaction by preventing a hypermetabolic state. Immersion in an ice-cold bath is also effective for fulminant hyperthermia. Patients who suffer an MH reaction should be treated in an intensive care unit with body temperature and pulse being monitored. Patients who recover from MH, however may suffer sequeli such as muscle disability from rhabdomyolysis or impaired function of major organs (5).

1.2 Pathophysiology of MH

1.2.1 Introduction

Although the exact mechanism of variable MH reactions is not understood, malfunction of intracellular Ca^{2+} homeostasis has been shown to play an important role (36). MH susceptible individuals show higher concentrations of cytosolic Ca^{2+} during MH

reactions and also in normal conditions without exposure to triggering drugs (37). In addition, an abnormal sarcoplasmic reticulum (SR) ryanodine receptor in the skeletal muscle has been reported to be responsible for the abnormal calcium release in ~50% of affected families (38).

1.2.2 Excitation-contraction coupling

Intracellular Ca^{2+} regulates a wide range of events in all cells, such as cell growth, mitochondrial function, gene expression and muscle contraction. Ca^{2+} plays a fundamental role in excitation-contraction (EC) coupling of skeletal muscles (39). The wave of depolarisation from nerves is detected by an L-type voltage-dependent Ca^{2+} channel called the dihydropyridine receptor (DHPR) located in the wall of the transverse tubule (T-tubule). DHPR transmits the signal to the functionally coupled calcium release channel, ryanodine receptor (RYR), and activates it to release Ca^{2+} from the SR to intracellular cytosol (Figure 1-1). The released Ca^{2+} binds to troponin and activates actin, and muscle contraction occurs. The intracellular free Ca^{2+} is rapidly transferred back to the SR by ATP-ase calcium pumps and stored within the lumen, and muscle relaxation occurs (40).

1.2.3 Dihydropyridine receptor

The DHPR is located in the T-tubule membrane and detects membrane depolarisation. It is an L-type calcium channel passing Ca^{2+} through to the cytoplasm. It is also a voltage sensor, and if it detects a signal from nerves, it transmits the signal to the RYR leading it to open and releasing Ca^{2+} from the SR. The DHPR is an asymmetric protein which consists of five subunits (41) (Figure 1-1). The α1-subunit (185 kDa) consists of four domains I to IV and is located in the T-tubule membrane (42). This subunit contains positive charges and senses plasma membrane depolarisation. It complexes with a cytoplasmic subunit (β, 54 kDa) and two intra membrane subunits (γ, 30 kDa and δ, 26 kDa). An extracellular subunit (α2, 143 kDa) is linked via a disulfide bridge to the δ-subunit. The DHPR is clustered with the T-tubule and RYR forming the triad, and the signal is transmitted through the loop between the II and III domains to the RYR (Figure 1-1), controlling release of Ca^{2+} and following EC coupling via the RYR (43). The activated RYR also transmits a current-enhancing signal to the DHPR through the II-III

loop (44).

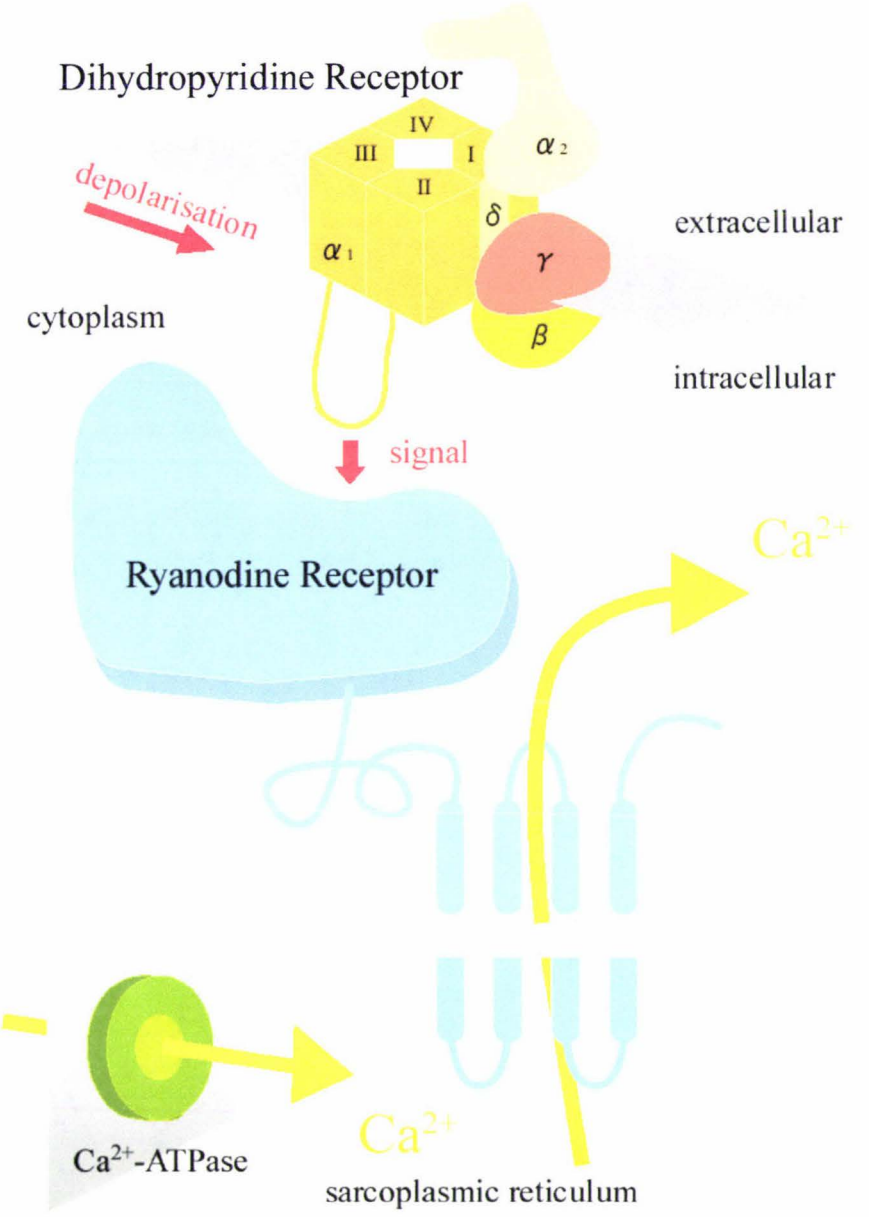

Figure 1-1 The excitation-contraction pathway of skeletal muscle

A depolarising signal is received by the DHPR and transmitted to the RYR through the II-III loop causing a release of calcium ions from the SR. One DHPR and one of four monomers of RYR are shown. Other associated proteins are omitted. The released calcium ions are pumped back to the SR lumen by a calcium transport ATPase. Diagram adapted from references (45) and (46).

1.2.4 Ryanodine receptor

The RYR is a large Ca^{2+} channel situated in the SR membrane (47) and is built up of four monomers, each with a molecular weight of about 560 kDa (48, 49). About 80 % of the protein is exposed in the cytoplasm forming the foot structure (50), and the remaining carboxyl terminal (C-terminal) region is embedded in the SR membrane (Figure 1-1). The RYR receives the signal from the activated DHPR, and opens the channel releasing Ca^{2+} from the SR lumen to cytoplasm. Three separate genes identified as *RYR1*, *RYR2* and *RYR3* have been found to encode the RYR (51), and each is predominantly expressed in skeletal muscle, cardiac muscle or brain and smooth muscle, respectively (52-54).

1.2.5 The proposed mechanism of MH reactions

As Ca^{2+} controls several important systems in cells, Ca^{2+} concentrations within the cytoplasm are under tight control. The activated RYR has a very short open time and is regulated by ATP, Mg^{2+} and Ca^{2+}. In addition, released Ca^{2+} within the cytoplasm is pumped back to the SR readily by a Ca^{2+}-ATPase (Figure 1-2, left). Hence, the metabolic state and muscle contracture do not last long. In contrast, an MH crisis shows dysfunctional control of Ca^{2+} release. In muscle specimens from MH susceptible swine, the RYR shows a prolonged duration of the open state and has a defect in a low-affinity Ca^{2+} binding site (55). In addition, Ca^{2+} release in MH susceptible muscles is reduced far later than in normal specimens (56). Hence, it is thought that the RYR does not close readily during MH reactions allowing large amounts of Ca^{2+} to pass through to the cytoplasm. The released Ca^{2+} induces muscle contraction and mitochondrial metabolism (Figure 1-2, right). Excessive muscle contraction causes membrane damage leading to rhabdomyolysis, and the overall higher metabolic activity causes increased CO_2 and heat production as well as increased O_2 consumption leading to acidosis, tachycardia and hyperthermia. These events may cause death because of cardiac arrhythmia or cardiac arrest.

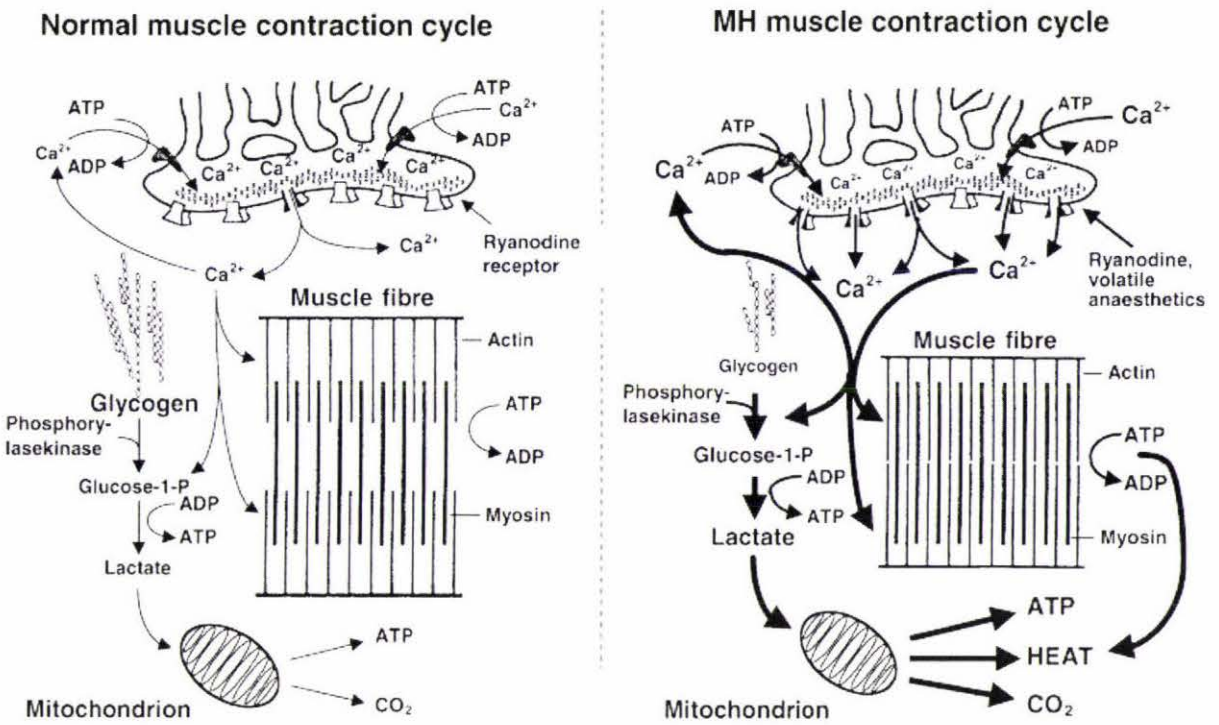

Figure 1-2 Proposed mechanism for induction of malignant hyperthermia

The activated RYR releases calcium ions from the SR to cytosol. Released intracellular Ca^{2+} within the muscle cell induces muscle contraction. The RYR closes immediately and Ca^{2+}-ATPase pumps rapidly transfer unbound Ca^{2+} back into the SR, and normalised Ca^{2+} concentration results in muscle relaxation (left). In MHS muscle cells, the RYR does not close readily causing an abnormally high release of Ca^{2+} into the cytoplasm. Hence, excess calcium ions induce a hypermetabolic state and excess muscle contraction (right). From reference (1).

1.3 Diagnosis of MH

1.3.1 The in vitro contracture test

As prediction of MH from clinical signs is difficult, attempts have been made to establish preoperative tests to diagnose MH susceptibility, but unfortunately, they have lacked reliability (57). To date, the gold standard and widely used method is the *in vitro* contracture test (IVCT), which is a method to determine the response of a patient's

muscle to the triggering agents halothane and caffeine *in vitro* (5, 6). The IVCT requires the surgical excision of a piece of quadriceps muscle to provide several muscle specimens for investigation. The fresh specimens are suspended in a bath, and the test drugs, halothane or caffeine, are added. Tension of the muscle is measured by a transducer before and after addition of the drugs.

The European MH Group developed a protocol for the IVCT in 1984. This protocol defines a positive response as 0.2 g or greater against 2 % v/v halothane or 2.0 mM caffeine. If both tests using halothane and caffeine show positive responses, the individual is diagnosed as MH susceptible (MHS). If both tests do not show positive responses at all, then the diagnosis is MH normal (MHN). If only the halothane test or only the caffeine test is positive, then the diagnosis is MH equivocal (MHE) although the person is regarded as clinically susceptible to MH. The North American MH Group has also developed an IVCT protocol in 1989 that differs slightly from the European protocol (8). It defines 0.5 and 0.3 g as a positive response to 3 % v/v halothane and 2.0 mM caffeine test, respectively. The North American protocol does not establish an MHE diagnosis. If one or both drug tests exhibit a positive response, then the diagnosis is MH positive (MH+), otherwise the patient is considered negative for MH (MH-). Therefore, it has been said that the North American protocol could result in more false positive or negative diagnoses than the European protocol (58).

1.3.2 Limitation of the IVCT

Unfortunately, the IVCT is not an absolute method for diagnosis of MH. It has been reported that the European protocol has 99 % sensitivity and 93.6 % specificity, and the North American protocol has 97 % sensitivity and 78 % specificity (59). This means that even the most reliable method, the European protocol, can produce 1 % false negative diagnoses and about 4 % false positive diagnoses. In fact, some cases of false negative diagnoses have already been reported (60). In addition, the IVCT is invasive and expensive, requiring minor surgery and temporary disability as well as a degree of uncertainty in diagnosis due to the equivocal nature of the test itself as well as the possibility of obtaining insufficient tissue. Hence, refinements in testing protocols or other methods for testing are required (61).

1.3.3 Other diagnostic methods

To improve reliability and discrimination between the MHS and MHN groups, the protocol for the IVCT has been modified with the introduction of drugs to replace or supplement halothane and caffeine. These include ryanodine, 4-chloro-m-cresol (4-CmC) and the phosphodiesterase-III inhibitor enoximone (62-64). 4-CmC may be a more reliable drug than halothane or caffeine. Multicentre evaluation has estimated its sensitivity and specificity as 96.1 % and 99 %, respectively (65). Other non-invasive diagnostic tests to replace the IVCT have also been developed.

Galloway *et al.* (1984) introduced phosphorus-31 nuclear magnetic resonance (^{31}P NMR) to determine relative concentrations of ATP, phosphocreatine (PCr) and inorganic phosphorus (Pi) in skeletal muscle (66). MHS muscle shows an abnormal metabolic state against triggering drugs, and hence, shows significantly higher Pi/PCr values than does MHN muscle (67). This method is not currently used for diagnostic testing, however because the value is changeable, and it is not sufficiently reliable to establish diagnoses (68). As abnormal Ca^{2+} release is an important phenomenon during MH reactions, Ca^{2+} release from the SR in skeletal muscle stimulated by drugs *in vitro* has been investigated. Censier *et al.* (1998) found that cultured skeletal muscle cells from MHS individuals showed abnormal intracellular calcium homeostasis in the presence of halothane (69). Later, coincidence of diagnoses from this method and from the IVCT was reported (70). This method does not replace the IVCT however, because it does not have higher sensitivity or specificity than can be obtained with the IVCT. It also requires skeletal muscle for cell culture, and is thus invasive and time consuming although the procedure could be developed from skeletal muscle obtained from needle biopsy and hence would be less invasive for patients than surgical excision for the IVCT (71). Klingler *et al.* (2002) have also introduced a diagnostic method using cultured skeletal muscle cells (72). These authors have determined H^+ release instead of Ca^{2+} after the administration of 4-CmC, although this method requires an expensive microphysiometer to detect secretion from cultured cells.

Blood samples have also been used to predict MH susceptibility. Anetseder *et al.* (2002) have introduced the *in vivo* caffeine test. After intramuscular injection of caffeine, MHS individuals show higher local carbon dioxide pressure (pCO_2) because of the high

metabolic state caused by caffeine, but MHN individuals do not (73). Sei *et al.* (1999) have found that *RYR1* is not expressed only in skeletal muscle, but also in B lymphocytes (74). As the type 1 RYR plays a critical role for calcium signalling in B lymphocytes, it is thought that these cells would show abnormal calcium homeostasis against drugs in MHS patients. In fact, a few reports have shown higher drug-induced Ca^{2+} release from MHS B lymphocytes isolated from blood (75, 76). These techniques do not require muscle biopsy and have the possibility of replacing the IVCT, although further investigation is required to confirm reliability, sensitivity and specificity.

1.4 Other disorders associated with MH

1.4.1 Central core disease

MH may be associated with other disorders especially myopathy. So far, the only disease that is clearly associated with MH is central core disease (CCD). CCD is a morphologically distinct myopathy with quite variable clinical features. It is characterised by muscle weakness and muscle cramps after exercise, and autosomal dominant inheritance is observed in most subjects. The association of this rare disorder with MH has been found from observation that most CCD patients have an abnormal response in the IVCT or show MH reactions during anaesthesia indicating that the two disorders can co-exist (77). Therefore, according to these observations, all patients with CCD must be considered at risk from MH unless the IVCT indicates otherwise.

1.4.2 Other disorders

Other disorders may also be associated with MH although evidence of association has still not been shown conclusively. King and Denborough (1973) reported an unusual syndrome within MHS patients in Australia and New Zealand (78). The syndrome, called King Syndrome is characterised by short stature, slowly progressive myopathy and an unusual facial appearance. The cause of the disease is unknown and the association with MH is still unclear, but some case reports have indicated co-existence of MH and King syndrome (79). Other myopathies including Duchenne muscular dystrophy, Evans myopathy and myoadenylate deaminase deficiency may have some relationship to MH (80) although this is still controversial.

The association of MH with sudden infant death syndrome (SIDS) has been indicated in the early 1980s because of the high rate of SIDS incidence within MHS families (81, 82). The cause and mechanism of SIDS is still unknown, but some reports have shown that overheating may be one of the causative factors (83, 84). MH can be triggered by overheating itself (25), and hence, it could be the cause of SIDS for some MHS infants.

1.5 Animal models

1.5.1 Porcine model

The homologous disorder to human MH has been found in some animals. Porcine MH was reported in 1966 and has been widely investigated as a model of human MH (85). It shows an autosomal recessive trait whereas human MH is autosomal dominant (86). Porcine MH is sometimes triggered by stress, such as fighting, and high temperature (87). It is called porcine stress syndrome indicating that human MH may be a human stress syndrome. The skeletal SR from MHS pigs shows an abnormal release of Ca^{2+} caused by halothane and caffeine (88, 89). In addition, linkage analysis has revealed that chromosome 6q is linked to the disorder and the susceptible locus encodes the RYR of skeletal muscle, *RYR1* (90). A major breakthrough occurred when the first mutation, R615C, was found to be associated with porcine MHS, which co-segregates with porcine MH phenotypes (91, 92). As porcine MH is associated only with the *RYR1* R615C mutation, a molecular genetic test was developed to predict porcine MH susceptibility by detecting this mutation within *RYR1* (93).

1.5.2 MH in other animals

MH has also been found in the dog (94), and Roberts *et al.* (2001) found a V547A mutation within canine *RYR1* which is linked to MH in dogs (95), although the homologous mutation has not been found in humans. MH is also found in the cat (96, 97) and in the horse (98, 99), however molecular genetic studies have not yet been performed in these animals.

1.6 Molecular genetics of human MH

1.6.1 RYR1 mutations

As with porcine MH, linkage analysis has shown that *RYR1* is a candidate gene associated with human MH and is located on chromosome 19q (100, 101). Later, an R614C mutation, homologous to porcine R615C, was found in human *RYR1*. This mutation co-segregates with the IVCT phenotype in some MH susceptible families, and both homozygous and heterozygous mutations clearly match the phenotype (102). Hence, *RYR1* is linked to MH and the heterozygous mutation within the gene can lead to susceptibility showing an autosomal dominant trait for this disorder. To date, over 60 mutations associated with MH and/or CCD have been found within *RYR1* (Table 1-1). A single-amino-acid deletion has also been reported to be associated with MH (103). *RYR1* mutations found so far are clustered in specific regions called "hot spots" – N-terminal (exon 2-17), central (exon 39-46) and C-terminal (exon 95-102) (Figure 1-3). The N-terminal and central hot spots are located in the foot region of the RYR exposed to the cytoplasm, and the C-terminal one is located in the channel region embedded in the SR membrane.

1.6.2 Functional effects of RYR1 mutations

Cultured skeletal muscle cells from an MHS individual show an abnormal response against halothane, and a mutant skeletal muscle RYR containing *RYR1* mutations also leads to high sensitivity to drugs (69). HEK-293 cells expressing the mutant RYR also show abnormal responses against drugs, although all mutations have not yet been investigated for their functional effect on the RYR (104, 105). Mutant RYR appears to be leaky resulting in higher resting Ca^{2+} concentrations in cytoplasm (106). Hence, causative mutations within *RYR1* may alter the RYR function as a calcium release channel. The difference of effect on RYR function between different mutations is still unclear. Some mutations, however appear to show higher sensitivity to drugs than do others (107).

	Exon	Nucleotide	Amino acid	Disorder	Proportion	Reference
RYR1	6	C487T	R163C	MH, CCD	2%	Quane *et al.*, 1993 (108)
mutations	9	G742A	G248R	MH	2%	Gillard *et al.*, 1992 (109)
	11	G1021A	G341R	MH	6%	Quane *et al.*, 1994 (110)
	39	C6487T	R2163C	MH	4%	Manning *et al.*, 1998 (111)
	39	G6502A	V2168M	MH	7%	Manning *et al.*, 1998 (111)
	40	C6617T	T2206M	MH	3%	Manning *et al.*, 1998 (111)
	45	G7303A	G2434R	MH	4%	Keating *et al.*, 1994 (112)
	100	C14477T	T4826I	MH	1 family	Brown *et al.*, 2000 (113)
	102	T14693C	I4898T	MH, CCD	4%	Lynch *et al.*, 1999 (114)
CACNA1S	26	G3256T	R1086C	MH	1 family	Jurkat-Rott *et al.*, 2000 (115)
mutations	26	G3257A	R1086H	MH	1 family	Monnier *et al.*, 1997 (116)

Table 1-1 Selected *RYR1* and *CACNA1S* mutations

Over 60 mutations within *RYR1* have been reported to date, which are associated with MH and/or CCD. Only two mutations have been identified within *CACNA1S* from MHS individuals. These two mutations are linked only to MH, and no *CACNA1S* mutations are known to be associated with CCD.

1.6.3 Molecular genetic testing

As *RYR1* mutations clearly co-segregate with MH susceptibility in some families, molecular genetic testing may be useful to predict susceptibility instead of the IVCT for certain families (117). It is possible to establish an MHS diagnosis by detecting a causative mutation because MHN individuals do not contain *RYR1* mutations, and individuals with mutations are always MHS (118, 119). This does not necessarily mean, however that all MHS patients have *RYR1* mutations. It has been reported that between 30 and 80 % of MHS families show linkage to *RYR1* (120). In fact, discordance between genotype and IVCT phenotype has been observed in some families (121, 122). Hence, molecular genetic testing may be useful in some individuals in specific families,

but it cannot be suitable for all cases. It may be useful to use as a supplemental method for the IVCT in some specific families (123).

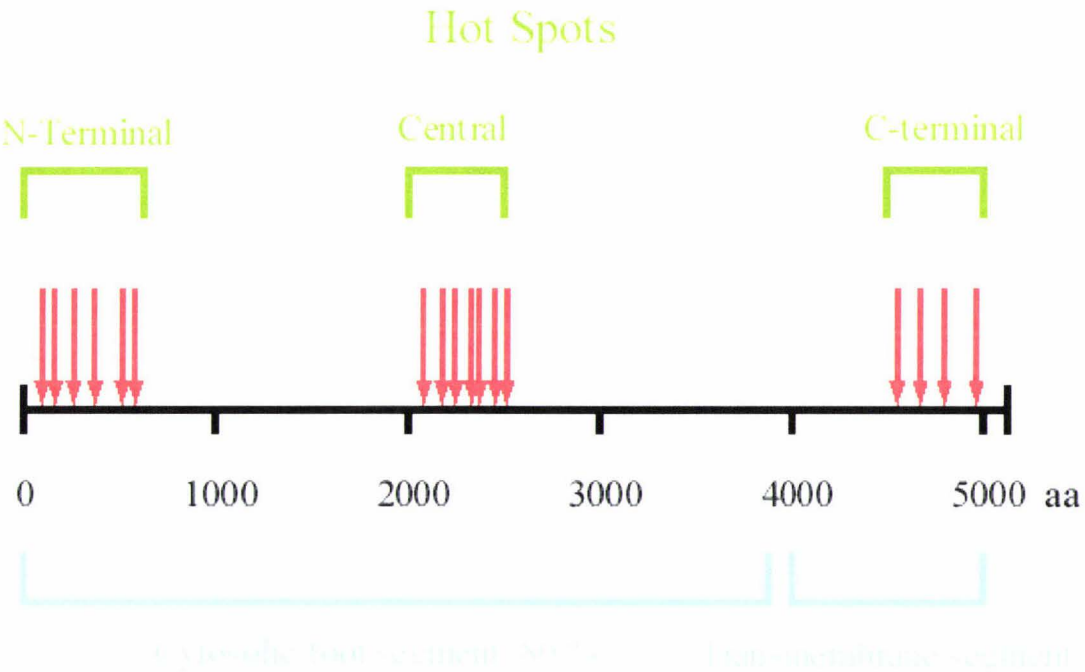

Figure 1-3 A linear representation of location of *RYR1* mutations

The RYR consists of 5,038 amino acids represented by a black line. Red arrows indicate the location of *RYR1* mutations found. They are clustered in N-terminal, central or C-terminal hot spots. Most hot-spot regions form the foot segment exposed in cytosol, and the C-terminal region is embedded in the SR membrane forming the transmembrane segment.

1.6.4 Other susceptible loci to MH

30-80 % linkage to *RYR1* indicates genetic heterogeneity of MH (120). This means that there must be other candidate loci associated with MH. In fact, linkage studies have identified other candidate loci on several chromosomes. Robinson *et al.* (1997) have performed a genome-wide scan of a MHS family, which does not have linkage on

chromosome 19q, encoding *RYR1* (124). These authors found strong linkage between MHS and chromosome 1q encoding the α-subunit of the DHPR. The gene (*CACNA1S*) was subsequently screened, and an R1086H mutation was found to co-segregate with MH susceptibility in this family (116). Later, a second mutation (R1086C) was found within this gene indicating that the *CACNA1S* gene may be a second candidate locus (115), although the functional effect of *CACNA1S* mutations is still unclear. Other candidate loci have been demonstrated on chromosome 3q (125), 5p (124), 7q (126) and 17q (127), however these are controversial because no mutations have been found within these loci, and potential candidate genes have not been identified for some of them.

1.7 Research goals

There were two separate and unrelated goals for the research described in this thesis. Both however, were aimed at identifying genetic factors causing MH in New Zealand families.

1.7.1 Screening RYR1 of the patient with exercise-induced MH

Recently, a male New Zealander suffered a fulminant MH crisis and died. The reaction was induced by exercise, but he did not have any signs of MH before the crisis and he did not have a family history of MH. Furthermore, molecular genetic analysis showed that he lacked *RYR1* mutations previously identified in New Zealand families. It is well known that MH reactions can be triggered by exercise, and in fact, mutations have been found in patients who showed exercise-induced MH-like reactions (128). It has not been confirmed, however that specific *RYR1* mutations are responsible for exercise-induced MH. It was possible that this patient had a novel *RYR1* mutation that is responsible for MH susceptibility caused by excess exercise. To determine this possibility, mRNA of the patient was extracted from his skeletal muscle followed by production of cDNA from mRNA using reverse transcriptase (RT). DNA fragments were amplified by PCR covering the entire *RYR1* cDNA. The fragments were purified and directly sequenced to detect any mutations and polymorphisms.

1.7.2 Linkage analysis within the CH family

To date, over 40 MH families have been identified in New Zealand. One of the largest MH families identified as the CH family has more than 1,400 individuals in total. Linkage analysis has shown that *RYR1* is responsible for MH susceptibility in this family (129), and in fact, the T4826I mutation in MHS patients was found to co-segregate with the phenotype in this family (113). It has also been observed, however that there is some discordance between genotype and phenotype showing that some MHS patients, as diagnosed by the IVCT do not have the T4826I mutation. Although the IVCT can produce false diagnoses, the rate of discordance in this family is higher than the probability of IVCT false diagnosis. Hence, it is thought that MH susceptibility in this family is not caused only by *RYR1*, but also by one or other traits in the discordant patients because of heterogeneity of MH. To search for other candidate loci that are susceptible to MH, a genome-wide scan was performed for patients selected from the CH family. Twenty-six individuals were selected from the family, and non-parametric analysis was adopted for the linkage analysis.

CHAPTER TWO : MATERIALS AND METHODS

2.1 Materials

Trizol™ reagent was purchased from Molecular Research Center, Inc., Cincinnati, OH, USA.

DEPC, chloroform, sodium hydroxide, HEPES and formamide were from BDH Laboratory Supplies, Poole, England. Ammonium chloride, magnesium sulfate, potassium acetate and potassium hydrogencarbonate were from Riedel-de Haen Fine Chemicals, Seelze, Germany. EDTA, DMSO, boric acid, formaldehyde and guanidine hydrochloride were from Ajax Chemicals, Auburn, Australia. MOPS was from USB™, Cleveland, OH, USA. Sodium citrate was purchased from Scientific Supplies Ltd., Auckland, New Zealand. Agarose LE was from Roche Molecular Biochemicals, Mannheim, Germany. NuSieve® GTG® agarose was from BioWhittaker Molecular Applications, Rockland, ME, USA. Tris was from Invitrogen™, Auckland, New Zealand. Acetic acid was from Rhone-Poulenc Chemicals Ltd., Aronmouth, UK. Bromophenol blue, xylene cyanol and ficoll were purchased from Sigma® Chemical, St. Louise, MO, USA.

Wizard™ Genomic DNA Purification Kit was from Promega Corp., Madison, WI, USA.

Taq DNA polymerase and reagents for PCR were purchased from Roche Diagnostics, Auckland, New Zealand. ELONGASE® Enzyme Mix and 1 kb plus DNA ladder were from Invitrogen™, Auckland, New Zealand. AmpliTaq Gold® PCR Master Mix and ABI PRISM® Linkage Mapping Primers were from Applied Biosystems, Foster City, CA, USA. Primers for PCR and sequencing were supplied from Professor Tommie McCarthy, University of Cork or purchased from Sigma® Genosys, Castle Hill, Australia.

DNase I and SUPERSCRIPT™ First-Strand Synthesis System were from Invitrogen™, Auckland, New Zealand.

QIAquick® or MinElute™ PCR Purification Kit or Gel Extraction Kit were purchased

from QIAGEN, New Zealand distributor: Biolab Scientific Ltd., Auckland, New Zealand.

Endonuclease *Hha*I and reagents were purchased from New England Biolabs, Inc., Beverly, MA, USA.

LightCycler-FastStart DNA Master SYBR Green I and LightCycler-Control Kit DNA were from Roche Applied Science, Penzberg, Germany.

All other chemicals and reagents used were of analytical grade or better.

2.2 Nucleic acid extraction

Investigation of genome and genes requires extraction of nucleotides from human samples. Genomic DNA was extracted for microsatellite analysis to perform a genome-wide scan or mutation analysis. Total RNA was extracted to synthesise complementary DNA (cDNA). cDNA was synthesised by reverse transcriptase (RT) using mRNA. Synthesised cDNA was used as a template for PCR to screen a gene. Genomic DNA was isolated from blood or skeletal muscle and total RNA was extracted from muscle samples. Fresh blood was obtained from patients in the MH family with informed consent. Ethical approval was obtained from the Whanganui-Manawatu and Massey University human ethical committees. Approval code numbers are 51/00 and 00/132, respectively. Samples were immediately transferred to Massey University and stored in 6 mL Vacutainer™ tubes containing citrate at 4°C or -20°C to prevent coagulation of the blood and DNA degradation. Skeletal muscle samples were obtained from a patient who showed a fulminant MH reaction after exercise. Samples were immediately frozen and stored at -70°C.

2.2.1 Isolation of RNA and DNA using the TRIzol™ reagent

TRIzol™ reagent is a mono-phasic solution for the isolation of total RNA from fluids, tissues or cells of a wide range of species including humans. It consists of phenol and guanidine isothiocyanate and is an improved method of the previous one developed in 1987 (130). During sample homogenisation or lysis, TRIzol reagent maintains the integrity of RNA and prevents RNase degradation. Added chloroform separates the

solution into an aqueous phase and an organic phase. The aqueous phase retains RNA exclusively, but DNA and proteins transfer to the organic phase. RNA in the aqueous phase is recovered by precipitation with isopropyl alcohol. DNA is recovered by ethanol precipitation at the following step, and proteins can also be isolated at the final step if needed. This technique allows the use of small quantities of tissue (50 mg) and cells (5×10^6), and large quantities of tissue (>1 g) and cells ($>10^7$). Total RNA isolated by this reagent is free of protein and DNA contamination, and can be used for several types of experiments including northern blot analysis, molecular cloning and PCR. Expected yields of RNA depend on species and types of tissue samples. The yield from human skeletal muscle is 1-1.5 μg per 1 mg tissue (manufacturer's instruction). RNA is easily degraded by RNase. As RNase is quite stable, it is important to guard against contamination by RNase and subsequent RNA degradation. All equipment coming in contact with RNA including tips, tubes and glassware, were treated with DEPC-treated water. Sterile water was treated with 0.01% (v/v) diethylpyrocarbonate (DEPC), and plastic and glass items were soaked in DEPC-treated water overnight, and then autoclaved. After RNA extraction, genomic DNA pellets can be solubilised in 8 mM NaOH. The expected yield from human skeletal muscle is 2-3 μg per 1 mg of tissue (manufacturer's instruction). Isolated DNA can be used for PCR or enzyme digestion.

Frozen skeletal muscle (50-100 mg) was placed on a cold steel plate and crushed to a fine powder using a mortar designed for rock crushing. Muscle tissues and steel tools were kept cold using liquid nitrogen. The powdered tissue was transferred to a 15 mL round-bottom centrifuge tube containing 0.75 mL of TRIzol reagent. The solution was homogenised using an ultra-Turax T25 and allowed to stand 5 minutes at room temperature. Addition of 0.2 mL of chloroform followed by centrifugation separated the solution into an aqueous phase and an organic phase. After removal of the aqueous phase, the RNA pellet was collected by precipitation with 0.5 mL of isopropanol. The pellet was washed with 1 mL of 75% ethanol and completely dried using a speedvac for 5 minutes. The RNA pellet was redissolved in 30 μL of DEPC-treated water.

After RNA isolation, the remaining aqueous phase overlying the organic phase was carefully removed. Addition of 0.3 mL of 100% ethanol and 5 minutes centrifugation precipitated a DNA pellet. The pellet was washed twice with 1 mL of 0.1 M sodium citrate in 10% ethanol. Following these washes, the pellet was suspended in 1.5 mL of

75% ethanol for 20 minutes. After 5 minutes of centrifugation using a speedvac, the DNA pellet was redissolved in 0.5 mL of 8 mM NaOH. The solution was allowed to stand overnight, and insoluble materials were removed by centrifugation. After redissolving the DNA, the pH was adjusted to 8.4 with 0.1 M HEPES subsequent to PCR.

2.2.2 *Isolation of genomic DNA using the Wizard™ kit*

The Wizard™ Genomic DNA Purification Kit allows fast genomic DNA extraction from whole mammalian blood. It is designed to isolate DNA from white blood cells in up to 12 mL of fresh blood. This technique is based on a four-step procedure (131). First of all, red blood cells are lysed using Cell Lysis Solution. This solution specifically lyses red blood cells and leaves white blood cells intact. Secondly, white blood cells and their nuclei are lysed and solubilised in Nuclei Lysis Solution. The cellular proteins are removed at the following step using Protein Precipitation Solution, and finally, genomic DNA is recovered by isopropanol precipitation. The expected yield is in the range of 5-15 µg per 300 µL whole blood (manufacturer's manual). Purified DNA is suitable for a variety of applications including amplifications, restriction endonuclease digestion and Southern blotting.

900 µL of Cell Lysis Solution from the kit or the hand-made solution (150 mM ammonium chloride, 10 mM potassium hydrogencarbonate, 0.1 mM EDTA, pH8.0) was placed in a 1.5 mL tube. Blood samples were thawed and thoroughly mixed. 300 µL of blood was added to the tube and mixed vigorously for 10 minutes. After centrifugation and supernatant removal, white blood cells were solubilised in 300 µL of Nuclei Lysis Solution and incubated at 37°C for solubilisation. Proteins were precipitated by the addition of 100 µL of Protein Precipitation Solution. DNA in the supernatant was recovered with 300 µL isopropanol followed by an ethanol wash with 300 µL of 70% ethanol. The DNA pellet was redissolved in 100 µL of DNA Rehydration Solution or 1× TE buffer (10 mM Tris, 1 mM EDTA, pH 8.0) and allowed to stand overnight. The samples were stored at -20°C until use. The Nuclei Lysis and Protein Precipitation Solution are proprietary reagents and Promega does not provide any information about their composition.

2.3 Polymerase chain reaction

2.3.1 Principles of PCR

The Polymerase Chain Reaction (PCR) is a technique to amplify DNA fragments (132). It is highly sensitive for the detection of nucleic acids, and uses multiple cycles of template denaturation, primer annealing, and primer elongation. Typical PCR reactions consist of 20 to 30 cycles with pre-determined times and temperatures (Table 2-1). Reaction cycles were performed using an FTS-320 thermal sequencer (Corbett Research) or GeneAmp® PCR System 2700 (Applied Biosystems). Typical reaction compositions are indicated in Table 2-2. After reactions, PCR products were stored at 4°C.

Initial denaturation (94°C, 1 cycle)	3 min
Amplification cycles – denaturation (94°C)	15 sec
primer annealing (annealing temperature)	30 sec
elongation (72°C)	30 sec
number of cycles	20-30
Final extension (72°C, 1 cycle)	5 min

Table 2-1 Typical conditions of PCR thermal cycles

Typical PCR reactions consist of three steps: 1 cycle of initial denaturation, 20-30 cycles of extension, and 1 cycle of final extension. Conditions were slightly modified for gene screening depending on the gene to analyse.

2.3.2 Primer design

Primer design is one of the most important factors to perform PCR reactions successfully. Primers already designed and supplied were used for most *RYR1* and *CACNA1S* screening reactions. Some primers however, were newly designed to screen

RYR1 and *CACNG3* according to following guidelines (133):

- 18 to 24 nucleotides in length. Primers must be long enough to anneal stably and specifically. 21 nucleotides were most preferred.
- 50% to 60% GC. The GC content varies the melting temperature (T_m). It is essential to set similar T_m for primer pairs. Large differences of T_m between primer pairs prevent specific annealing and amplification. 62% GC was most preferred.
- Avoid complementary sequences at the 3' end of primer pairs. This induces formation of primer-dimers and prevents amplification.
- Avoid a GC-rich 3' end. This induces production of unspecific bands.
- Avoid palindromes. These induce high internal secondary structure and prevent stable annealing.

Components	Quantity
Template DNA	10^4-10^6 copies
Forward primer	0.1-0.5 μM
Reverse primer	0.1-0.5 μM
10× reaction buffer	1×
Magnesium chloride	1.0-3.0 mM
dNTP mix	200 mM each dNTP
DNA polymerase	1-4 units/100 μL reaction

Table 2-2 Typical reaction components for PCR

The quantities of each component are in the range shown in this table for most PCR reactions. The optimal quantities of each component, however are dependent on the templates and the regions to amplify.

2.3.3 *Annealing temperature*

Another important aspect is primer annealing temperature. A temperature which is too high does not facilitate annealing of primers to the template, and a temperature which is too low induces unspecific priming. Typically, annealing temperature is set about 5°C below the T_m of the primers.

T_m differs in nucleotides of primers, and is calculated using the following formula (134):

$$T_m = 81.5 + 16.6(\log_{10}[Na^+]) + 0.41(\%\ G + C) - 675/n$$

where n=number of bases in the primer, and $[Na^+]$=the molar salt concentration of monovalent cations (Na^+ or K^+). Reasonable annealing temperatures range from 55°C to 70°C. 60°C was the most preferred.

2.3.4 *Enzymes*

A thermostable DNA polymerase was used for elongation. The most frequently used enzyme is *Taq* DNA polymerase. This enzyme is stable against prolonged incubations at high temperature (95°C) and can perform fast amplification (over 1 kb/min). *Taq* DNA polymerase is suitable for most routine applications, but other polymerases can enhance results. *Taq* polymerase is considered a slightly low fidelity polymerase because it lacks 3'-5' exonuclease (proofreading) activity. Hence, other high fidelity polymerases are often used for some procedures including cloning and site-directed mutagenesis. ELONGASE® Enzyme Mix is a mixture of *Taq* and *Pyrococcus species* GB-D thermostable DNA polymerases. This mixture contains a proofreading enzyme, which edits the nascent strand allowing higher fidelity and amplification of larger targets. Another consideration is required in the use of *Taq* polymerase for microsatellite analysis. It often introduces an A at the 3' end. Therefore, genotypes may be shifted because of the extra nucleotide. AmpliTaq Gold® PCR Master Mix was used for secondary microsatellite analysis and ELONGASE Enzyme Mix was used for some *RYR1* PCR reactions. *Taq* DNA polymerase was used for all other PCR reactions.

2.3.5 *Touchdown PCR*

Touchdown PCR is a technique to increase sensitivity by using a stringent initial annealing temperature (135) and is often used with primers of differing T_m. Thermal cycles start with annealing temperature above the estimated T_m, followed by incremental decrease in every cycle to the suitable annealing temperature. Primers cannot anneal stably on non-specific sequences in the initial cycles, hence only specific targets will be amplified. Touchdown PCR was performed for some *RYR1* screening reactions, especially GC-rich regions.

2.3.6 *Hot-start PCR*

Hot-start PCR is a very effective technique to increase PCR specificity. Although the optimal activation temperature for *Taq* DNA polymerase is 72°C, the enzyme is still active at room temperature (136). Therefore, non-specific products are often generated during PCR sample preparations and at the start of thermal cycling. Hot-start PCR inhibits enzyme activity to react until after the initial denaturation, and increases specific fragment production. Typical methods are delayed addition of the enzyme and the limitation of enzyme activity. For all PCR reactions except microsatellite marker analysis, reaction components were mixed without the *Taq* DNA polymerase and incubated for initial denaturation. During the denaturation (94°C), the enzyme was added manually to each sample. AmpliTaq Gold DNA polymerase is a chemically modified form of AmpliTaq DNA polymerase. As a chemical moiety is attached to the enzyme, it is inactive at room temperature. After the initial activation step (95°C, 5 minutes), the enzyme becomes active. Because the enzyme is inactive during sample set-up and the first ramp of thermal cycles, non-specifically annealed primers will not be extended.

2.3.7 *Additives*

Additives that affect DNA melting temperature often improve product specificity and yield for some targets especially with a high GC content. Within GC-rich regions, high secondary structure can prevent primer annealing and enzymatic elongation. PCR additives including formamide, dimethyl sulfoxide (DMSO) and glycerol lower the T_m

aiding primer annealing and helping the DNA polymerase extend through regions of secondary structure (137). Formamide, DMSO or glycerol were added to some *RYR1* screening samples at final concentrations of 5%, 2% or 10% (v/v), respectively.

2.3.8 RT-PCR

RT-PCR combines cDNA synthesis from RNA templates with PCR. cDNA synthesis is carried out by using reverse transcriptase (RT). RT-PCR can be performed either in two-step or one-step reactions. In two-step RT-PCR, each step is performed separately. cDNA is synthesised first in RT buffer, and then one tenth of the reaction is removed for PCR. In one-step RT-PCR, the RT reaction and PCR is carried out sequentially in a single tube. Total RNA extracted from skeletal muscle was used as a template for RT reactions. As isolation of high-quality RNA is essential for successful RT reactions, RNA was purified by degradation of any contaminating genomic DNA using DNase I (see section 2.5.1). Two-step RT-PCR was adopted for *RYR1* screening using SUPERSCRIPT™ First-Strand Synthesis System. The first-strand cDNA synthesis was catalysed by SUPERSCRIPT II RNase H^- Reverse Transcriptase. This enzyme has been engineered to retain the full DNA polymerase activity found in RNase H^+ M-MLV RT and to synthesise first-strand cDNA from a total RNA preparation. The enzyme exhibits increased thermal stability and may be used at temperatures up to 50°C.

Random hexamers were used to prime the first-strand synthesis for most reactions. These nonspecific primers are typically used when a particular mRNA is difficult to copy in its entirety. 0.5-1.0 μg of total RNA was mixed with 1 μL of random hexamers (50 ng/μL), 1 μL of 10 mM dNTP mix and DEPC-treated water to achieve a 10 μL total volume. The mixture was incubated at 65°C for 5 minutes for annealing, and then placed on ice. A cocktail reaction mixture was added to the solution. The reaction mixture contained 2 μL of 10× RT buffer (200 mM Tris-HCl, pH 8.4, 500 mM $MgCl_2$), 4 μL of 25 mM $MgCl_2$, 2 μL of 0.1 M DTT and 1 μL of RNASEOUT™ Recombinant RNase Inhibitor (40 units/μL). The solution was then incubated at 25°C. After 2 minutes, 1 μL of SUPERSCRIPT II RT (50 units/μL) was added, and the solution was incubated for 10 minutes at 25°C. Then the solution was transferred to 42°C and incubated for 50 minutes. The reaction was terminated by incubation at 70°C for 15 minutes. The mixture was placed on ice and 1 μL of RNase H (2 units/μL) was added and incubated

at 37°C for 20 minutes. After RT reactions, 1-2 μL of 10-fold reaction product was used as a template for PCR. Oligo(dT) was used for some RT-PCR reactions for more specific priming. It hybridises to 3' poly(A) tails that are found in the vast majority of eukaryotic mRNAs. The amount and complexity of cDNA is considerably less than when random hexamers are used because poly(A) constitutes 1% to 2% of total RNA. The procedure was identical to that described for the random hexamers, apart from the following adjustments. 1 μL of 0.5 μg/μL oligo(dT) was used in place of 1 μL of random hexamers in the annealing step. After the addition of the cocktail of reaction mixture, the solution was incubated directly at 42°C. Hence the 25°C pre-incubation steps were omitted. After reactions, 2 μL of 10-fold reaction product was used for PCR.

2.4 Nucleic acid quantification

2.4.1 Gel electrophoresis

Gel electrophoresis is one of the most popular and effective techniques to analyse nucleic acids. Double-stranded DNA is negatively charged as a total molecule because of phosphate ions. As the charges on each base are decreased by hydrogen bonding with complementary strands, only the length of the DNA affects the length of electrophoresis on the gel regardless of nucleic acid sequences. Gels were prepared using agarose, and agarose LE was most preferred. Agarose LE is suitable for separation of DNA fragments with a size range of 0.2-15 kb depending on the concentration of agarose LE applied (manufacturer's instructions).

NuSieve® GTG® agarose was used for some gel preparations. This low melting temperature agarose is suitable for separation of short nucleic acids (<1 kb). The gels were electrophoresed using a running buffer. 1× TAE (40 mM Tris-acetate, 1 mM EDTA, pH 8.0) was used mostly, and 0.5× TBE (45 mM Tris-borate, 1 mM EDTA, pH 8.0) was occasionally used for the separation of short DNA fragments. Generally, TAE is suitable for long DNA and TBE is suitable for short DNA fragments. DNA samples were loaded on the gel with 5× DNA loading buffer (0.4% bromophenol blue, 0.1% xylene cyanol FF, 15% ficoll in water). The gels were electrophoresed for 30-60 minutes at 80 V or 100 V for TAE or TBE, respectively. The DNA fragments were visualised using ethidium bromide under UV. Normally, ethidium bromide was added in

the melted agarose before loading, at a final concentration of 0.4 μg/mL. It was sometimes omitted from the gel for clearer photographs; after electrophoresis, the gel was soaked in the running buffer containing 0.5 μg/mL ethidium bromide for 45 minutes. Then, the gel was soaked in 1 mM magnesium sulphate for 20 minutes for washing. The DNA bands observed were slightly clearer than using the gel containing ethidium bromide, especially for very short fragments.

This method is not suitable for RNA because it does not have double helical structure. The charges of each base or high-order structure of the molecule significantly affect electro-mobility. Therefore, denaturants such as urea and formaldehyde are required to separate fragments depending on their length only. Denaturants prevent hydrogen bonding between nucleotides and high-order structure in the molecule. 1× MOPS (1 M MOPS, 250 mM sodium acetate, 5 mM EDTA, pH 7) was used as the running buffer for RNA gels. The gels were prepared using agarose LE; 0.45 g of agarose LE was melted in 18.8 mL of DEPC-treated water and the solution was warmed at 55°C, 6 mM of 5× MOPS and 5.3 mL of formaldehyde were added to the solution, and the gel was allowed to set within a fume hood. The gel was submerged in 1× MOPS and electrophoresed before sample loading for 5 minutes at 40 V for clear photographs. RNA was concentrated by ethanol precipitation after extraction from muscle. RNA samples containing 10-30 μg of total RNA were mixed with 100 μL of HEPES/EDTA (10 mM HEPES, 1 mM EDTA, pH 7.6). After addition of 0.1 volume of 2 M potassium acetate and 2.5 volumes of 100% ethanol (-20°C), the solution was allowed to stand overnight at -20°C. The RNA pellet was collected by centrifugation, and redissolved in 20 μL of prepared sample buffer (50 μL of deionised formamide, 16 μL of formaldehyde, 20 μL of 5× MOPS buffer, 14 μL of DEPC-treated water). RNA was denatured at 60°C for 10 minutes, and then loaded on the gel with 1 μL of 10 mg/mL ethidium bromide and 1 μL of RNA loading buffer (50% glycerol, 0.4% bromophenol blue, 1 mM EDTA in DEPC-treated water). The high concentration of ethidium bromide was required as ethidium bromide is positively charged and consequently moves in the opposite direction to the RNA. Electrophoresis was carried out in a fume hood at 40 V until the bromophenol blue reached the middle of the gel.

2.4.2 *Spectrophotometry*

UV/Visible spectrophotometry is often used for nucleic acid quantification and assessment of purity. Concentrations of nucleic acids can be calculated using the absorbance at 260 nm (A_{260}). The formula is following:

$$\text{Concentration } (\mu\text{g/mL}) = A_{260} \times \text{Factor}$$

where Factor is the established concentrations of DNA and RNA, which have an absorbance of 1.0 at this wavelength with 50 or 40 μg/mL for DNA or RNA, respectively. Purity of nucleic acid samples can be established using an absorbance ratio:

$$\text{Absorbance ratio} = \frac{\text{Absorbance at } \lambda_1}{\text{Absorbance at } \lambda_2}$$

where λ_1 is the maximal absorbance of the substance of interest, and λ_2 is that of an impurity. For the DNA and RNA purity check, λ_1 is 260 nm and λ_2 is 280 nm for protein contamination. Pure DNA or RNA has an A_{260}/A_{280} ratio of 1.8 or 2.0, respectively. Ratios less than 1.7 for DNA or less than 1.65 for RNA indicate protein contamination. This procedure was performed using an Ultrospec 3000 UV/Visible Spectrophotometer (Pharmacia Biotech) with 100 μL cuvettes.

2.4.3 *Real-time PCR using a LightCycler*

Genomic DNA was quantified by real-time PCR. The LightCycler is a rapid PCR machine, which can monitor PCR reactions in real-time. It requires only 10-20 μL of sample volumes in glass capillaries, and performs rapid thermal cycling using the thermal chamber and a carousel with up to 32 samples. The thermal chamber and glass capillaries account for extremely rapid thermal transfer to the reaction mixture. As a result, the time required for each cycle is about 15-20 seconds and total time for one reaction is only 20 minutes. Fluorescent DNA-binding dyes included in the reaction mixture allow the LightCycler to detect exact amounts of PCR product in real-time. The LightCycler is suitable for variations of procedures including mutation detection, melting temperature analysis and quantification.

Real-time PCR using the LightCycler can perform kinetic quantification of DNA samples. During a PCR reaction, DNA fragments are produced with accelerated speed. Figure 2-1 shows a typical PCR amplification curve. Each curve has three segments: an early background phase, an exponential growth phase (log linear phase), and a plateau phase. The background fluorescence is greater than that from PCR products at the background phase. The log linear phase begins when sufficient product has accumulated to be detected above background, and the exponential curve bends toward a plateau at the final plateau phase. At these last two phases, amplification is described as (138):

$$N = N_0 \times E^n$$

where N=number of amplified molecules, N_0=initial number of molecules, E=amplification efficiency, n=number of cycles.

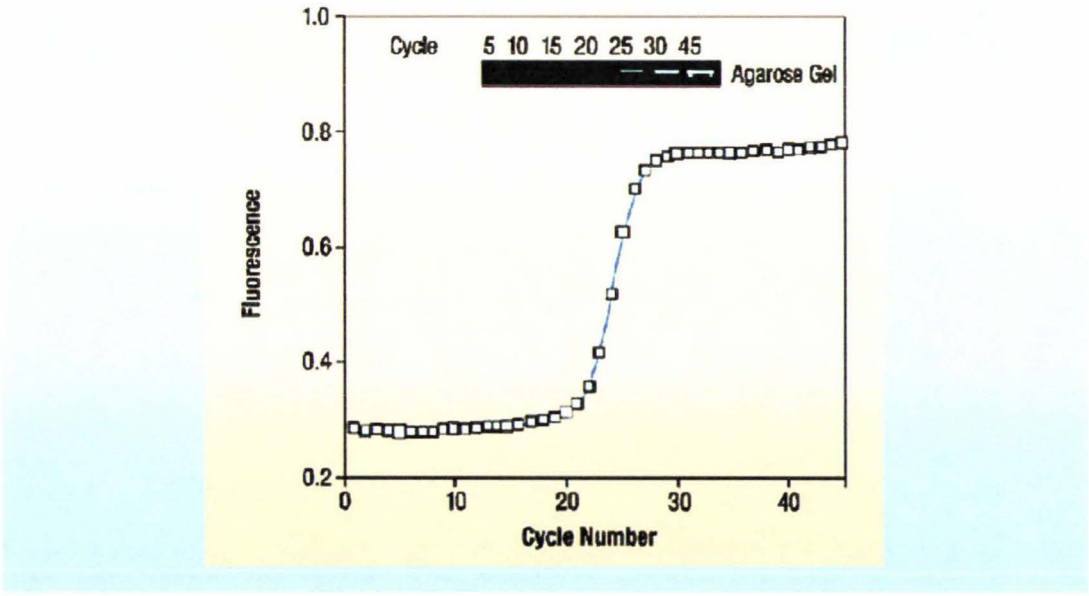

Figure 2-1 Typical PCR amplification curves

LightCycler can monitor PCR samples in real-time detecting the fluorescence at each cycle. It can identify the log linear phase for calculation of the amplification efficiency, whereas DNA fragments can be observed only at the plateau phase by electrophoresis. From Technical Note No. LC 10/2000 (Roche Molecular Biochemicals).

The amplification efficiency, E, can be calculated at the log linear phase by using the following formula:

$$E = 10^{-1/slope}$$

The log linear phase lasts only 2-5 cycles in a run. They cannot be detected by agarose electrophoresis (Figure 2-1), but with real-time PCR monitoring on a LightCycler, these log linear cycles are easily identified and measured using an intercalating dye, such as SYBR Green®. SYBR Green binds all double-stranded DNA regardless of the sequence, and emits a fluorescent signal during annealing and extension steps of each PCR cycle. The accumulation of amplified DNA is measured by the increase in fluorescence over time. The specificity of the amplification product can be evaluated by combining PCR with melting curve analysis. Non-specific products such as primer dimers are differentiated by measuring T_m.

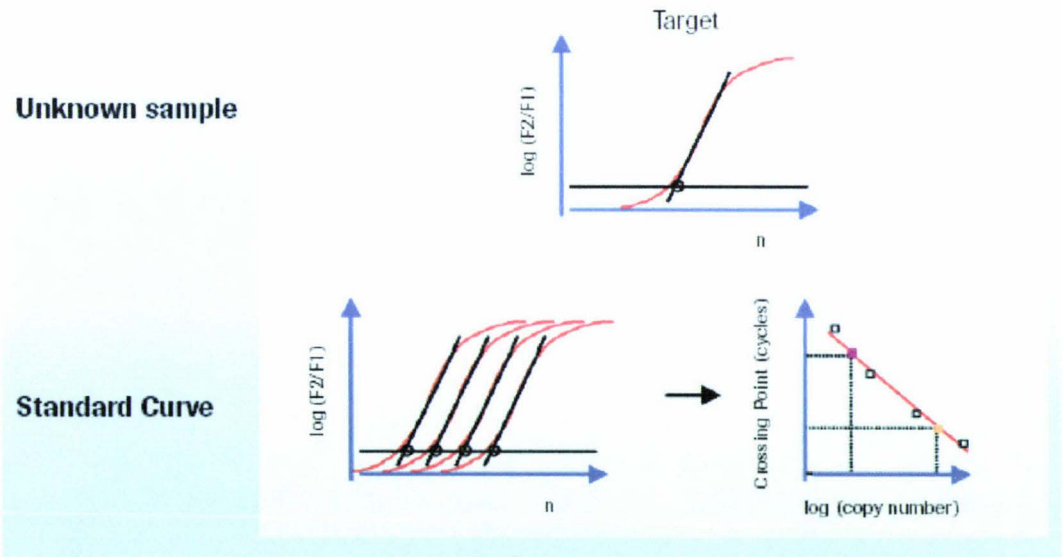

Figure 2-2 Concepts of quantification using external standard samples

The standard curve is created using standard samples with known DNA concentrations. The concentrations of unknown samples are calculated by using a crossing point within the standard curve. LightCycler can perform accurate quantification because it detects the exact amount of PCR products at each reaction cycle. From Technical Note No. LC 10/2000 (Roche Molecular Biochemicals).

Monitoring PCR and quantification was performed by using LightCycler Software version 3.5.3. The software detects the fluorescent signals and calculates the slope for kinetic quantification. The concentrations of unknown samples are calculated by using a crossing point on the standard curve created by external standard samples (Figure 2-2). LightCycler-Control Kit DNA provides control DNA with the exact concentration (15 ng/μL) for external standards. The kit also provides primers specific for the human β-globin gene. Five dilution series (1.5 pg/μL to 15 ng/μL) were analysed to create an accurate standard curve, and then unknown samples were analysed using same β-globin primers. The concentrations were calculated automatically by the software using the standard curve. SYBR Green was adopted as a fluorescent dye for all reactions. LightCycler-FastStart DNA Master SYBR Green I is a mixture including the dye and modified *Taq* DNA polymerase allowing Hot-start PCR. The components of a reaction are listed in Table 2-3, and Table 2-4 shows thermal cycle conditions.

Components	**Volume (μL)**
Control or unknown DNA	2
25 mM $MgCl_2$	2.4
β-globin primer mix (20 μM each)	2
Faststart DNA Master Mix	2
PCR-grade water	11.6
Total	20

Table 2-3 The reaction components for LightCycler quantification

The reaction mixture was placed in a glass capillary kept at 4°C. Sample preparations were always carried out at 4°C avoiding sunlight because of sensitivity of the enzyme.

stage	# of cycles	Step 1	Step 2	Step 3	Fluorescent detection
Activation	1	95 °C, 10 min	—	—	No
Amplification	45	95 °C, 15 sec	55°C, 5 sec	72°C, 10 sec	Single acquisition at 83°C
Melting curve	1	95 °C, 0 sec	65°C, 15 sec	Ramp 65-95°C at 0.1 °C/sec	Continuous
Cooling	1	40 °C, 30 sec	—	—	No

Table 2-4 The thermal cycles for LightCycler quantification

The initial activation step was needed for FastStart DNA Master Mix to perform Hot-start PCR. Detection of fluorescence was carried out at 83°C after the elongation step so as to avoid detection of the signal from the primer-dimers.

2.5 Nucleic acid purification

2.5.1 RNA purification by DNA degradation

After RNA isolation from skeletal muscle, RNA samples sometimes contained genomic DNA. As DNA could inhibit RT-PCR, RNA purification was performed by DNA degradation using DNase I. DNase I digests single- and double-stranded DNA and is suitable for RNA purification procedures. 1 μg of RNA sample was mixed with 1 μL of 10× DNase I reaction buffer (200 mM Tris-HCl, 20 mM $MgCl_2$, 500 mM KCl, pH 8.4), 1 μL of DNase I Amp Grade (1 unit/μL) and DEPC-treated water to adjust the final volume to 10 μL. The solution was incubated at room temperature for 15 minutes. Addition of 1 μL of 25 mM EDTA and incubation at 65°C for 15 minutes inactivated the enzyme. RNA samples were then ready for RT-PCR. Careful attention was paid to sample incubation (15 minutes at room temperature) because higher temperatures and longer time could lead to Mg^{2+}-dependent hydrolysis of the RNA.

2.5.2 DNA purification using QIAGEN kits

PCR products needed to be purified for direct sequencing or endonuclease digestion. QIAGEN kits using QIAquick® or MinElute™ columns provide fast DNA purification

procedures from PCR products or agarose gels after electrophoresis. These columns have a unique silica-gel membrane, which absorbs DNA fragments in the presence of high salt while contaminants pass through the columns. The membrane of QIAquick and MinElute column can absorb up to 5 μg and 10 μg of DNA, respectively (manufacturer's instruction). These columns are designed to give high concentrations of purified DNA fragments for subsequent reactions. QIAquick and MinElute column give a final volume at elution of 30 μL and 10 μL, respectively. PCR products or fragment purification for agarose gels was carried out according to the manufacturer's instruction.

2.6 Mutation screening

2.6.1 Direct sequencing

After purification of PCR products, 2-20 ng/μL of DNA fragments were directly sequenced using ABI PRISM™ 377 or ABI 3730 Genetic Analyser with Big Dye terminator chemistry. Sequencing primers were diluted to 0.8 or 3.2 pmol/μL for use. This procedure was performed at the Allan Wilson Centre Genome Service by Ms Lorraine Berry (Massey University). The sequencing data were analysed using CLUSTAL W (139).

2.6.2 Endonuclease digestion

Two mutations have been found to date within *CACNA1S* and the R1086H mutation has been found in more than one family (140). Screening of these mutations can be performed by *Hha*I endonuclease digestion. *Hha*I recognises GCG/C sequence, and mutations R1086C (C3256T) and R1086H (G3257A) disrupt the recognition site. Hence, *Hha*I digestion followed by agarose gel electrophoresis can be used to ascertain whether or not samples have a mutation at the site. A 226-bp-long fragment was directly used for enzyme digestion after PCR. 20 μL of PCR product was mixed with 5 μL of 1× NEBuffer 4 (20 mM Tris-acetate, 10 mM magnesium acetate, 50 mM potassium acetate, 1 mM DTT, pH 7.9), 0.5 μL of bovine serum albumin (10 mg/mL) and water. Then, 1 μL of *Hha*I (20 units/mL) was added to the mixture and reaction tubes were incubated at 37°C for 2.5 hours. The final volume of the reaction mixture was 50 μL. Digested fragments were analysed by agarose electrophoresis using 3.5% NuSieve GTG agarose.

2.7 Genetic linkage analysis

2.7.1 Microsatellite marker analysis

Genomic DNA extracted from blood was used as a template for PCR. Fragments covering microsatellite markers were amplified and their polymorphism was determined to establish the patients' genotypes. All samples needed to be quantified and have the same concentrations because PCR and genotyping of markers were performed with several samples at the same time, and a difference in DNA concentration could induce huge differences in PCR products preventing signal detection of small amount of products for genotyping. Genomic DNA was isolated using the Wizard kit and DNA samples were initially quantified by spectrophotometer. The manufacturer's instructions in the Wizard kit, however recommend not relying on the results of spectrophotometry because the results may not be reliable. Therefore, DNA samples were also quantified by real-time PCR with a LightCycler, and concentrations were estimated for each sample from the average between the results of spectrophotometry and these from real-time PCR. After estimation, each sample was diluted to 100 ng/μL. For a genome-wide scan, DNA samples were sent to Australia, and PCR and genotyping were performed at the Australian Genome Research Facility, Parkville Victoria, Australia. 400 microsatellite markers were used to analyse the entire genome at 10 cM intervals on average (141-143). After analysis, collected data were provided in an Excel format. For a secondary linkage analysis, PCR and genotyping were performed manually. DNA samples were diluted to 50 ng/μL, and PCR was carried out to amplify 10 marker regions. PCR primers were labelled with a fluorescent dye, FAM, VIC or NED.

PCR was carried out using AmpliTaq Gold PCR Master Mix. Reaction components were: 1.2 μL of 50 ng/μL DNA, 1 μL of microsatellite marker primer mix (5 μM each), 7.5 μL of AmpliTaq Gold PCR Master Mix and 5.3 μL of sterile water. The final volume was 15 μL. Table 2-5 shows the thermal cycles for PCR.

Stage	# of cycles	Step1	Step2	Step3
Activation	1	95°C, 12 min	—	—
Amplification 1	10	94°C, 15 sec	55°C, 15 sec	72°C, 30 sec
Amplification 2	20	89°C, 15 sec	55°C, 15 sec	72°C, 30 sec
Final extension	1	72°C, 10 min	—	—

Table 2-5 The thermal cycles for microsatellite marker analysis

AmpliTaq Gold DNA Polymerase required the initial activation step. PCR was performed by using GeneAmp PCR System 2700.

Ten PCR products were obtained for each DNA sample. They were separated into two groups (five PCR products each) according to their dye label and fragment length. In each group, PCR products were mixed directly at the same ratio (FAM:VIC:NED=1:1:1). Mixed samples were analysed for genotyping by ABI 3730 Genetic Analyser (Applied Biosystems) at the Allan Wilson Centre Genome Analysis Service (Massey University). Data were viewed and the genotype was determined using ABI PRISM® GeneMapper Software version 3.0. As the length or dye of each fragment was different in the same group, the detection of dye signal and genotyping was carried out for five samples at the same time in a single capillary.

2.7.2 Installation of software

GENEHUNTER and GENEHUNTER-PLUS were used for linkage analysis of autosomes and X chromosome, respectively (144, 145). GENEHUNTER version 2.1 release 5 was downloaded from the author's website (http://www.fhcrc.org/labs/kruglyak/Downloads/index.html), and GENEHUNTER-PLUS version 1.2 was downloaded from its homepage (http://galton.uchicago.edu/genehunterplus/). As these programmes do not run on MS-DOS or Windows, they were run on a Linux PC. As a Linux PC was not available, KNOPPIX® was used for running both programmes on Linux. KNOPPIX is a Linux distribution on a bootable CD-ROM, which does not require any installation on a PC and can run Linux software. KNOPPIX was obtained from its website

(http://www.knoppix.org/).

2.7.3 Preparing input data

After genotyping, haplotypes of each individual were determined on every marker. Numbers of allele and allele frequencies were also calculated for each marker. GENEHUNTER and GENEHUNTER-PLUS use the input data format called the LINKAGE format, which is used in the popular linkage analysis software, LINKAGE package (146). The input data consist of two files, datafile and prefile. The datafile contains general information on loci and locus order, description of loci, information of recombination and programme-specific information. The important information is order and description of loci. Marker information should be described according to their order in a certain format as in a following example:

```
3   6 # D1S468

0.346153846   0.057692307   0.192307692   0.057692307   0.153846153   0.192307692
```

The 3 on the first line is obligatory, followed by the number of alleles for the marker. The name of the marker after a # is recognised and printed out in the output data by the software. Allele frequencies calculated for each allele are described in the second line. The datafile should be written in a text format and have an extension '.dat'.

The prefile contains family information and haplotypes for family members. It is also written in a text format and the extension is '.pre'. Each line of this file should have the following structure:

```
CH      9       7       8       1       0       1 1   3 5...
(a)     (b)     (c)     (d)     (e)     (f)     (g)
```

(a) Family name

(b) Individual ID

(c) Father's ID

(d) Mother's ID

(e) Sex (1=male, 2=female)

(f) Affection status (1=unaffected, 2=affected)

(g) Haplotype for each marker

A 0 in affection status or marker haplotype indicates unknown data.

2.7.4 Settings of the software

Table 2-6 shows the settings adopted for analysis using both GENEHUNTER and GENEHUNTER-PLUS. The 'count recs' command activates the recombination counting mechanism during analyses. After each pedigree is analysed, the observed recombination is shown for each map interval alongside the actual distance of the interval. When there is significantly more recombination than expected in an interval, this often indicates an error in the pedigree information or genotype data. Because of the time and memory requirements of the mapping algorithms in GENEHUNTER, a maximum pedigree size must be set to keep the calculations within the ability of the computer. The 'max bits' command sets the pedigree size for analysis. A larger number allows the software to handle a larger pedigree, but it requires more memory and time for analysis. 19 was the maximum number for the system used for analysis in this project. It could not be set over 19, otherwise the computer could not finish the calculations because of lack of memory. Microsatellite markers used for a genome-wide scan had about 10 cM intervals in average. Therefore, analysis 10 cM at the top and bottom of chromosomes could sometimes not be completed. To scan each end of chromosomes, calculations were carried out beyond the regions where markers were available. The 'off end' command was set to 10, and it means that the software calculates 10 cM before the first marker and after the last marker.

Command	Setting	Summary
haplotype	on	determine likely haplotypes for individuals
postscript output	on	activate postscript graphing capability
count recs	on	turn recombination counting on
max bits	19	determine how large a pedigree may be analysed
discard	off	eliminate less informative individuals
skip large	off	determine how large pedigree are dealt with
off end	10	select how far to compute scores beyond ends of map
map function	kosambi	choose map function to convert cM ↔ recombination fraction

Table 2-6 Settings for linkage analysis

Both GENEHUNTER and GENEHUNTER-PLUS have several alterable parameters including analysis methods, output data style and pedigree size for analysis. Settings were described in an '.ini' file and they were read every time before analysis. Other settings were set as default.

CHAPTER THREE : SCREENING OF MUTATIONS

3.1 Introduction

Recently, a New Zealand male, identified as M818, suffered a fulminant MH crisis, which resulted in death. This patient had no family history of MH and the reaction was triggered by exercise, rather than anaesthesia. Post-mortem muscle tissue had been stored at -70°C, and this was used to extract DNA for molecular genetic analysis. In New Zealand, at least 40 families have been identified as MHS, and ten families have been characterised for mutations in *RYR1* (113, 128, 147). Screening for these known mutations had already been carried out for the M818 patient, but none were identified. As exercise-induced MH is quite rare, consequently there are few published case reports. One *RYR1* mutation, R401C, was identified, however from Australian patients who showed exercise-induced rhabdomyolysis, a symptom of MH (128). The R401C mutation was also found in individuals of one New Zealand family, where the proband had had several triggering anaesthetics before MH was diagnosed. It is not clear whether the R401C mutation is responsible for exercise-induced MH, neither has it been clearly shown that some specified mutations are likely to cause exercise-induced MH reactions. It is possible, however that the M818 patient had a novel mutation responsible for his MH susceptibility, because exercise-induced MH is very unusual and he is the first case reported of exercise-induced MH in New Zealand. As he lacked all of the *RYR1* mutations found in New Zealand to date, it was important to screen the entire *RYR1* cDNA. The identification of the three hot spot regions may simply be due to an accident as these regions are often screened preferentially and the rest of the cDNA ignored. cDNA was synthesised from total RNA extracted from the muscle sample, and *RYR1* was screened by PCR and direct sequencing. Two *CACNA1S* mutations which are associated with MH were also screened by endonuclease *Hha*I digestion of PCR products amplified from genomic DNA.

3.2 Screening of *CACNA1S* mutations

Two mutations within *CACNA1S*, R1086C and R1086H, have been reported to be associated with MH (115, 116). *CACNA1S* is the only gene aside from *RYR1* where mutations associated with MH have been identified. These two mutations alter the recognition site of endonuclease *Hha*I, hence the existence of mutation can be observed by agarose gel electrophoresis following enzyme digestion of a specific PCR product. A 226-bp-long fragment was synthesised by PCR using *Taq* polymerase, and digested by *Hha*I. If the fragment does not have these mutations, two fragments, 36 bp and 196 bp, will be observed. If the fragment contains a mutation at the *Hha*I site, then a fragment size of 226 bp would be observed. Genomic DNA was isolated after RNA extraction from skeletal muscle using the TRIZOL reagent, and the quality was checked by agarose electrophoresis (Figure 3-1). Using this DNA sample as a template, a 226-bp-long fragment was amplified by PCR using GeneAmp PCR System 2700. 1 ng of the DNA sample and 2 ng/μL of the forward primer 25i5, 5'-CTTGGTGCTGACCTGTCCTGTT and 2 ng/μL of the reverse primer 25i3, 5'-GATCAGACATTTTTCTCCTGGGG were used for the reaction. 30 cycles were carried out for amplification with 62°C as an annealing temperature for 30 seconds. The amplified DNA fragment was purified, and incubated with *Hha*I followed by electrophoresis for the mutation check. Figure 3-2 clearly shows the two bands for the M818 patient indicating that this patient does not have a mutation at this site.

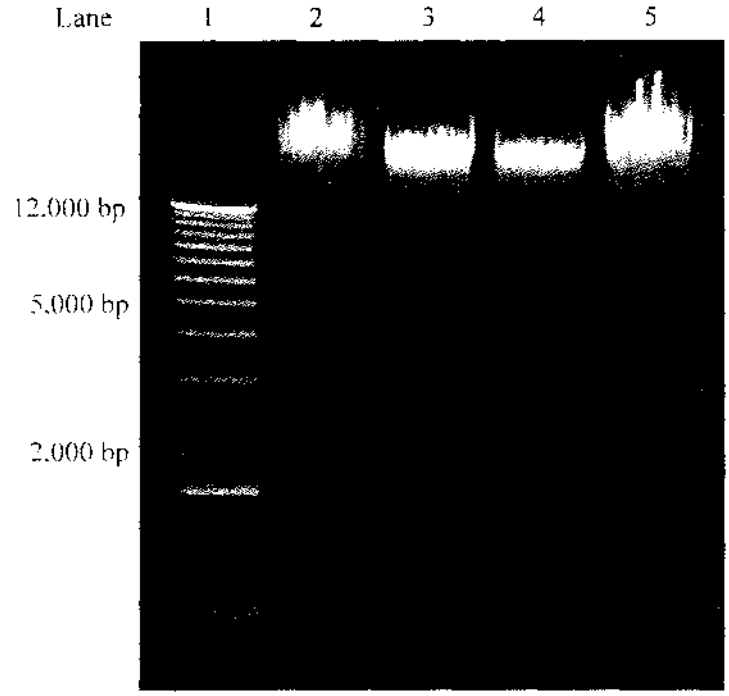

Figure 3-1 Quality check of genomic DNA

Extracted genomic DNA was analysed by agarose electrophoresis to check its quality. 600 ng DNA was electrophoresed on the 1% agarose gel for 1 hour at 80 V. 1× TAE was used as a running buffer. After electrophoresis, the gel was soaked in 100 mL 1× TAE containing 20 μg of ethidium bromide for 1 hour, and then washed with 1 mM $MgSO_4$ for 30 minutes.

Lane	1	5 μL of 1 kb plus DNA ladder
	2	DNA from the M818 patient
	3	DNA from M394
	4	DNA from M514
	5	DNA from M775

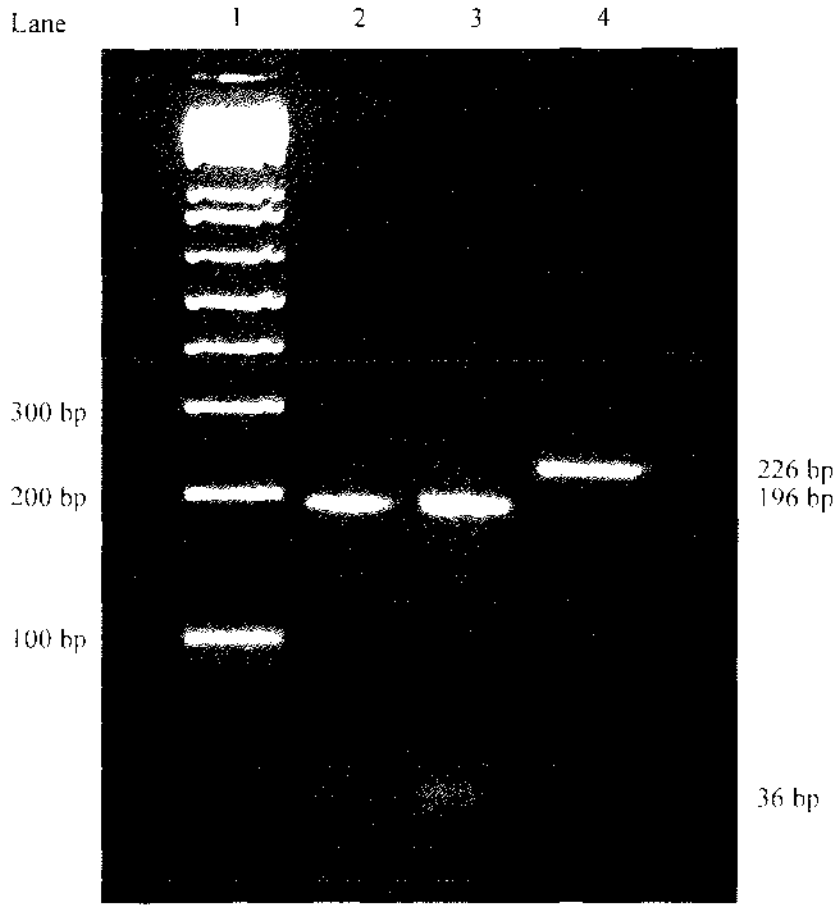

Figure 3-2 Detection of *CACNA1S* mutations

A 226-bp fragment was digested by *Hha*I. Each fragment was electrophoresed on 3.5% NuSieve GTG agarose gel for 1 hour at 80 V using 1× TAE as a running buffer. Fragments were stained with 2 µL of 10 mg/mL ethidium bromide and visualised by UV. Cut 36- and 196-bp fragments indicate the absence of the mutations.

Lane	1	10 µL of 1 kb plus DNA ladder
	2	M818 patient
	3	Positive control (MHN individual without mutations)
	4	Negative control (without *Hha*I)

3.3 Screening of *RYR1* cDNA

The cDNA representing *RYR1* (ryanodine receptor of skeletal muscle) is 15,117 bp long containing GC-rich region (75%) at the C-terminus. Screening of mutations within a

gene can be performed by several procedures; restriction fragment length polymorphism (RFLP) digests and single-stranded conformational polymorphism (SSCP) or direct screening. RFLP digests are performed using endonucleases. PCR fragments are incubated with one or more enzymes and then analysed on an agarose gel. If there is a mutation within the recognition site of the enzyme, it will alter the site and different length of fragments will be observed on the gel. This technique is effective, and widely used for detection of known mutations. It is not suitable, however to screen unknown mutations, especially within a large gene.

SSCP is a technique which can be used to detect mutations in DNA, to the extent of one base change. Even one nucleic change affects electro-mobility of single-stranded short DNA fragments (up to 300 bp). This polymorphic difference in strand mobility can be observed on a non-denaturing polyacrylamide gel. This technique however, was not adopted for screening *RYR1* because this gene is so large that hundreds of DNA fragments would be required to cover the entire gene. Sample and gel preparations for the huge number of fragments are time-consuming and not ideal for this project. Furthermore, SSCP is not reliable. The sensitivity of SSCP for detecting mutations has been reported as ranging from 35% to nearly 100% (148, 149). Therefore, screening of *RYR1* was carried out by direct DNA sequencing using an automated sequencer. This technique involves sequencing the amplified DNA fragments directly detecting the peak of each nucleotide. Mutations are easily detected by observing peak length and overlapping peaks for two nucleotides. Direct screening is a fast, easy and reliable method to analyse the gene sequence, and hence is suitable for detecting unknown mutations from the entire gene especially for large genes such as *RYR1*.

Amplification of *RYR1* fragments using cDNA as a template was accomplished using over 40 PCR primer pairs. Total RNA was extracted from skeletal muscle of the M818 patient. 100 mg muscle was used for each extraction procedure. As the muscle sample was limited, procedures were also carried out with rat muscle for practice and for a positive control. Isolated RNA samples were quantified by spectrophotometry (Table 3-1) and RNA electrophoresis (Figure 3-3) to check their purity and RNA integrity.

Sample source	$A_{260/280}$	Conc. (μg/mL)	Yield (μg RNA/mg tissue)
rat	1.82	3055	0.917
human	1.98	775	0.233

Table 3-1 Concentrations and the $A_{260/280}$ ratios of extracted RNA samples

RNA was dissolved in DEPC-treated water in a final volume of 30 μL. The $A_{260/280}$ ratios and concentrations were determined by spectrophotometry. RNA was checked for its quality by electrophoresis before RT-PCR.

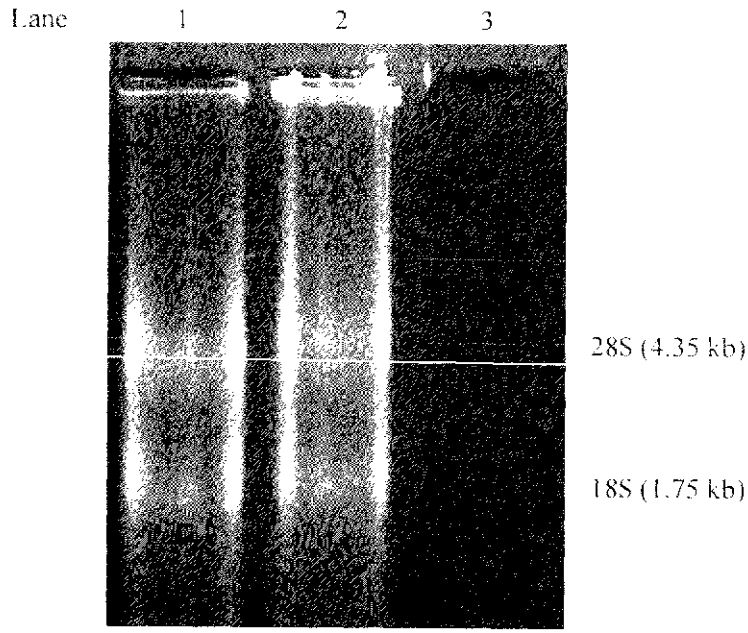

Figure 3-3 RNA electrophoresis

RNA samples isolated from skeletal muscle were analysed on a 1.5% agarose gel containing 17.6% formaldehyde. 30 μg RNA in the sample buffer was loaded in each lane. Electrophoresis was carried out at 40 V for 5 hours in 1× MOPS running buffer. The 28S (4.35 kb) and 18S (1.75 kb) ribosomal RNA bands were observed indicating no contamination and RNA degradation. RNA markers were not available.

Lane 1 Rat RNA
2 M818 RNA
3 Blank

After quantification and purification, RNA was used as a template for RT-PCR. 24 PCR fragments were synthesised to cover the entire *RYR1* cDNA. Figure 3-4 shows the strategy for *RYR1* screening. Primers used for PCR and sequencing are listed in Table 3-2 and an example of the PCR products are shown in Figure 3-5. Appendix 1 lists sequences of all PCR and sequencing primers employed and Appendix 2 shows the sequence of the entire *RYR1* including primers and mutations found to date.

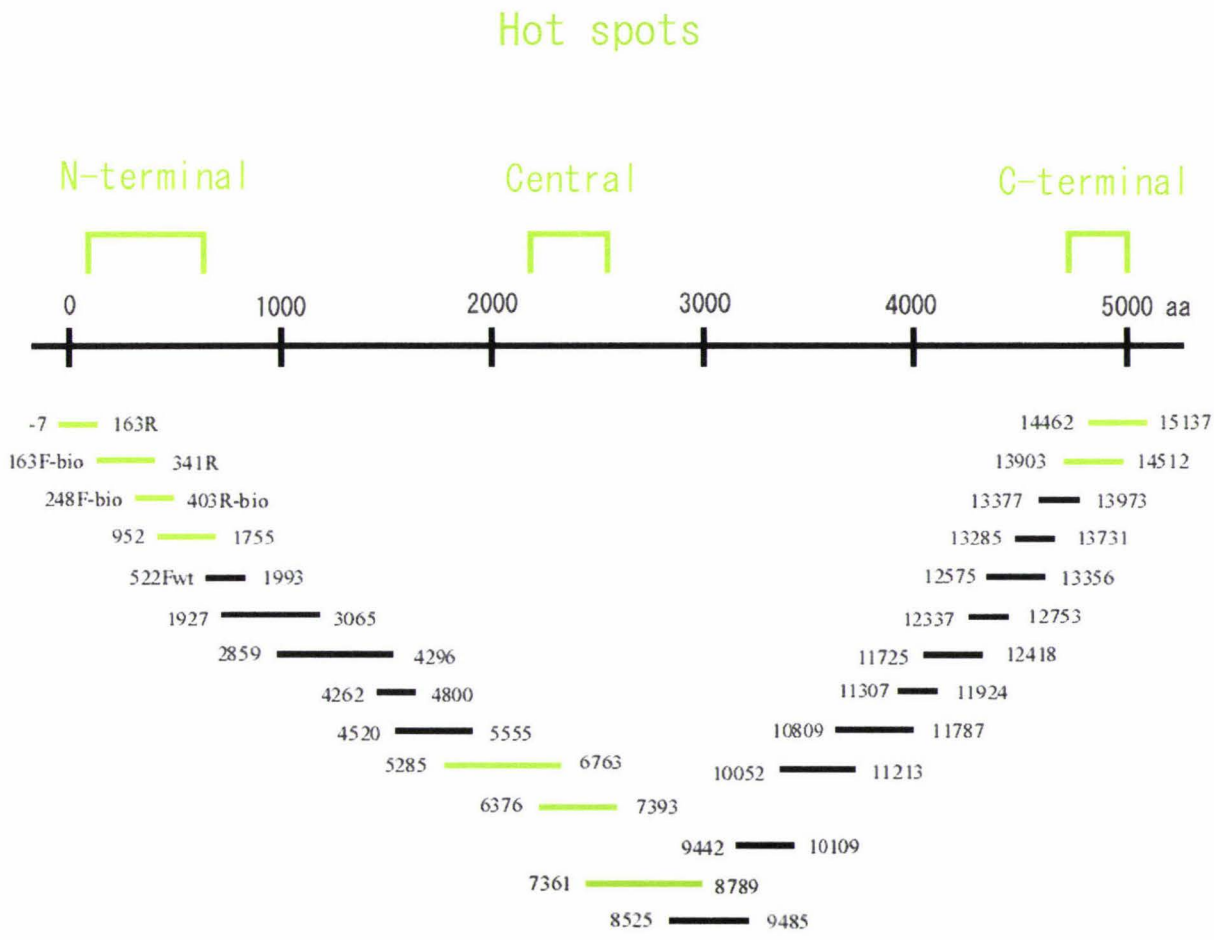

Figure 3-4 Strategy for the amplification of *RYR1* cDNA

24 DNA fragments in total were amplified. A black line at the top represents *RYR1* cDNA, and lower lines indicate the fragments amplified by each PCR reaction. Names of the forward and reverse primers are given. *RYR1* mutations identified to date are clustered on three regions; N-terminal, Central or C-terminal hot spots, as shown in green. The green lines represent the PCR fragments covering these hot spots.

Forward primers	Reverse primers	Product size (bp)	Annealing temperature (°C)	RT priming	Sequencing primers employed
-7	163R	546	60	dT	163R-seq
163F-bio	341R	629	59	dT	163F-bio, 248R-seq
248F-bio	403R-bio	523	61	dT	1204
952	1755	824	59	dT	522R-bio
522Fwt	1993	567	60	RH	522Fwt
1927	3065	1159	59	dT	2447, 2536
2859	4296	1441	55	RH	2859,3277, 3880, 4296
4262	4800	559	58	RH	4800
4520	5555	1056	60	RH	4766, 5137, 5430
5285	6763	1499	62	RH	5285, 5880
6376	7393	1038	65	dT	7039, 7393
7361	8789	1449	57	RH	7699, 8025, 8582
8525	9485	980	57	dT	9022, 9485
9442	10109	687	61	dT	9696, 9769
10052	11213	1196	53	RH	10884
10809	11787	999	60	RH	10809
11307	11924	637	56	RH	11307
11725	12418	713	56	RH	11725
12337	12753	434	60	RH	12753
12575	13356	803	58	dT	13356
13285	13731	467	58	RH	13731
13377	13973	606	59	RH	13377
13903	14512	630	59	RH	14512
14462	15137	782	60	dT	15137

Table 3-2 PCR and sequencing primers for screening of *RYR1* cDNA

RYR1 cDNA was synthesised by RT using random hexamers (RH) or oligo(dT) (dT) for primers. cDNA was amplified by PCR using PCR primers at their specific annealing temperatures. PCR products were checked by gel electrophoresis, purified, and directly sequenced using an automated DNA analyser using specific sequencing primers.

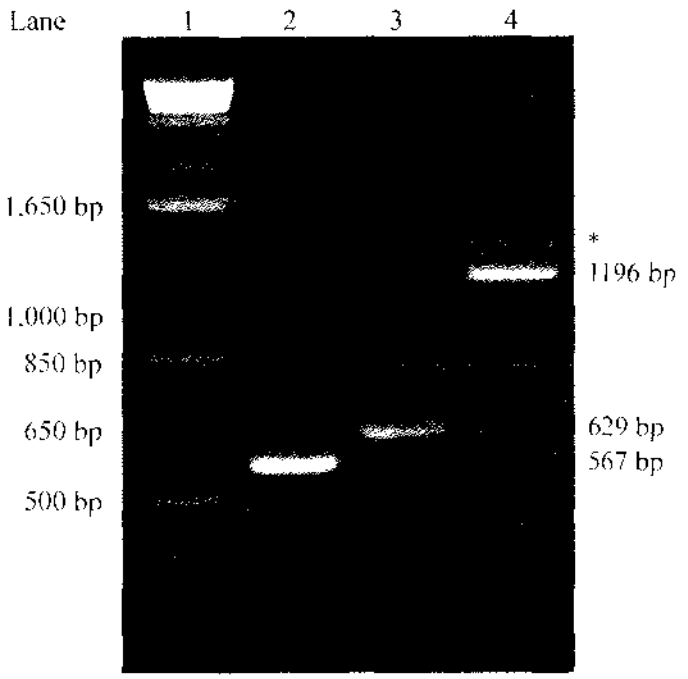

Figure 3-5 PCR products for *RYR1* screening

Example of PCR products checked by electrophoresis for their quality and specificity before direct screening. A single band was observed for some PCR products (lane 2 and 3), but unspecific bands were observed for other products (lane 4, asterisk) requiring gel excision for the purification step. Samples were electrophoresed on a 2% agarose gel for 1 hour at 100 V. 1× TBE was used for a running buffer. The gel was stained in 100 mL 1× TBE containing 20 µg of ethidium bromide for 1 hour, followed by the wash with 1 mM $MgSO_4$ for 30 minutes.

Lane	1	10 µL of 1 kb DNA ladder
	2	567 bp fragment (522Fwt-1993 primer set)
	3	629 bp fragment (163F-bio-341R primer set)
	4	1196 bp fragment (10052-11213 primer set)

Amplified DNA fragments were purified from PCR samples directly or from the gel after electrophoresis using the QIAGEN kit. Purified fragments were estimated for their concentration on an agarose gel with DNA quantitation standards. 2-20 ng of DNA was used for direct screening by automated sequencing. Sequencing data indicated that the M818 patient contained no mutations within *RYR1*, although eight polymorphisms, which do not introduce amino acid changes, were identified within the gene (Table 3-3).

Three of the eight were novel polymorphisms first observed in the patient M818 (129). Two of the eight were heterozygous and the others were homozygous. An example of the detection of polymorphisms is shown in Figure 3-6. The position of polymorphisms found from M818 is shown in Figure 3-7.

Exon	Nucleotide change	Amino acid	Homo/heterozygous
7	G549A	Leu198	Homo
8	T648C	Gly216	Hetero
11	C1077T	Ala359	Homo
15	G1668A	Ser556	Homo
19	T2286C	Pro762	Homo
24	A2943G	Thr981	Homo
24	C3018T	Tyr1006	Hetero
39	C6463T	Leu2155	Homo

Table 3-3 Polymorphisms found from *RYR1* cDNA of M818

M818 cDNA was amplified by PCR and directly sequenced. No mutations were identified, but eight polymorphisms were found in total. Three novel polymorphisms are described in red.

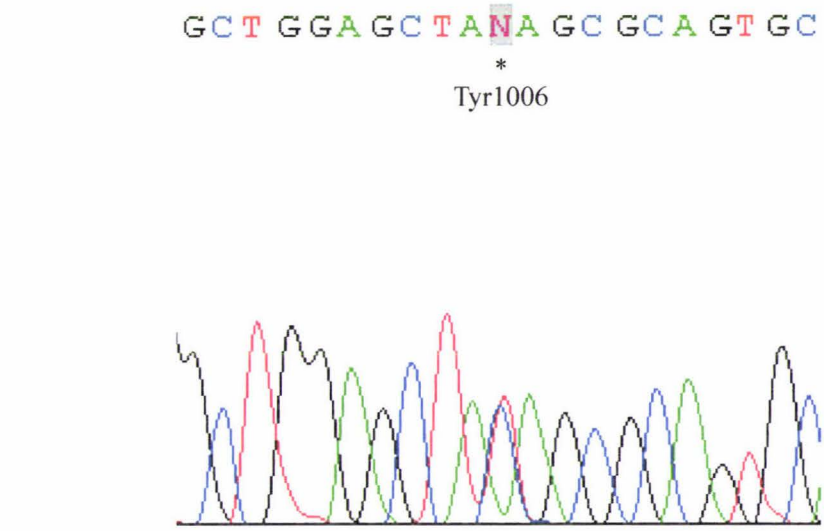

Figure 3-6 Detection of the Tyr1006 polymorphism

M818 cDNA was amplified by PCR using 1927/3065 primers, and the fragment was sequenced using the 2447 primer as the sequencing primer. The sequencing data was viewed by using Chromas version 1.45 (downloaded from Technelysium http://www.technelysium.com.au/index.html). As the Tyr1006 polymorphism was heterozygous, two peaks of C and T with the same height were observed.

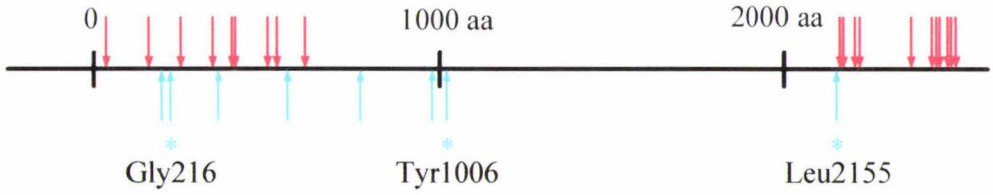

Figure 3-7 The position of polymorphisms found in M818 cDNA

The sequence of *RYR1* is represented as a black line. Selected reported mutations at the time are indicated with red arrows. Polymorphisms found in the M818 patient are indicated with cyan arrows below. All eight polymorphisms are clustered in the region between N-terminal and central hot spots. Three novel polymorphisms are highlighted with an * and their names.

Sequencing of the entire *RYR1* cDNA also identified an amino acid change, A1832G (Figure 3-8). This procedure was performed several times using different primers and cDNA templates, but the results were identical. This change, however is homozygous, and glycine has a similar structure to alanine, so this change is unlikely to introduce a significant effect on RYR function. In addition, glycine at this position is highly conserved through a wide range of species including *RYR1* isoforms *RYR2* and *RYR3* (Figure 3-9), hence it is unlikely that only human *RYR1* has alanine at this position. This amino acid change is not a mutation causative of MH, but a sequencing error of the sequence in GenBank as previously reported (150). Accession numbers of sequences in Figure 3-9 are: human *RYR1*; NM_000540, pig *RYR1*; P16960, rabbit *RYR1*; P11716, mouse *RYR1*; AAP29981, fish *RYR1*; AAB58117, bullfrog *RYRα*; A54161, *c.elegans RYR1*; NP_504753, human *RYR2*; NP_001026, rabbit *RYR2*; P30957, mouse *RYR2*; NP_076994, human *RYR3*; NP_001027, mink *RYR3*; CAA69029, chicken *RYR3*; S66572, *Drosophila RYR*; NP_476994.

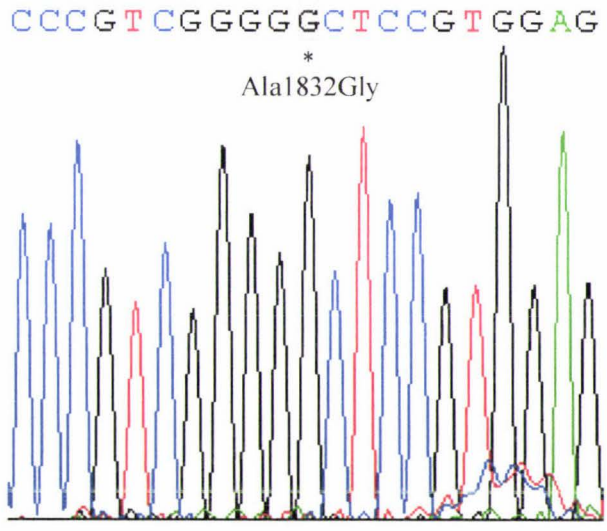

Figure 3-8 Detection of the sequencing error A1832G

A 1499-bp fragment was amplified using 5285/6763 primers, and sequenced using the 5285 primer. Only the G signal was detected instead of C.

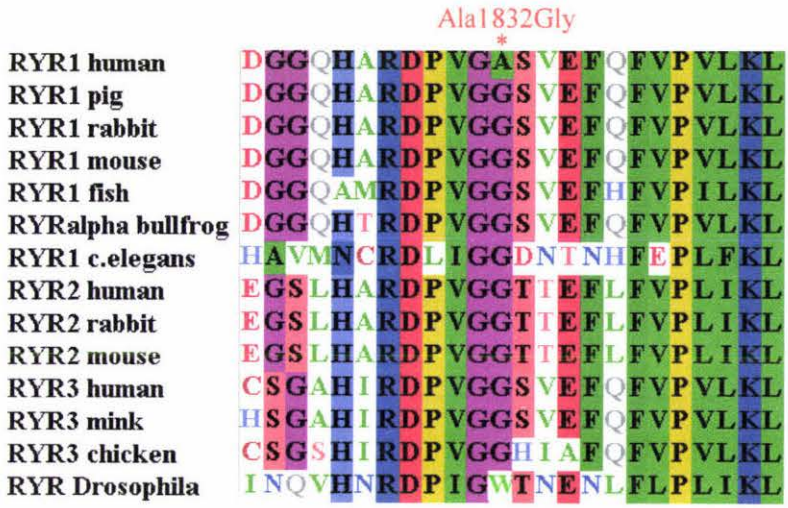

Figure 3-9 Alignment of sequences from several species

Sequences of RYR from major species were aligned using CLUSTAL W. Conservative positions with the same or similar amino acids are highlighted with coloured bars. The amino acid at the position of 1832 is glycine for most species except Drosophila. Ala1832Gly found from M818 *RYR1* is not a causative mutation, but a sequencing error.

3.4 Chapter summary

The M818 patient with no family history of MH died of exercise-induced MH. The patient's cDNA was synthesised from total RNA extracted from skeletal muscle. The entire coding region of *RYR1* was screened by PCR followed by direct DNA sequencing. After the analysis however, no mutations were found within *RYR1*, although eight polymorphisms were identified. This indicates that the direct sequencing approach was robust enough to detect sequence variations. There was no evidence of any splice site mutations as the cDNA sequence obtained was able to be aligned with the published sequence with no gaps (see Appendix 2). A restriction fragment polymorphism within *CACNA1S* was also screened, however the result of restriction endonuclease digestion indicated an absence of either of the mutations at this site. It is possible that an alternative mutation exists within the *CACNA1S* gene but as no other *CACNA1S* mutations have been identified, it was not considered worthwhile to continue with sequencing the cDNA representing this gene (72.51 kb). As there was no family history

of MH for proband M818, there were no samples or information available making linkage analysis possible. Therefore, the cause of MH in this individual remains unknown and further investigation has been postponed until such time as more information about the family is obtained.

CHAPTER FOUR : A GENOME-WIDE SCAN

4.1 Introduction

4.1.1 Basics of linkage analysis

Linkage analysis is a technique used to search a candidate locus related to a phenotype using genetic linkage, which is an exception of Mendel's law (law of independent assortment). All chromosomes come in pairs, one inherited from each parent. These maternal and paternal alleles contain the same genes in the same order, but the sequences are not identical. Two alleles are often mixed by recombination during meiosis, and one of two mixed chromosomes is transferred to an offspring (Figure 4-1). It is normally easy to find out whether a particular sequence comes from mother or father because these two sequences are not usually identical, especially at marker loci. The exception is where marker loci are identical in which case the markers are classed as non-informative.

Genetic markers are DNA sequences that show polymorphisms within a population. They are present in every chromosome and can be typed using techniques including PCR. In Figure 4-1, if A is a disease gene and B and C are genetic markers, recombination is likely to occur much more frequently between A and C than between A and B because markers A and B are close together. This allows the disease gene to be mapped relative to the markers B and C. If a marker is far from the disease gene, there is a good chance that recombination will occur between the marker and the gene and maternal and paternal alleles will be mixed up (A and C). In contrast, if two sequences are very close together, they will recombine only rarely. These alleles will tend to stay together (A and B). Therefore, by detecting the markers and analysing the movement of the markers (by recombination) in a family, marker loci that tend to associate with candidate loci can be linked with a disorder. Thus genotype can be linked with phenotype and particular genes within a defined chromosomal locus can be termed candidate genes.

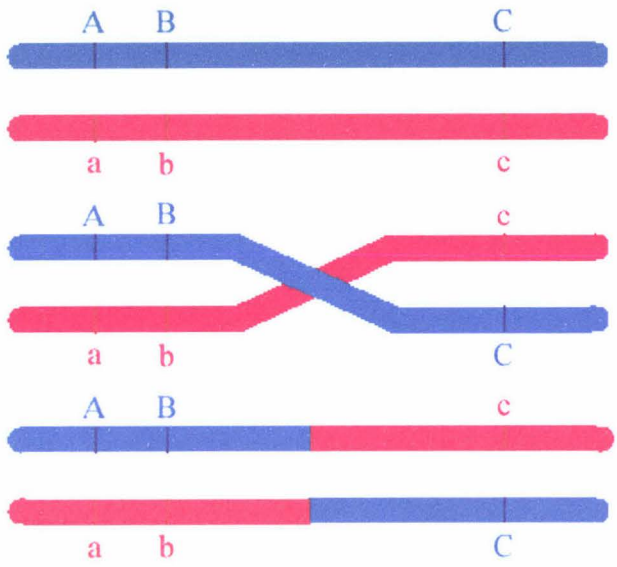

Figure 4-1 Principle of linkage analysis

Each chromosome is inherited from mother (red) or father (blue) (top). Crossingover often occurs during meiosis (middle), and as a result, two chromosomes are mixed with each other (bottom). After recombination and meiosis, one mixed chromosome is transferred to an offspring. Three DNA sequences are shown, labelled A, B and C. The capital letters represent the paternal alleles and the lower case letters represent the maternal alleles. The allele A tends to stay together with the allele B rather than the allele C because B is closer and recombination rarely occurs between A and B.

Commonly used types of DNA markers are restriction fragment length polymorphisms (RFLP), variable number of tandem repeat polymorphisms (VNTR), and microsatellite polymorphisms that were used in this project. The microsatellite marker has been widely used to date, especially for a genome-wide scan for linkage analysis. This type of marker is highly informative because alleles can be determined reliably, and there are large numbers of alleles at specific loci. Allele frequency is known for specific populations for many microsatellite markers providing additional power to the linkage analysis.

A genome-wide scan is a technique to carry out linkage analysis for the entire genome. It requires analysing several hundreds of marker loci in ~20 cM intervals (cM; a centimorgan is equivalent to 1% recombination between two loci and corresponds to

~1×10^6 base pairs of DNA in humans). This is a powerful approach for searching for disease genes when there is no information about candidate genes. A genome-wide scan can allow identification of candidate loci from the entire genome and eliminate other unrelated regions. It has been used widely to date for studies of multiallelic genetic disorders or common diseases, such as diabetes, schizophrenia and asthma (139, 151).

4.1.2 Parametric and non-parametric linkage analysis

Linkage analysis can be divided into two groups, parametric and non-parametric linkage analysis. In linkage analysis, "parametric" means to estimate parameters describing the disease, such as the mode or model of inheritance and the penetrance values. Parametric linkage analysis is more widely used and powerful with a small number of samples rather than non-parametric linkage (NPL) analysis. It is useful to perform parametric linkage analysis if the disease is caused by only one gene, or if there is only one gene which largely contributes to the existence or absence of the disorder. If the parameters are not correct, it is not powerful and false results can be produced. If the penetrance values are incorrect, powerful analysis cannot be performed even if there is only one disease gene. Hence, if the disorder is heterogeneous or parameters are unknown as is the case for many common diseases, NPL analysis is performed instead of parametric analysis. Parameters for the disease are not required for NPL analysis. The mode of inheritance, penetrance values or genetic heterogeneity does not affect the analysis. It is not as powerful as parametric analysis however, with small numbers of samples.

Many linkage studies have been performed for MH to date, and these studies always adopted parametric analysis because the mode of inheritance is well known (autosomal dominant). A penetrance value has been estimated as nearly 1.0 which means that all individuals with the trait show the disease status, and this estimation allowed accurate parametric linkage analysis leading to identification of candidate genes and loci including *RYR1* (100, 101). One paper has reported a genome-wide scan for MH by parametric analysis followed by identification of *CACNA1S* as another candidate gene (116, 124). MH is a heterogeneous disorder, however, and several genes may be involved in MH susceptibility for some individuals (120). A penetrance value can be estimated as nearly 1.0 for some genes including *RYR1* and *CACNA1S* because these genes are expressed dominantly in skeletal muscle, but other genes may have different

penetrance values depending on expression level or contribution to the existence of the disorder. In cases such as these parametric analysis may not be powerful enough to identify candidate loci with several genes involved and wrong penetrance values estimated.

Therefore, non-parametric linkage analysis was adopted in this project for a family which has discordance between the MHS phenotype and *RYR1* mutation genotype. Some MHS family members do not have a *RYR1* mutation which was identified from other MHS members in the same kindred. This observation indicates that there is more than one gene involved in MH in this family and hence non-parametric linkage analysis may be more suitable for this family than parametric analysis because non-parametric analysis is still powerful with several disease genes with unknown penetrance values.

4.1.3 Programmes for linkage analysis

Dedicated software is required to facilitate linkage analysis. There are many programmes available for linkage analysis that are based on different algorithms (Table 4-1). Most programmes are not supported by Windows, but require DOS or UNIX operating systems. In addition, large pedigrees or many markers significantly increase the time for calculation (Table 4-2). Hence, a PC with high computing power running UNIX OS or MS-DOS is needed for analysis.

The most widely used software is LINKAGE (FASTLINK) for parametric analysis and GENEHUNTER for non-parametric analysis. GENEHUNTER is especially used for a genome-wide scan because this technique is used to search candidate loci from the entire genome and in this case information of the disorder (how many genes involved or their penetrance values) is normally not available before the analysis. GENEHUNTER is known as powerful non-parametric software, but it can also carry out parametric analysis although its parametric analysis is not considered as powerful as that of LINKAGE or FASTLINK. In this project, non-parametric analysis may be more suitable than parametric analysis using FASTLINK, and hence GENEHUNTER was used for non-parametric linkage analysis also performing parametric analysis at the same time.

Algorithm	Programme	Solution	Size restriction
Elston-Stewart	LINKAGE FASTLINK MENDEL VITESSE	exact	~8 loci, less with loops (larger for VITESSE)
Lander-Green	CRI-MAP GENEHUNTER MENDEL	exact	~20 people ($2n - f \leq 20$)
Markov chain Monte Carlo	PANGAEA SimWalk2	estimate	much larger (>1000 individuals, >30 loci)

Table 4-1 Algorithms and restrictions of linkage analysis programmes

Each programme is based on different algorithms and has some restrictions. The Elston-Stewart algorithm can handle only up to 8 marker loci for one analysis, and Lander-Green can handle unlimited marker loci, but cannot analyse large pedigrees. The n and f indicate the number of non-founders and founders, respectively. Markov chain Monte Carlo can analyse huge amounts of data, although this algorithm computes with estimate solutions.

	Increase in computation time with increase in:		
Algorithm	**people**	**markers**	**missing data**
Elston-Stewart	linear	exponential	severe (modest for VITESSE)
Lander-Green	exponential	linear	modest
Markov chain Monte Carlo	linear	linear	mild

Table 4-2 Factors influencing computation time

Computation time increases according to the amount of data depending on the algorithms of the programmes. The Markov chain Monte Carlo is influenced the least on an increase in amount of data.

4.1.4 LOD and NPL scores

Programmes for linkage analysis produce several values after analysis as output data including LOD or NPL scores, p-values and information content. In these output values, LOD or NPL scores are most valuable to estimate linkages on the loci analysed. The LOD score, so-called in parametric linkage analysis, is the logarithm (base 10) of the ratio of the likelihood of the observed genotypes compared with the likelihood under non-linkage. Programmes calculate highest LOD scores between the two marker loci in the range of recombination fraction (θ) from 0.0-0.5. Recombination fraction of 0.0 means that the two marker loci are exactly same (no recombination), and 0.5 means no linkage between the loci (free recombination). It cannot be over 0.5 because if the two marker loci are far enough apart, recombination occurs twice returning to the same loci. Traditionally, a LOD of 3 or more is taken as significant linkage (152). If significant linkage is on a specific marker locus, disease genes should be nearby.

The equivalent value in non-parametric linkage analysis is known as NPL scores. The calculation process is not the same as for parametric analysis for LOD scores, and each algorithm has a different calculation process. Values of 3.5 or over for NPL scores are considered as significant linkage (152). The criteria are still controversial because each algorithm has a different calculation process and solution, and it is not known which algorithm is most powerful. The criteria may be needed to be determined for each algorithm and parametric and non-parametric analyses.

4.1.5 The CH family

To date, at least 40 families have been identified as MHS in New Zealand. One of the largest families is a Maori family, known as the CH family. The CH family has over 1,400 documented individuals in total, and a T4826I mutation has been identified within *RYR1* in this family (113). The mutation clearly co-segregates with phenotype and all individuals who have this mutation show strong MH susceptibility by the IVCT. 22 discordances between MH susceptibility and phenotype, however has also been found in this family (113). Some MHS individuals were diagnosed as MHS by the IVCT, but did not have the T4826I mutation. MH is known to be heterogeneous and other genes have been linked to the disorder. Linkage to chromosome 1 at the *CACNA1S* locus was

studied in a discordant branch of the CH family (153). While this was incomplete, the results suggested that the *CACNA1S* locus was not implicated in MHS in this family.

The IVCT is not 100% specific and can produce false diagnoses, but discordance occurs much more frequently in the CH family than the probability of false diagnoses of the IVCT. Therefore, it is possible that other genes are responsible for MH susceptibility in this family. It is still not clear, however which other genes are associated with MH, even though five candidate loci have been reported. A genome-wide scan for MH has not been performed in New Zealand to date and therefore analysis of the entire genome and a search for novel candidate loci in New Zealand families was appropriate approach. The CH family is large and has significant numbers of discordant MHS patients without the T4826I mutation or linkage to *RYR1*, chromosome 19q, so this family is an ideal population for a genome-wide scan to identify other candidate loci associated with MH.

26 individuals were selected for the genome-wide scan. 16 were MHS individuals who did not have the T4826I mutation, 2 were MHS patients containing the mutation, 2 were MHE without the mutation, 1 was MHN, and others had not been diagnosed by the IVCT. As the family was large and complicated, the analysis was performed in the three branches separately: the EA, ES and TAME branches (Figure 4-2). Each branch had a common ancestor and consisted of individuals who were both MHS with and without the mutation.

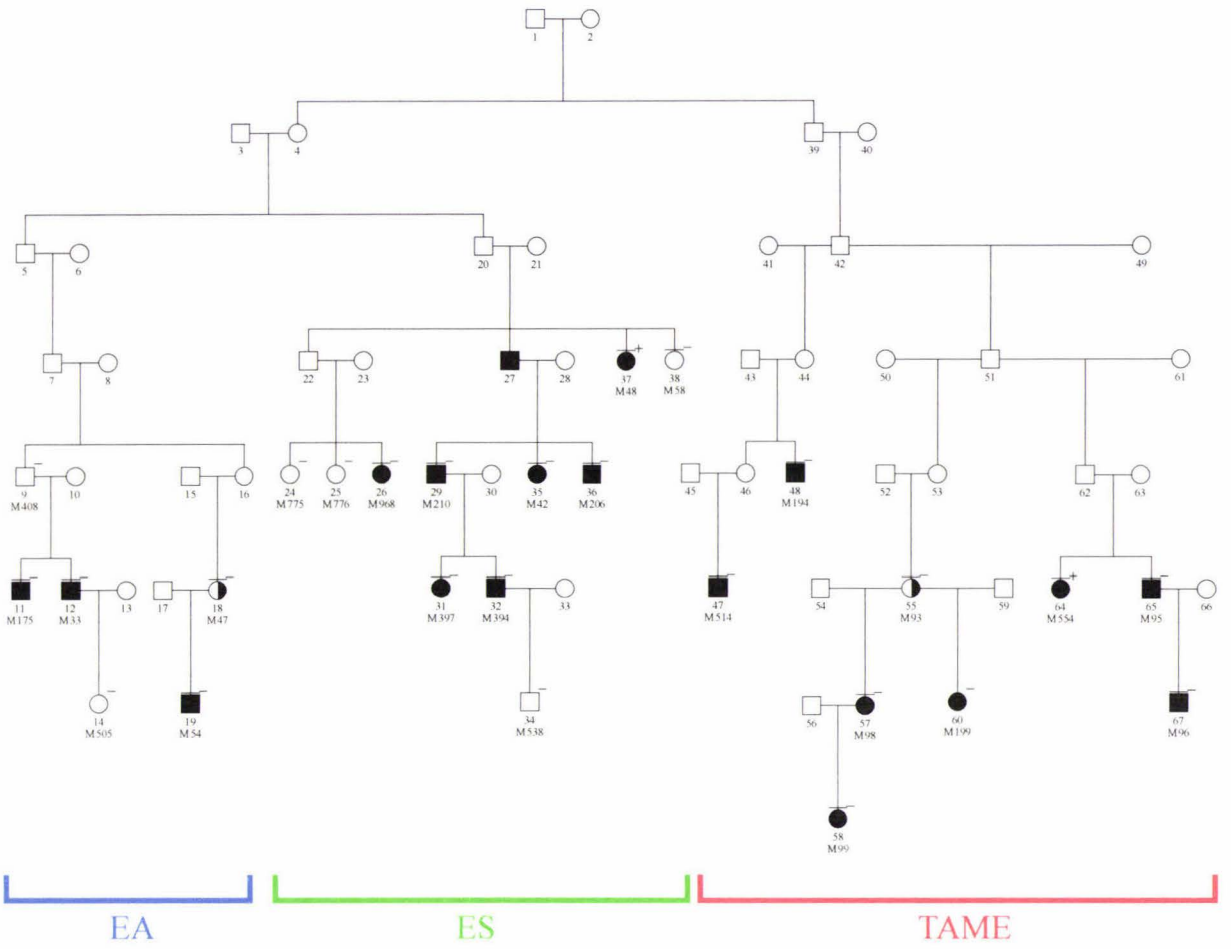

Figure 4-2 The CH family members selected for the genome-wide scan

Analysis was performed for the EA (blue), ES (green) and TAME (red) branches separately. The closed symbols indicate MHS individuals and half-closed symbols represent MHE. A bar on the top of the symbol means the IVCT tested, so an open symbol with the bar indicates the MHN patients and open symbols without the bar indicate the unknown individuals who have not been diagnosed by the IVCT. The + and – represent the presence and absence of the T4826I mutation, respectively. All individuals are identified with an ID number used for the input data of GENEHUNTER, and the 26 individuals selected for the genome-wide scan are also identified with a DNA number (M number).

4.2 A genome-wide scan

4.2.1 Preparation of samples and input data

Genomic DNA was extracted from whole blood samples of the selected 26 individuals. Integrity of the DNA was checked by gel electrophoresis. An example of the DNA check was described previously (see section 3.2, Figure 3-1). DNA samples were quantified by using UV spectrophotometry and real-time quantitative PCR to estimate concentrations. A standard curve for LightCycler quantification was created using the LightCycler-Control Kit DNA (Figure 4-3) which uses the β-globin gene as a target. Unknown DNA samples were amplified with the same primers and quantified using the standard curve created (Figure 4-4). Melting curve analysis determined the specificity of PCR products amplified (Figure 4-5). This step was always required because SYBR Green binds to all double-stranded DNA fragment including specific and non-specific products. The $A_{260/280}$ ratios and estimated concentrations are listed in Table 4-3.

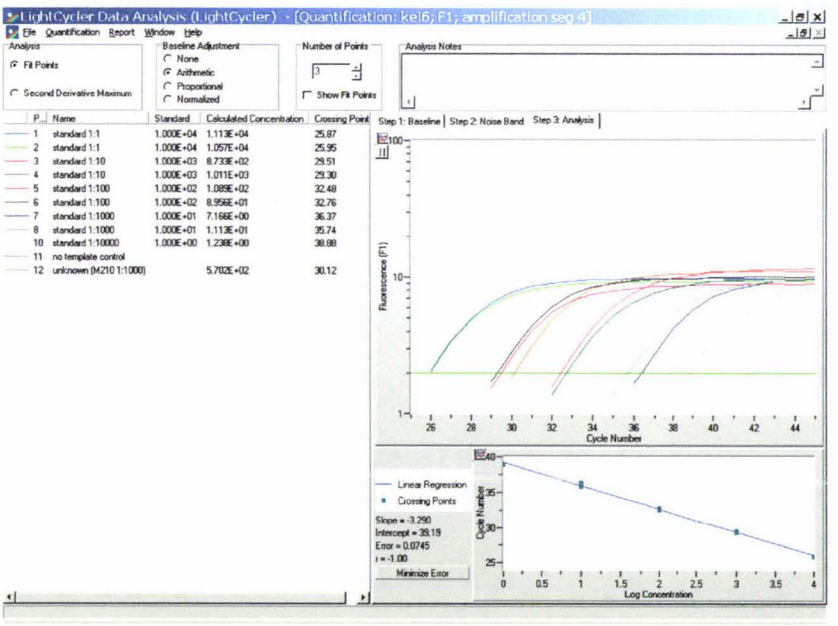

Figure 4-3 A standard curve used for real-time quantification PCR

A standard curve was created using several DNA samples in stepwise known concentrations (1.5 pg/μL to 15ng/μL). The created standard curve (right bottom) was used for quantification of all 26 individuals.

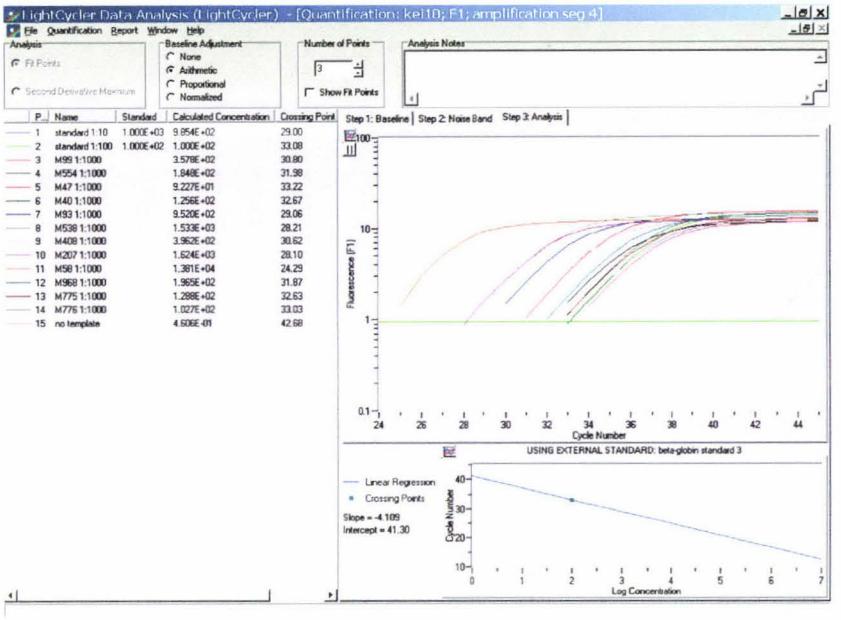

Figure 4-4 DNA quantification using a standard curve

LightCycler Software imports the standard curve previously created, and automatically calculates the concentrations of unknown DNA samples by a crossing point on the standard curve. Each reaction contained negative control (pink, no template).

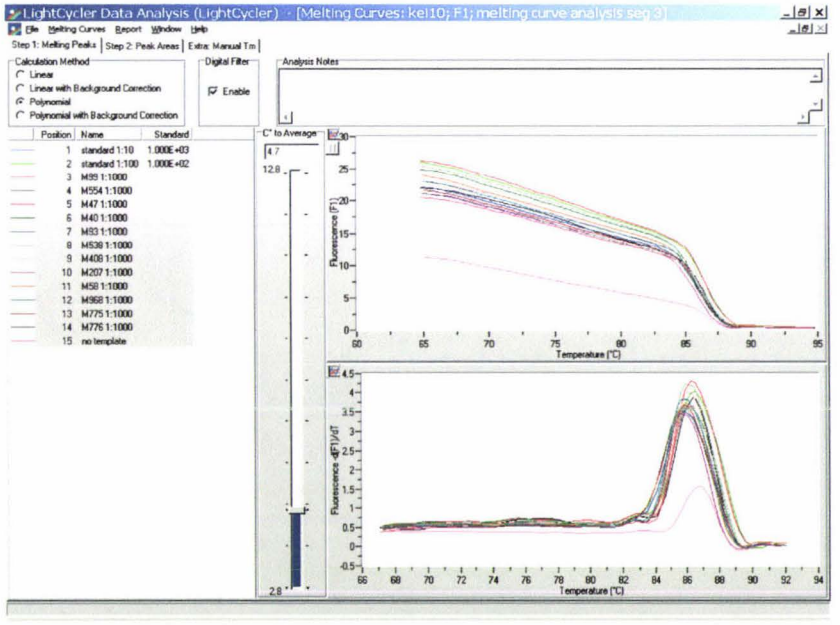

Figure 4-5 Melting curve analysis

The single peak (86-87°C) on this analysis indicates the specific PCR product and reliability of DNA quantification. The negative control (pink) is also included.

ID	DNA number	$A_{260/280}$	Conc. (A_{260})	Conc.	Average
9	M408	1.84	443	574	509
11	M175	1.88	284	199	242
12	M33	1.90	123	155	139
14	M505	1.80	205	210	208
18	M47	1.47	171	132	152
19	M54	1.85	256	158	207
24	M775	1.84	319	185	252
25	M776	1.88	157	157	157
26	M968	1.81	173	307	240
29	M210	1.85	1026	923	975
31	M397	1.87	506	334	420
32	M394	1.82	348	301	325
34	M538	1.90	423	608	516
35	M42	1.82	1425	1079	1252
36	M206	1.65	2623	2885	2754
37	M48	1.74	431	275	353
38	M58	1.92	80	215	148
47	M514	1.88	185	233	209
48	M194	1.89	165	121	143
55	M93	1.64	708	1038	873
57	M98	1.80	123	280	202
58	M99	1.78	240	565	403
60	M199	1.85	1885	2282	2084
64	M554	1.80	188	261	225
65	M95	1.90	275	418	347
67	M96	1.84	345	612	479

Table 4-3 The $A_{260/280}$ ratios and concentrations of 26 individuals

Quantification was performed by spectrophotometer and LightCycler, and final concentrations were estimated. The unit of concentration is ng/μL.

150 µL of 100 ng/µL dilution samples were prepared for each quantified DNA sample and they were sent to the Australian Genome Research Facility for PCR and genotyping using 400 microsatellite marker loci. Information of all microsatellite markers are listed in Appendix 3. Genotypes were analysed twice. If a sample failed, it was repeated once. All genotyping data was returned in excel spread sheets (Table 4-4).

Sample	Marker	Allele 1	Allele 2	Allele 1	Allele 2
M175	D1S2667	134	144	133.3	143.88
M194	D1S2667	136	140	135.4	139.5
M199	D1S2667	134	140	133.42	139.49
M206	D1S2667	148	150	148.18	150.31
M210	D1S2667	148	150	148.07	150.15
M33	D1S2667	Failed	Failed	Failed	Failed
M394	D1S2667	142	150	141.69	150.16
M397	D1S2667	142	150	141.61	150.15
M408	D1S2667	134	142	133.39	141.52
M42	D1S2667	148	150	148.08	150.3
M47	D1S2667	138	140	137.5	139.5
M48	D1S2667	148	148	148.21	148.21
M505	D1S2667	142	148	141.45	148.08
M514	D1S2667	138	142	137.18	141.53
M538	D1S2667	142	148	141.45	147.91
M54	D1S2667	138	138	137.32	137.32
M554	D1S2667	144	148	143.63	147.88
M58	D1S2667	148	148	148.07	148.07
M775	D1S2667	148	148	148.07	148.07
M776	D1S2667	148	148	148.18	148.18
M93	D1S2667	134	152	133.39	152.32
M95	D1S2667	144	148	143.56	147.91
M96	D1S2667	144	144	143.62	143.62
M968	D1S2667	134	148	133.36	148.05
M98	D1S2667	152	152	152.08	152.08
M99	D1S2667	140	152	139.16	151.98

Table 4-4 An example of genotyping data

The genotyping data were provided in a excel file. This table shows an example of data for one microsatellite marker (D1S2667). The software detects the exact fragment length (bp) of PCR products (decimal) and automatically estimates genotypes (integer). The analysis was repeated once if it failed, and if both analyses were not successful, the genotype was described as "Failed" and haplotype was determined as 0 (unknown).

The data provided were arranged by chromosome and marker location. Haplotypes were determined according to genotypes and allele frequencies were calculated for each marker (Table 4-5).

Allele (bp)	Haplotype	Allele frequency
134	1	0.1
136	2	0.02
138	3	0.08
140	4	0.08
142	5	0.12
144	6	0.1
148	7	0.32
150	8	0.1
152	9	0.08

Table 4-5 An example of haplotype and allele frequency

This table shows haplotype and allele frequency of the D1S2667 marker calculated from the provided data (Table 4-4). Haplotype was determined according to the fragment length, and allele frequency was calculated depending on the frequency in the CH family.

All data including haplotype, number of alleles and allele frequency were collected and described in a text file for input data as in the following example:

```
32 0 0 5
0  0.0  0.0  0
1 2 3 4 5 6 7 8 9 10 11 12 13 14 15 16 17 18 19 20 21 22 23 24 25 26 27
28 29 30 31 32
1  2
0.990000 0.010000
1
0.001000 0.999000 0.999000
3  6 # D1S468
0.346153846 0.057692307 0.192307692 0.057692307 0.153846153 0.192307692
3  5 # D1S214
0.307692307 0.019230769 0.269230769 0.192307692 0.211538461
3  7 # D1S450
0.115384615 0.403846153 0.192307692 0.076923076 0.096153846 0.019230769
0.096153846
3  9 # D1S2667
0.1 0.02 0.08 0.08 0.12 0.1 0.32 0.1 0.08
3  5 # D1S2697
0.076923076 0.634615384 0.173076923 0.096153846 0.019230769
.
.
.
3 3
0.160 0.104 0.063 0.040 0.138 0.078 0.089 0.105 0.115 0.101 0.097 0.114
0.088 0.123 0.077 0.114 0.061 0.056 0.132 0.078 0.047 0.101 0.102 0.099
0.183 0.169 0.089 0.010 0.136 0.076 0.138
1 0.05 0.5
```

The above example shows partial data of the datafile of chromosome 1. 5 of 32 microsatellite markers are shown in this example. The datafile contains information about allele order on the top, marker name, number of alleles and allele frequency in the middle and distance between each marker at the end. Family information and haplotype was described in the prefile as follows:

```
CHEA  7   0   0   1  0   0 0  0 0  0 0  0 0  0 0 ...
CHEA  8   0   0   2  0   0 0  0 0  0 0  0 0  0 0 ...
CHEA  9   7   8   1  0   1 1  3 5  1 7  1 5  2 2 ...
CHEA  10  0   0   2  0   0 0  0 0  0 0  0 0  0 0 ...
CHEA  11  9   10  1  2   1 1  1 5  1 7  1 6  2 2 ...
CHEA  12  9   10  1  2   1 1  1 3  7 7  0 0  2 2 ...
CHEA  13  0   0   2  0   0 0  0 0  0 0  0 0  0 0 ...
CHEA  14  12  13  2  0   1 6  3 3  2 7  5 7  2 2 ...
CHEA  15  0   0   1  0   0 0  0 0  0 0  0 0  0 0 ...
CHEA  16  7   8   2  0   0 0  0 0  0 0  0 0  0 0 ...
CHEA  17  0   0   1  0   0 0  0 0  0 0  0 0  0 0 ...
CHEA  18  15  16  2  2   1 1  3 4  5 6  3 4  1 2 ...
CHEA  19  17  18  1  2   1 3  3 4  2 5  3 3  1 2 ...
```

The above example shows the partial prefile of the CHEA family for chromosome 1. The haplotype is shown for 5 of 32 markers used for this chromosome. The prefile contains family name, ID number, family information and haplotype for each marker according to the order described in the datafile.

4.2.2 Data analysis

Data analysis was performed using GENEHUNTER and GENEHUNTER-PLUS (144, 145). GENEHUNTER is a powerful programme widely used for non-parametric linkage analysis. Non-parametric linkage analysis does not require estimating the penetrance of the disease, and can perform powerful analysis for heterogeneous disorders. It is well known that MH is autosomal dominant in humans, and a previous report using a parametric genome-wide scan with estimation of the penetrance for 1.0 has identified a mutation within *CACNA1S* (116).

In this project however, non-parametric linkage analysis was performed because MH is heterogeneous and several genes may be involved for the CH family. The penetrance of MH is not known assuming that the disorder is heterogeneous. GENEHUNTER is considered as a powerful non-parametric analysis programme, but it can also perform parametric linkage analysis. Hence, both parametric and non-parametric linkage analyses were performed for the EA, ES and TAME branches. The latest version of GENEHUNTER is 2.1 release 5. This version, however cannot perform analysis on sex chromosomes. GENEHUNTER-PLUS is a modified programme of GENEHUNTER

and can handle sex chromosomes. The latest version of this programme, however is 1.2, which is a modification of GENEHUNTER version 1.2. As GENEHUNTER-PLUS modified from version 2.1 of GENEHUNTER was not available, data analysis was performed using GENEHUNTER for autosomes, and GENEHUNTER-PLUS was used for the X chromosome even though candidate loci were not expected on the X chromosome as there is no evidence that MH is X-linked. The datafile was imported in to the software, and the prefile was screened for computation. Multipoint parametric and non-parametric linkage analysis was performed at the same time. Output data was provided in a text format as in the following example:

```
analyzing pedigree CHEA...
using non-originals:  9 11 12 16 18 19 14
position  LOD score    NPL score    p-value    information
 -10.00   -0.114055     0.032280    0.250000    0.078725
  -8.00   -0.130391     0.035335    0.250000    0.091834
  -6.00   -0.148896     0.038617    0.250000    0.107016
  -4.00   -0.169908     0.042120    0.250000    0.124595
  -2.00   -0.193839     0.045835    0.250000    0.144975
   0.00   -0.221207     0.049744    0.250000    0.168692
   2.33   -0.319311    -0.031047    0.437500    0.189127
   4.66   -0.431348    -0.111347    0.437500    0.218920
   7.00   -0.557603    -0.190405    0.500000    0.260247
   9.33   -0.694416    -0.267451    0.500000    0.317415
  11.66   -0.827529    -0.341730    0.500000    0.408818
  13.01   -0.827329    -0.368105    0.500000    0.404628
  14.35   -0.833182    -0.396116    0.500000    0.408726
  15.70   -0.843582    -0.425641    0.500000    0.419994
```

The above example shows a partial output data of the CHEA family on chromosome 1.

The output data contains LOD score for parametric linkage analysis, NPL score for non-parametric linkage analysis, p-value and information content. Most attention was paid to the NPL score because non-parametric linkage analysis may be more suitable in this project rather than parametric analysis due to heterogeneity of MH, and in fact, non-parametric analysis identified some linkage on several chromosomes whereas parametric analysis did not identify linkage on any chromosome from any branch. The

LOD scores for parametric analysis were under 2 for all chromosomes. Figure 4-6 shows the result of the genome-wide scan by multipoint non-parametric linkage analysis.

Figure 4-6 A genome-wide scan for the CH family

This figure shows the NPL scores (Z_{all}) on each chromosome for three CH branches: EA (blue), ES (green) and TAME (red). Multipoint non-parametric linkage analysis was carried out using GENEHUNTER (autosome) and GENEHUNTER-PLUS (chromosome X).

4.3 The EA branch

Six individuals were analysed from the EA branch. Detailed information for these

individuals is listed in Table 4-6. Five weak linkages were identified from this branch. These are on chromosome 1, 10, 16, 18 and 19. Output data of these chromosomes are shown in Appendix 4. NPL scores were 2-3 for each of these loci (Figure 4-7).

ID	DNA number	Sex	IVCT result (halothane/caffeine ,g)	T4826I mutation
9	M408	Male	Unknown	Negative
11	M175	Male	MHS (3.7/0.9)	Negative
12	M33	Male	MHS (1.5/0.2)	Negative
14	M505	Female	Unknown	Negative
18	M47	Female	MHE (0.3/0.1)	Negative
19	M54	Male	MHS (1.4/1.0)	Negative

Table 4-6 Status of individuals of the EA branch

Six individuals were selected from the EA branch for the genome-wide scan. 4 of 6 patients were tested by the IVCT and the results of both halothane and caffeine tests are shown. All individuals were previously screened for the T4826I mutation (all negative).

RYR1 is located on chromosome 19q and *CACNA1S* is on chromosome 1q, but neither is located at the candidate loci found from the EA family. Database searching was performed to identify any candidate genes located within the five loci, but no genes related to calcium homeostasis were identified except on chromosome 16. On chromosome 16, *CACNG3*, the γ-subunit of DHPR is close to the highest peak of the NPL scores (Figure 4-8). The γ-subunit of DHPR is believed to stabilise RYR to the closed state, and hence this gene may be associated with MH.

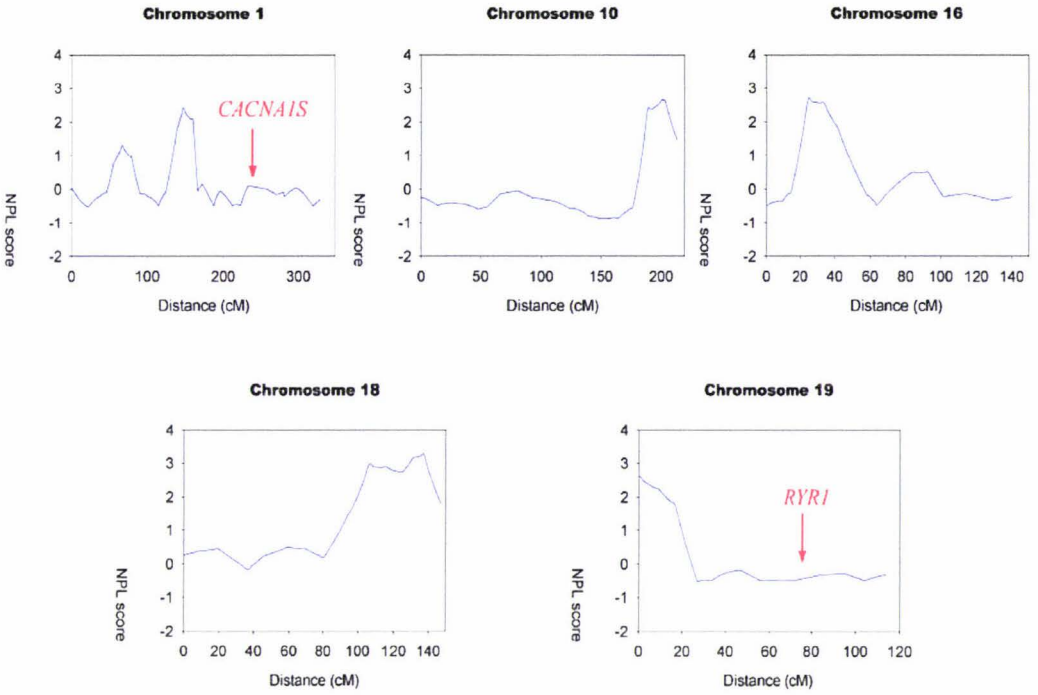

Figure 4-7 Candidate loci identified from the EA branch

Weak linkages (2-3 for NPL scores) were identified on five chromosomes, 1, 10, 16, 18 and 19. No candidate genes were found within these loci, however except on chromosome 16. Two genes which are known to be linked to MH, *CACNA1S* (chromosome 1) and *RYR1* (chromosome 19) are indicated in red arrows.

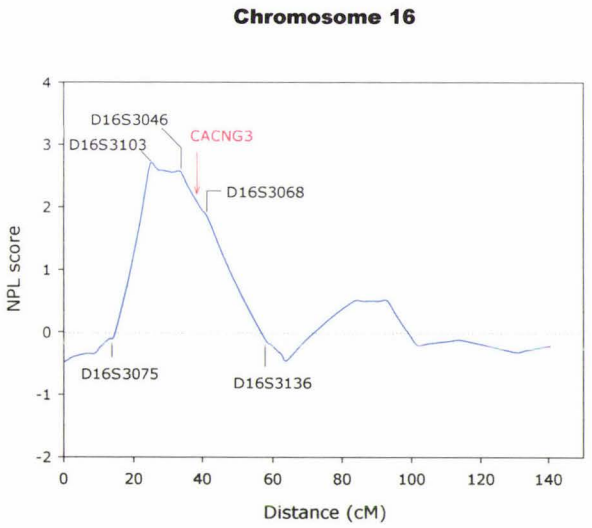

Figure 4-8 A candidate gene on chromosome 16

The *CACNG3* gene is located within the candidate locus identified on chromosome 16 in the EA branch. Microsatellite markers used are shown within the candidate locus.

4.4 The ES branch

Eleven individuals were selected for the analysis from the ES branch (Table 4-7). The analysis, however had to be performed excluding one individual because of the lack of computer memory. The sole MHN individual, M58 was eliminated because a negative sample is less significant for analysis than positive individuals. The analysis was also performed including the M58 individual instead of the M48 patient, and the result was not significantly different. Analyses were performed several times and it seemed to be most reliable to eliminate the M58 individual. After the analysis, two very strong linkages (7-8 for NPL scores) were identified on chromosome 6 and 12 (Figure 4-10). Appendix 4 also shows output data of the ES branch on these chromosomes. Candidate genes, however could not be found within these loci because they were too large to identify any one gene. There are also many genes of unknown function.

ID	DNA number	Sex	IVCT result (halothane/caffeine ,g)	T4826I mutation
24	M775	Female	Unknown	Negative
25	M776	Female	Unknown	Negative
26	M968	Female	MHS	Negative
29	M210	Male	MHS (1.5/0.5)	Negative
31	M397	Female	MHS (2.9/0.95)	Negative
32	M394	Male	MHS (1.7/0.6)	Negative
34	M538	Male	Unknown	Negative
35	M42	Female	MHS	Negative
36	M206	Male	MHS	Negative
37	M48	Female	MHS	Positive
38	M58	Female	MHN	Negative

Table 4-7 Status of individuals of the ES branch

Eleven individuals were analysed by the genome-wide scan although M58 was omitted for the analysis. The scores of the IVCT were not available for some patients because the diagnoses were established prior to the adoption of the European IVCT.

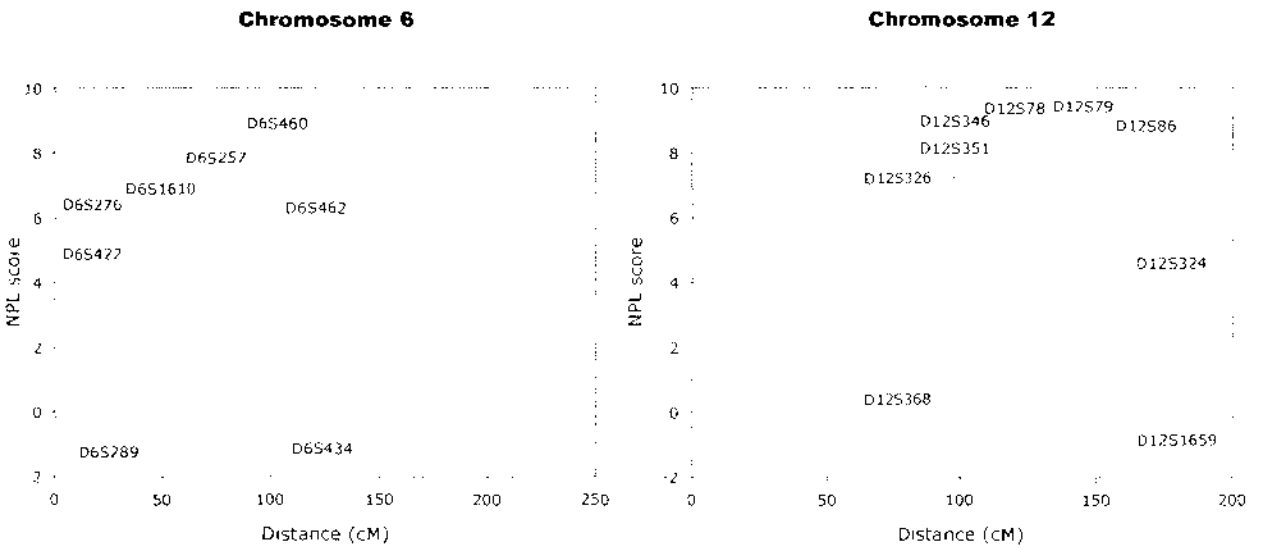

Figure 4-9 Candidate loci on chromosome 6 and 12

Two strong linkages were found on chromosome 6 and 12 from the ES branch, and the highest NPL scores were 7-8. The names of microsatellite markers are given. As these candidate loci are so large, candidate genes could not be identified.

4.5 The TAME branch

Nine individuals were used from the TAME branch, although this branch is quite complicated. Information of the individuals is shown Table 4-8. Oddly enough, no linkage was observed over the entire genome using both parametric and non-parametric analysis. All LOD scores and NPL scores were under 2.

ID	DNA number	Sex	IVCT result (halothane/caffeine ,g)	T4826I mutation
47	M514	Male	MHS (2.2/0.45)	Negative
48	M194	Male	MHS (1.3/0.2)	Negative
55	M93	Female	MHE (0.7/0.1)	Negative
57	M98	Female	MHS (1.7/1.0)	Negative
58	M99	Female	MHS (0.6/0.2)	Negative
60	M199	Female	MHS (0.4/0.2)	Negative
64	M554	Female	MHS (3.6/5.5)	Positive
65	M95	Male	MHS (1.7/0.7)	Negative
67	M96	Male	MHS (0.7/0.2)	Negative

Table 4-8 Status of individuals of the TAME branch

Nine individuals were selected from the TAME branch including the M554 individual who is MHS and has the T4826I mutation.

4.6 Chapter summary

A genome-wide scan was performed using 26 individuals from the CH family including MHS patients who do not contain the T4826I mutation. Parametric and non-parametric linkage analysis was performed for three branches of the CH family. No significant linkage was identified by parametric linkage analysis, but several weak and strong linkages were found by non-parametric analysis. Five weak linkages were identified in the EA branch, and the gene of the γ-subunit of DHPR is located at one of five candidate loci. Two strong linkages were found from the ES branch, but no candidate genes were identified because of the length of the loci. No linkages at all were observed from the TAME branch.

CHAPTER FIVE : SECONDARY LINKAGE ANALYSIS

5.1 Introduction

A genome-wide scan found five weak linkages with MHS in the EA branch, and *CACNG3*, the γ-subunit of DHPR is situated in one of the candidate loci, at chromosome position 16p12. Six individuals were used in this analysis and as this is a small number, the results may not be very significant. Numbers of samples affect linkage analysis significantly, and 6 samples are insufficient for a conclusive result. In addition, the microsatellite markers used for the initial genome-wide scan were placed at approximately 10 cM intervals on average. The candidate locus on chromosome 16p12 spanned over 20 cM, and there is a large number of genes located within this region. Therefore, to shorten the candidate region to facilitate the search for candidate genes and confirm linkage to this region, secondary linkage analysis on chromosome 16p12 was performed using 10 microsatellite markers positioned at approximately 1.7 cM intervals and 14 individuals over four generations from the EA branch were included.

Figure 5-1 shows the pedigree of the EA branch used for secondary analysis. 14 individuals were used including the six used in the initial genome-wide scan. The MH status of the additional 8 individuals is shown in Table 5-1. Table 5-2 shows the information of 10 microsatellite markers used for this secondary analysis.

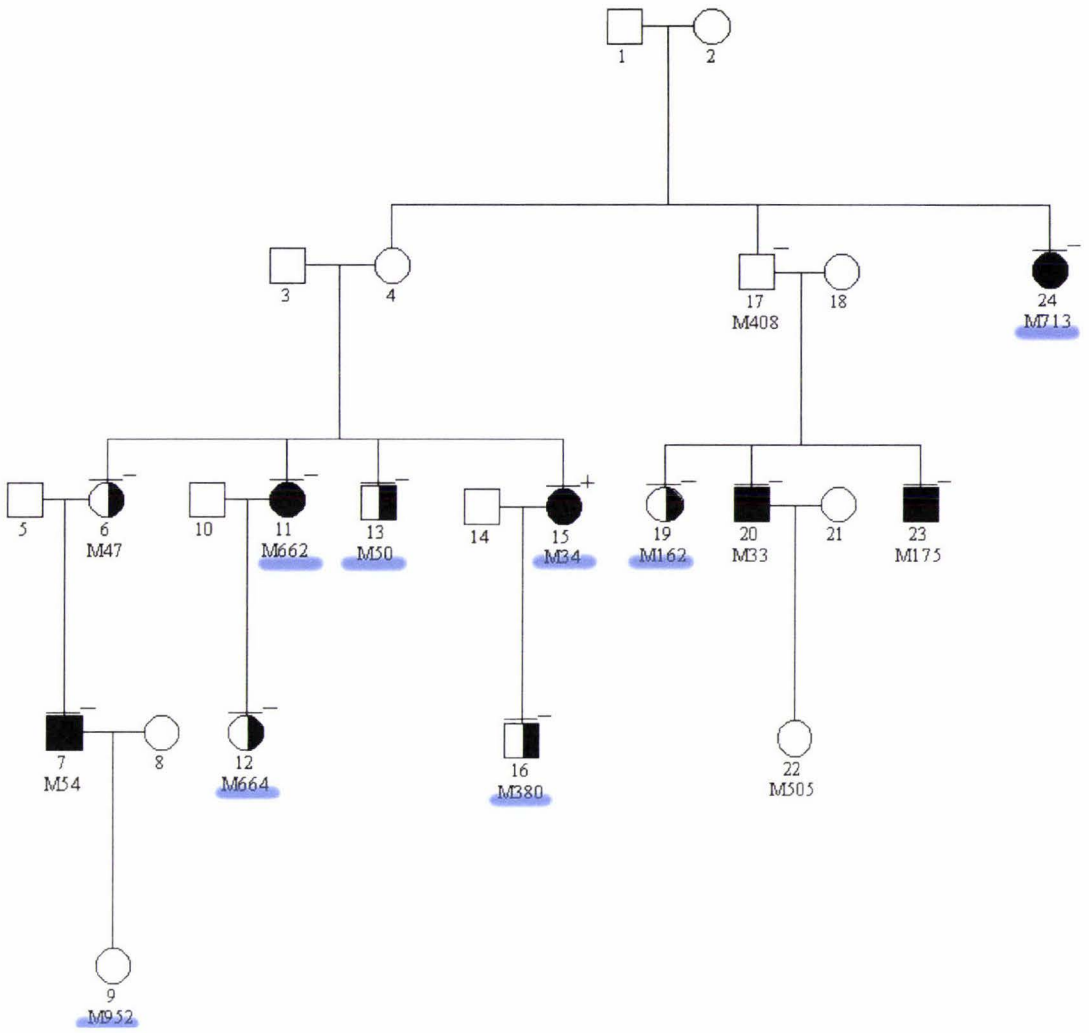

Figure 5-1 The EA family used for secondary linkage analysis

8 family members, highlighted with blue were added to the original 6 and 14 individuals in total were used for linkage analysis on chromosome 16p12. DNA numbers are shown for all 14 samples. Different ID numbers from the initial analysis are given to each member. The individual of ID 1 of this family tree is the same person with ID 7 of the pedigree in Figure 4-2.

ID	DNA number	Sex	IVCT result (halothane/caffeine ,g)	T4826I mutation
6	M47	Female	MHE (0.3/0.1)	Negative
7	M54	Male	MHS (1.4/1.0)	Negative
9	M952	Female	Unknown	Negative
11	M662	Female	MHS (0.6/0.2)	Negative
12	M664	Female	MHE (0.4/0.0)	Negative
13	M50	Male	MHE (0.3/0.0)	Negative
15	M34	Female	MHS (3.4/1.7)	Positive
16	M380	Male	MHE (0.3/0.05)	Negative
17	M408	Male	Unknown	Negative
19	M162	Female	MHE (0.3/0.0)	Negative
20	M33	Male	MHS (1.5/0.2)	Negative
22	M505	Female	Unknown	Negative
23	M175	Male	MHS (3.7/0.9)	Negative
24	M713	Female	MHS (0.6/0.3)	Negative

Table 5-1 Status of individuals used for the secondary linkage analysis

Eight individuals (red) from the EA branch were added for secondary analysis. They include 4 MHE patients.

Marker	Location	Fragment	heterozygosity	Dye label
D16S3103	31.1	316-344	81	VIC
D16S499	33.1	209-217	69	FAM
D16S410	34.6	134-140	69	FAM
D16S3041	37.6	252-282	88	NED
D16S3046	39.3	87-113	74	FAM
D16S412	41.6	101-125	71	FAM
D16S403	42.7	142-160	85	VIC
D16S420	43.2	179-205	81	FAM
D16S401	45.5	160-185	77	FAM
D16S3068	46.6	223-239	77	FAM

Table 5-2 Microsatellite markers used for the secondary linkage analysis

Ten microsatellite markers were used for further linkage analysis on chromosome 16p12. They occur at 1.7 cM intervals on average. Location indicates the distance in cM from the p-terminus of the chromosome. Each marker was labelled with FAM (blue), VIC (green) or NED (yellow).

5.2 Linkage analysis on chromosome 16p12

DNA samples for the additional eight individuals were quantified by spectrophotometry. Table 5-3 shows the $A_{260/280}$ ratios and concentration. Integrity of the DNA was also checked by agarose gel electrophoresis as shown previously (see Figure 3-1).

All 14 DNA samples were diluted to 50 ng/μL, and 10 marker loci were amplified by PCR, and quality of PCR products were checked by electrophoresis (Figure 5-2). The fragment length was detected by ABI PRISM GeneMapper Software version 3.0 (Figure 5-3). Haplotype was determined manually according to the fragment length and allele frequencies were calculated as previously (see section 4-2). Collected data were described as the datafile and prefile, and analysed using GENEHUNTER.

ID	DNA number	$A_{260/280}$	Concentration (ng/μL)
9	M952	1.90	1070
11	M662	1.88	440
12	M664	1.90	360
13	M50	1.86	285
15	M34	1.52	106
16	M380	1.90	237
19	M162	1.72	1528
24	M713	1.86	340

Table 5-3 The $A_{260/280}$ ratios and concentrations of additional individuals

Concentrations of new eight individuals were determined by using spectrophotometer. LightCycler quantification was not performed for these samples.

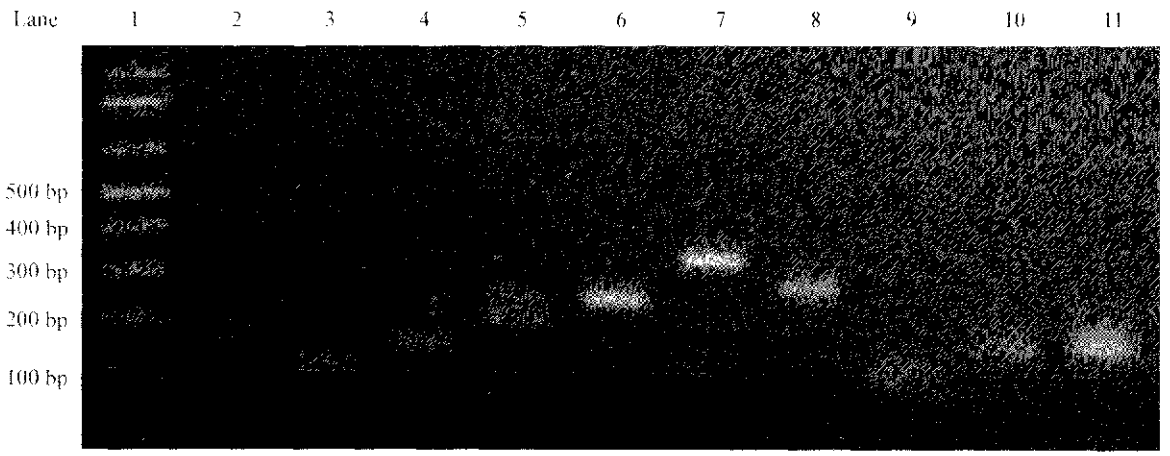

Figure 5-2 Amplification of microsatellite marker loci

PCR products were analysed by agarose electrophoresis before genotyping procedure. This figure shows the 10 PCR products of the M54 individual. Procedures were carried out reported previously (see section 3.3, Figure 3-5). Some marker loci show a single band, and some have two bands because of different length of alleles. Lane 1; 5μL of 1 kb plus DNA marker, 2; D16S403, 3; D16S3046, 4; D16S410, 5; D16S420, 6; D16S3068, 7; D16S3103, 8; D16S3041, 9; D16S412, 10; D16S401, 11; D16S499.

Figure 5-3 Genotyping using GeneMapper Software

This software detects the exact length of DNA fragment using a fluorescent dye, FAM (blue), NED (yellow) or VIC (green). This example shows the partial genotyping data of the M175 individual. Fragment peaks of D16S410 (FAM, fragment length of 130.4, 134.3 bp), D16S403 (VIC, 139.2, 143.5), D16S420 (FAM, 188.28) and D16S3068 (FAM, 229.73, selected in the lower box) are shown. Yellow peaks are standard markers (140, 150, 160 and 200 bp).

A problem arose for input data preparation because equivocal diagnosis could not be described for linkage analysis. The programme can recognise only three parameters for the disease status (0=unknown, 1=not affected, 2=affected), and so equivocal status cannot be included in the computation. In the initial genome-wide scan, the sole MHE individual M47 was treated as affected status. MHE individuals are considered as clinically susceptible to MH although their actual susceptibility is unclear. One MHE sample only would not affect the analysis significantly for the initial genome-wide scan. In the secondary analysis however, five individuals out of 14 were MHE and this number could affect the power of analysis significantly. Some MHE individuals may be positive, but some may be MHN. As it was not feasible to distinguish between MHS or

MHN for the MHE group, linkage analysis was performed three times according to the different disease status (unknown, not affected or affected) for these five MHE individuals. Appendix 5 shows all output data performed obtained from secondary linkage analysis although there was no significant difference between the results of analysis with unknown status and that of affected status (Figure 5-4). Oddly enough, the data with the unaffected status were same as that with the unknown status except for LOD scores (see Appendix 5).

Both parametric and non-parametric analysis identified no strong linkage on chromosome 16p12 because of an apparent discordance in the M662 individual. All LOD and NPL scores were under 3. Figure 5-5 shows the haplotype of 14 individuals. The haplotype 3-4-3-2-2-4-1-3-2-2 is widely conserved in MHS and MHE individuals in this family. The M662 and M664 individuals do not have the haplotype because of discordance in the M662 patient. The M952 individual, whose clinical status is unknown also does not contain this haplotype. This patient could be MHN. As the location of *CACNG3* is very close to the highest peak, this gene may be the candidate gene associated with MH although the NPL score is low. On the other hand the common haplotype associated with 11/14 of this branch may have occurred by chance and may not be associated with MH at all.

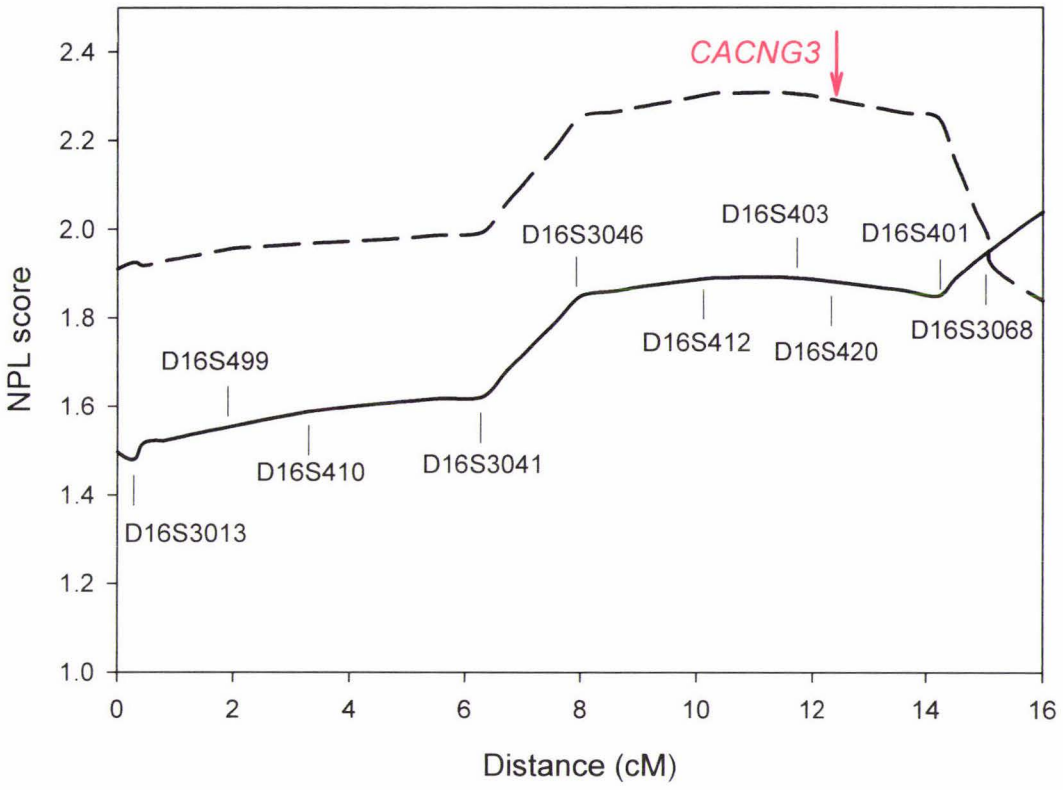

Figure 5-4 Secondary linkage analysis on chromosome 16p12

Secondary linkage analysis was performed on the candidate locus found from the initial genome-wide scan in the EA branch. Multipoint non-parametric linkage analysis was carried out by GENEHUNTER. The NPL score with the unknown status for the MHE individuals (hash line) is higher than that with the affected status (solid line), although they are not significantly different. The names of ten microsatellite markers employed are given. *CACNG3* (indicated in red) is located close to the highest peak.

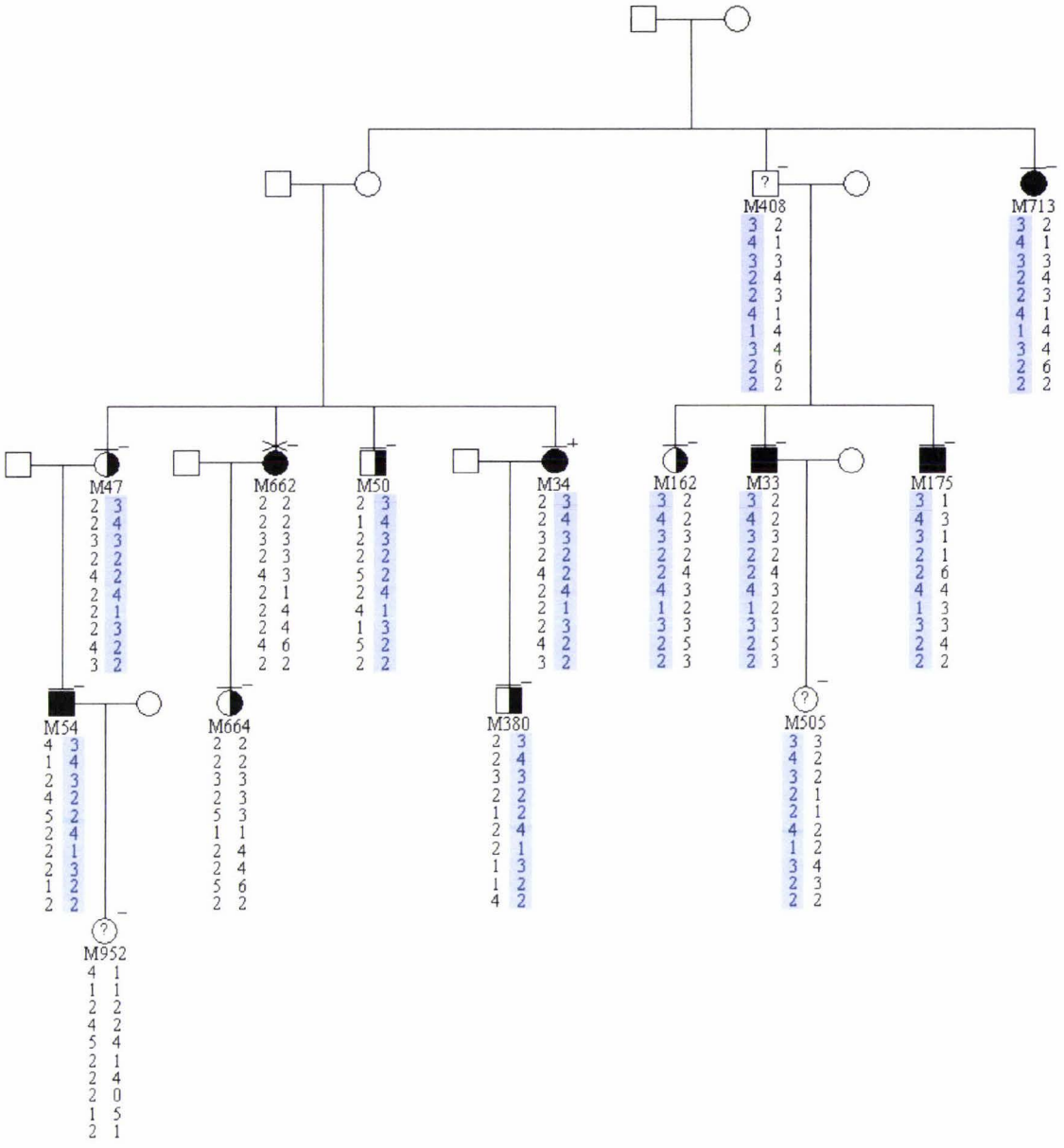

Figure 5-5 Haplotype of the EA family on chromosome 16p12

The haplotype 3-4-3-2-2-4-1-3-2-2 (highlighted with blue) is inherited widely in the MHS and MHE patients. There is discordance, however on the M662 patient (indicated with the cross), so she and her daughter M664 do not have this haplotype despite of their apparent MH susceptibility.

5.3 Screening of *CACNG3*

Although secondary linkage analysis identified discordance and no strong linkage, the *CACNG3* gene is still a potential candidate gene. Observation of discordance in linkage analysis is not rare and it is not conclusive that the locus with discordance is not associated with the disorder. MH is heterogenous and in fact, a genome-wide scan identified five candidate loci from the EA family. Two individuals M662 and M664 are MHS and MHE, respectively but did not have the haplotype widely shared in other patients used for the secondary analysis. As susceptibility to MH of these two patients may be from other traits on other loci, the locus on chromosome 16p12 can still be considered a candidate locus that may be associated with MH for other members in the EA family. *CACNG3* is the sole candidate gene identified from candidate loci found from the initial genome-wide scan, and no other genes of interest which appear to be related to calcium signalling or homeostasis were identified. Therefore, it was worthwhile to screen this gene because of the small size of its coding regions and it was feasible to do so from genomic DNA.

CACNG3 (the γ-subunit of DHPR) is a 106,861 bp-long gene, but most regions are introns or untranslated regions. Translated sequences cover just 1 kb on four exons encoding 315 amino acids. Because resources for RNA preparations were not available for all members in the EA branch, screening could not be carried out using cDNA. Genomic DNA was used as a template to screen the coding regions and four PCR reactions were carried out. Translated regions were directly screened by using the ABI 3730 Genetic Analyser. PCR primers are described in Table 5-4, and sequences of *CACNG3* are shown in Appendix 6.

Screening of *CACNG3* did not identify any mutations or polymorphisms within the four exons. The template was genomic DNA and sequencing covered all boundaries between introns and exons including the recognition sites for RNA splicing. 5' upstream and 3' downstream untranslated regions were not screened as these regions do not affect amino acid sequences of the protein but may have a role in post-transcriptinal regulation such as stability of mRNA. Therefore, translation of this gene is likely to be accurate resulting in a wild-type protein. This result indicates that *CACNG3* is not likely to be associated with MH in the EA family and not a candidate gene of MH.

Exon	Size (bp)	Forward primer	Reverse primer
1	435	G3_e1F 5'-GGTTACCCGGCTGCAGAGTGA	G3_e1R 5'-CAGAGTCTGGGCACCTGCACA
2	201	G3_e2F 5'-ATAGCGGTGAGGACCCAGGCT	G3_e2R 5'-TCCTCCCAGAGAGACCCGAGA
3	402	G3_e3F 5'-GACTGCAGAGCATCAACCCCA	G3_e3R 5'-GCCCTGAGTAGCATTGCTTCC
4	798	G3_e4F 5'-GGTGGTTGGATTTCCCAGCTA	G3_e4R 5'-AAATGTGGGAGAGGGCTGAGT

Table 5-4 Primers for *CACNG3* screening

Four PCR reactions were performed to cover the translated regions in four exons. An annealing temperature of 60°C was adopted for all reactions. Thermal cycles were accomplished by using FTS-320 thermal sequencer. PCR products were purified and directly sequenced using the forward primer as the sequencing primer for each fragment.

5.4 Chapter summary

Further linkage analysis was performed on the 15 cM candidate loci between D16S3103 and D16S3068 identified by the initial genome-wide scan. 14 individuals were used for the analysis. Strong linkage could not be identified due to discordance between genotype and reported phenotype. LOD and NPL scores were all under 3. The haplotype 3-4-3-2-2-4-1-3-2-2 was conservative through the MHS and MHE patients in this family, except for two discordant individuals. *CACNG3* is located close to the highest peak, but DNA sequencing did not identify a mutation within this gene showing that it is not associated with MH.

CHAPTER SIX : DISCUSSION AND FUTURE WORK

6.1 The M818 patient

By screening *RYR1* cDNA and endonuclease *Hha*I digestion, it was found that the M818 individual did not have any mutations within *RYR1* and did not have either of the two reported *CACNA1S* mutations, R1086C and R1086H. It is possible that MH patients do not have mutations or linkage with *RYR1* because MH is heterogeneous and other genes are likely to be involved in the disorder. The M818 patient showed an exercise-induced MH reaction, and it is possible that this type of MH is both phenotypically and genotypically distinct from MH associated with anaesthesia. In fact, 5 other chromosomal loci have been reported as candidate loci, so MH in this patient may have been linked to one of these or a novel locus. Further analysis of this individual was not feasible as the there was no family history and samples from other family members were not available.

CACNA1S is the only other candidate gene apart from *RYR1* where mutations have been identified. The R1086H mutation has been found in European and American families, and it is possible that the M818 individual has a novel mutation within the gene. Most molecular genetic studies, however have been carried out with *RYR1* and only two mutations have been reported within *CACNA1S*. No mutations have been found within other genes, and even gene products are still unknown for some candidate loci. The cDNA of *CACNA1S* is more than 6 kb in size and as only two mutations linked to MH have been identified in this gene, it was not feasible to screen the entire gene for novel mutations. Therefore, analysis of genomic DNA or cDNA from the M818 patient was not continued.

In the future, if novel candidate genes and mutations are identified in New Zealand families, it may be worthwhile to return to M818 and screen for these.

6.2 The CH family

After the initial genome-wide scan, five weak linkages were found in the EA branch. Secondary linkage analysis was performed on the region of chromosome 16p12 including *CACNG3*, using additional individuals from the branch. Unfortunately, only weak linkage was observed because of discordance, and no mutations were identified within *CACNG3*, so this gene is not likely to be associated with MH. The γ-subunit of DHPR has eight isoforms, from *CACNG1* to *CACNG8*. *CACNG3* is one of these, and it is not expressed predominantly in skeletal muscle (154). The *CACNG1* gene is predominantly expressed in skeletal muscle, and almost no gene product from *CACNG3* has been observed in skeletal muscle on a gel. Therefore, *CACNG3* may not be related to MH. No other obvious candidate genes were identified within the five loci identified in the EA branch. It is possible that each of these five loci may be associated with MH, but some of them could be false positives. These results may not be significant because only small numbers of individuals were used for the analysis. Factors influencing power of analysis are:

- Pedigree size and structure
- Information content of markers
- Distance of markers from the disease locus
- Genetic heterogeneity
- Magnitude of genetic effect

In this project, non-parametric linkage analysis was adopted using GENEHUNTER. Non-parametric analysis does not require information about genetic heterogeneity and magnitude of genetic effect. In addition, multipoint linkage analysis allows searching the disease gene using each marker as a starting point. This means that the distance of markers from the disease locus does not have an affect on the power of the analysis. Therefore, if the marker information (location, order and allele frequencies) is correct, only family information and size is a significant factor. As five candidate loci found from the EA branch have not been conclusively proven to be linked to MH, further linkage analysis within these loci is required to determine whether they are actual

positive loci and also to narrow the region to facilitate the identification of candidate genes. Increasing the numbers of samples will increase the power and provide more reliable results. False positives will also be revealed by further analyses.

Although weak linkage was observed on chromosome 16p12, this locus may not be associated with MH because there are two individuals who do not share the candidate haplotype. This does not always mean the absence of linkage, so it is still possible this region is associated with MH. The problem, however is that equivocal diagnosis could not be described for linkage analysis. 5 of 14 individuals were MHE in the secondary analysis, and it is still controversial whether MHE is truly MHS or MHN. Generally, genetic linkage is observed within only MHS individuals, and there are not many cases showing linkage including MHE individuals. Mutations or candidate loci are seldom identified in MHE individuals although they are all recognised as clinically susceptible to MH. Importantly, the T4826I mutation has not been found in any MHE individuals in the CH family.

Secondary linkage analysis was carried out three times with different disease status for five MHE individuals in the EA family. It did not produce significant differences in NPL scores, but unusual data was obtained if these MHE individuals were treated as MHN (status 1, unaffected). LOD scores were all abnormally low (up to -7) and other data including NPL scores were the same as that of analyses with the disease status as affected or unknown (see Appendix 5). This is probably because the programme could not continue computation properly with MHE individuals categorised as MHN and this potentially incorrect family information resulted in an error producing exactly the same data as for the unknown status. This observation indicates that it is not feasible to handle MHE individuals as MHN for this type of linkage analysis and some MHE patients may be truly MHS. It is not conclusive that all MHE patients should be treated as MHS, and some MHE individuals could be MHN. The analysis with the MHE patients categorised as affected produced slightly lower NPL scores compared to that using MHE as unknown. It may be best for MHE individuals to be described as unknown for linkage analysis to avoid computation errors. More accurate definition of phenotype is clearly required, but as the IVCT remains the "gold standard" test, the MHE classification is likely to remain for the foreseeable future.

Hence, it is still not clear whether the region on chromosome 16p12 is associated with MH for the EA family. Some additional MHN individuals may need to be included in the analysis in the future. If MHN individuals share the haplotype of interest, it clearly suggests that this locus is not linked the disorder. This would be stronger evidence than discordance showing that the locus is not candidate.

Two strong linkages were identified on chromosome 6 and 12 in the ES branch. Ten individuals were used for the genome-wide scan, excluding the negative individual M58, hence the results seem to be more reliable that for the EA branch. A previous report suggested that NPL scores >5.4 would show significant linkage (151), so scores of ~8 for both loci seem to be significant.

The M48 individual is an MHS patient who has the T4826I mutation within *RYR1*. Interestingly, this patient shares the candidate loci with other MHS patients who do not have the *RYR1* mutation. If these two loci are also associated with MH, it means that the M48 patient has three possible traits causing MH susceptibility, whereas the other patients have two. It is known that MH is heterogeneous, but it has not yet been reported to be a result of a combination of several gene defects. No patient has been identified who has mutations within both *RYR1* and *CACNA1S*. Therefore, the magnitude of the effect of one gene on MH susceptibility is unknown. MH may be a complex disorder with a threshold mechanism (155). Several genes may be involved in MH susceptibility, and if the total magnitude goes over the threshold, the patient may show clear susceptibility which is detectable by the IVCT. *RYR1* is likely to be the most important gene for susceptibility. The patients in the CH family who have a *RYR1* mutation always show strong susceptibility for the IVCT (1-5 g for both drugs), whereas MHS patients who do not have *RYR1* mutations show only mild contractures in the IVCT (~1 g). Patients who are not linked to *RYR1*, but have the *CACNA1S* mutation, also showed mild susceptibility (116).

Therefore, it is thought that *RYR1* mutations significantly affect the function of RYR and MH susceptibility, but other genes may be less important. One mutation within *RYR1* or *CACNA1S* may be enough to go over the threshold and show susceptibility, whereas several mutations in other genes may be needed for a clear MHS status. *RYR1* and *CACNA1S* are predominantly expressed in skeletal muscle and proteins from these

genes, especially *RYR1* play important role in EC coupling. This is why individuals who have a mutation within *RYR1* show strong susceptibility for the IVCT. Individuals who have some other traits, without abnormality in *RYR1* and *CACNA1S* may show lower IVCT scores.

The IVCT however, is not perfect and produces variable results, and only the highest score is recorded from 2-3 tests for each halothane and caffeine test and the average is not considered. Hence, the difference in the IVCT score between patients who have an *RYR1* mutation and those who do not may be just because of limitations in the test. It is possible however, that patients without an *RYR1* mutation may show milder susceptibility due to two candidate loci, which independently have weak MH susceptibility. This observation was also found in the EA branch.

Candidate genes were not able to be identified from the two loci found in the ES branch because the loci are too large (over 100 cM) with hundreds of genes to assess. There are also many functionally unknown genes within these regions. MH is caused by abnormal calcium homeostasis, so the candidate genes should be involved in this process in some way. Such genes however, could not be identified within these loci, including all subunits of DHPR and proteins which modify RYR and calcium release such as triadin and calsequestrin. All genes known to have a role in calcium homeostasis are located in other regions of the genome. As the mechanism and proteins involved in calcium signalling and homeostasis are not clearly understood, novel candidate genes may be able to be identified within these loci in the future. Most of isoforms of the γ-subunit of DHPR have been identified recently, and it is possible that other unidentified isoform genes of DHPR subunits exist (154, 156). Further linkage analysis on chromosome 6 and 12 is required to fine map these regions. More markers with shorter intervals and more individuals for analysis should produce more reliable scores and narrow the candidate regions.

In the TAME branch, no linkage was identified through the entire genome. Although the reason for this is unclear, there may be some errors in the marker analysis or the family data. The CH family is a Maori family and the pedigrees of Maori often become complicated because of their unique culture. They often marry with their cousins or close relatives and have several partnerships often within the same family. Hence,

family pedigree and data become complicated and errors can occur as much of the genealogical information is provided "word of mouth". In addition, family structure can significantly affect linkage analysis. The TAME family has a much more complex structure than the EA and ES branch, and a more extensive analysis of this family may be required before informative linkage data can be obtained for this branch. All three branches have a common ancestor (ID 1 and 2 in Figure 4-2), but they do not share the same candidate loci. The EA family does not show linkage to the candidate loci found in the ES family and vice versa. As the TAME family is complicated, it is possible that there are several candidate loci within each small branch. In addition, because the structure of the pedigree affects the power of analysis, the complicated pedigree of the TAME branch might reduce the power of analysis for GENEHUNTER.

Accurate family information is critical for linkage analysis. Only one error can cause significantly false results. To obtain correct information and perform reliable linkage analysis, it will be required to collect all data and construct a more complete database. Family structure and information needs to be re-examined for the TAME family.

The IVCT diagnosis could be another factor producing incorrect information. The European protocol has been adopted for the IVCT in New Zealand, but it has 99% sensitivity and 93.6% specificity and can produce false diagnoses (59). In the CH family, out of 130 individuals tested by the IVCT, 22 individuals were diagnosed as MHS although they do not have the T4826I mutation. This means that sensitivity and specificity for this family is 100% and 76.6%, respectively (129) if there is linkage only to *RYR1*. There are also many MHE individuals in the CH family. About 35% of tested individuals (45 individuals) were diagnosed as MHE (Table 6-1).

Genotype	MHS	MHE	MHN	Total
T4826I positive	36	0	0	36
T4826I negative	22	45	27	94
Total	58	45	27	130

Table 6-1 The IVCT result of the CH family

The IVCT was carried out for 130 individuals from the CH family. No MHE and MHN individuals contained the T4826I mutation, but 22 individuals were diagnosed as MHS although none of them carried the mutation, which indicates discordance between genotype and IVCT phenotype. From reference (129).

Healy *et al.* (1996) suggested unreliability of the IVCT using the diagnostic threshold suggested by the European protocol (0.2 g for both halothane and caffeine test). Generally, the halothane test tends to produce a higher score than the caffeine test producing more MHE individuals against halothane. These authors suggested the use of thresholds at 0.8 and 0.4 g for halothane and caffeine tests, respectively to avoid large numbers of MHE diagnoses and false positive diagnoses (118). This suggestion may be useful for the CH family. There are many MHE patients in the family and most of them are MHE against halothane. Only two individuals were diagnosed as MHE due to abnormal contracture using caffeine. The threshold of the IVCT may need to be re-assessed depending on the family tested. This will only be possible with the identification of causative mutations or linkage to other loci.

This idea, however does not answer all the questions raised by this study of the CH family. Even if the Healy's threshold is adopted for the family (0.8/0.4 g for halothane/caffeine), there are still 9 individuals who do not have the T4826I mutation showing strong MH susceptibility. To obtain 100% specificity, the threshold would need to be set as 1.8/1.2 g which are unrealistic scores and would exclude many individuals who are MHS (129). This would be clinically inappropriate. Linkage analysis in this project was performed mainly with these strong positive patients who do not share the *RYR1* mutation, and most of the 9 patients were included for the analysis. Therefore, it is hard to believe that lack of identification of linkage in the TAME family was caused

by incorrect information from the IVCT results only (Table 6-2). 9 discordances in 130 samples (6.9%) are unlikely to be all false positives. There could be some other susceptible loci in the EA and ES families that could also be in the TAME branch. Further linkage analysis clearly is required as well as a more definition assignment of phenotype.

	Threshold (h/c, g)	MHS	MHE	MHN	Unknown
EA	0.2/0.2	6	5	0	3
	0.8/0.4	3	1	7	3
ES	0.2/0.2	7	0	1	3
	0.8/0.4	7	0	1	3
TAME	0.2/0.2	8	1	0	0
	0.8/0.4	4	1	4	0

Table 6-2 Numbers of each disease status in three branches

This table shows the number of individuals for each disease status in three families used for linkage analysis. The data of the EA branch are from individuals for secondary linkage analysis. Each branch has one MHS patient who has the T4826I mutation (M34 in the EA, M48 in the ES and M554 in the TAME). The 0.8/0.4 threshold re-classes some MHS and MHE patients as MHN, but there are still some individuals who are MHS and do not contain the mutation. The IVCT scores were not available for some MHS individuals in the ES family.

In this project, analysis was performed using GENEHUNTER which can carry out parametric and non-parametric linkage analysis. No significant linkage was observed however, by parametric analysis (under 2 LOD scores for all chromosomes). More importance was attached to non-parametric analysis because MH is heterogeneous in the CH family and parametric analysis is not powerful with several traits. Nevertheless, parametric analysis may be necessary for further analysis. The LINKAGE package is most commonly used for parametric linkage analysis. A different algorithm from that of

GENEHUNTER is used, so more reliable results may be produced. It is not clear why parametric analysis did not show strong linkage. It may be because of heterogeneity of MH, but could also be because parametric analysis using the algorithm of GENEHUNTER is not very powerful. It may be useful to perform both parametric and non-parametric linkage analysis using the LINKAGE package and GENEHUNTER, respectively. High NPL scores by GENEHUNTER and low LOD scores by the LINKAGE package may indicate the heterogeneity of MH. It is still controversial which method or which programme is most reliable although both parametric and non-parametric analyses are not very different (157, 158). It is quite difficult, however to find disease genes by linkage analysis, and one analysis is rarely sufficient to identify a disease-linked gene (151, 159). Hence, further linkage analysis using several methods with several different programmes will be required for candidate loci found in the EA and ES branch to identify true linkages.

The ES branch seems to be the most worthwhile family for further linkage analysis in three branches studied in this project. The highest number of samples was analysed for this branch, and there were no MHE patients included. Although there were some MHS patients tested prior to the introduction of the European protocol, most discordance between strong MH susceptibility and lack of the T4826I mutation is observed in this family. Secondary linkage analysis on chromosome 6 and 12 using several algorithms and programmes with more individuals may identify more reliable and stronger linkage.

Linkage analysis requires high specifications especially memory for computation. In this project, GENEHUNTER was run on a Linux PC by using KNOPPIX because a machine with Linux installed was not available. KNOPPIX can run Linux programmes without installation, but it uses a large amount of memory. KNOPPIX runs all programmes on memory only, not using a hard disk, hence most of the memory was used for KNOPPIX itself and there was not enough memory for linkage analysis. As a result, the M58 individual was eliminated for analysis of the ES branch because of lack of memory, although this individual was MHN and not very important for the analysis. More individuals will need to be used for further linkage analysis to identify shorter candidate loci with more reliable scores, and then a PC with more memory or higher capability for computation will be needed. As KNOPPIX uses a large amount of memory, it is unlikely to be suitable for linkage analysis programmes. Another Linux

distribution should be used. GENEHUNTER is a programme written in C, and another option would be to compile the source code of the programme and run it on MS-DOS.

In conclusion, several candidate loci were identified from the EA and ES branches of the CH family. Further linkage analysis, however is required with more markers and samples. Secondary analysis should be performed using both parametric and non-parametric linkage analysis using several programmes on a PC, which has enough power and memory for heavy computation. Family or marker data need to be reviewed especially for the TAME branch. Information about New Zealand MH families should be collected and rearranged to allow easy acquisition of correct information. Once candidate genes are identified, they can be selected for mutation screening by DNA sequence analysis. Eventually, using this approach it should be possible to identify novel causative mutations in the CH family. This will allow the development of DNA tests for all members of the CH family. In addition, the identification of novel genes with a putative role in calcium release will allow further investigation of calcium signalling and homeostasis at the biochemical and physiological level. In future, this information may aid in the understanding of factors affecting anaesthesia.

REFERENCES

1. Wappler, F. (2001) Malignant hyperthermia. *Eur. J. Anaesth.*, **18,** 632-652.

2. Stowell, K.M., Brown, R.L., James, D., Couchman, K.G., Hodges, M. and Pollock, A.N. (1999) Malignant hyperthermia in New Zealand. *NZ BioScience,* **7,** 12-17.

3. Denborough, M. and Lovell, R. (1960) Anaesthetic deaths in a family. *Lancet,* **2,** 45.

4. Denborough, M., Forster, J., Lovell, R., Maplestone, P. and Villiers, J. (1962) Anaesthetic deaths in a family. *Br. J. Anaesth.*, **34,** 395.

5. Kalow, W., Britt, B.A., Terreau, M.E. and Haist, C. (1970) Metabolic error of muscle metabolism after recovery from malignant hyperthermia. *Lancet,* **2,** 895-8.

6. Ellis, F.R., Harriman, D.G., Keaney, N.P., Kyei-Mensah, K. and Tyrrell, J.H. (1971) Halothane-induced muscle contracture as a cause of hyperpyrexia. *Br. J. Anaesth.*, **43,** 721-2.

7. European Malignant Hyperpyrexia Group. (1984) A Protocol for the Investigation of Malignant Hyperpyrexia (MH) Susceptibility. *Br. J. Anaesth.*, **56,** 1267-1269.

8. Larach, M.G. (1989) Standardization of the Caffeine Halothane Muscle Contracture Test. *Anesth. Analg.*, **69,** 511-515.

9. Kalow, W., Britt, B.A. and Chan, F.Y. (1979) Epidemiology and inheritance of malignant hyperthermia. *Int. Anesthesiol. Clin.*, **17,** 119-39.

10. Friesen, C.M., Brodsky, J.B. and Dillingham, M.F. (1979) Successful use of dantrolene sodium in human malignant hyperthermia syndrome: a case report. *Can. Anaesth. Soc. J.*, **26,** 319-21.

11. Denborough, M. (1998) Malignant hyperthermia. *Lancet,* **352,** 1131-1136.

12. Hackl, W., Mauritz, W., Schemper, M., Winkler, M., Sporn, P. and Steinbereithner, K. (1990) Prediction of malignant hyperthermia susceptibility: statistical evaluation of clinical signs. *Br. J. Anaesth.*, **64,** 425-9.

13. Larach, M.G., Rosenberg, H., Larach, D.R. and Broennle, A.M. (1987) Prediction of malignant hyperthermia susceptibility by clinical signs. *Anesthesiology,* **66,** 547-50.

14. Rosenberg, H. (1988) Clinical presentation of malignant hyperthermia. *Br. J. Anaesth.*, **60,** 268-73.

15. Larach, M.G., Localio, A.R., Allen, G.C., Denborough, M.A., Ellis, F.R., Gronert, G.A., Kaplan, R.F., Muldoon, S.M., Nelson, T.E., Ording, H. *et al.* (1994) A clinical grading scale to predict malignant hyperthermia susceptibility. *Anesthesiology,* **80,** 771-9.

16. Evans, T.J., Parent, C.M. and McGunigal, M.P. (2002) Atypical presentation of malignant hyperthermia. *Anesthesiology,* **97,** 507-8.

17. Claxton, B.A., Cross, M.H. and Hopkins, P.M. (2002) No response to trigger agents in a malignant hyperthermia-susceptible patient. *Br. J. Anaesth.*, **88,** 870-3.

18. Kalow, W. and Britt, B.A. (1973) Drugs causing rigidity in malignant hyperthermia. *Lancet,* **2,** 390-1.

19. Tegazzin, V., Scutari, E., Treves, S. and Zorzato, F. (1996) Chlorocresol, an additive to commercial succinylcholine, induces contracture of human malignant hyperthermia-susceptible muscles via activation of the ryanodine receptor Ca^{2+} channel. *Anesthesiology,* **84,** 1380-5.

20. Herrmann-Frank, A., Richter, M., Sarkozi, S., Mohr, U. and Lehmann-Horn, F. (1996) 4-Chloro-m-cresol, a potent and specific activator of the skeletal muscle ryanodine receptor. *Biochim. Biophys. Acta.*, **1289,** 31-40.

21. Wappler, F., Scholz, J., Fiege, M., Kolodzie, K., Kudlik, C., Weisshorn, R. and Schulte am Esch, J. (1999) 4-chloro-m-cresol is a trigger of malignant hyperthermia in susceptible swine. *Anesthesiology,* **90,** 1733-40.

22. Franks, R.D., Aoueille, B., 3rd, Mahowald, M.C. and Masson, N. (1982) ECT use for a patient with malignant hyperthermia. *Am. J. Psychiatry,* **139,** 1065-6.

23. Levenson, J.L. (1989) Tricyclic antidepressants and malignant hyperthermia. *Am. J. Psychiatry,* **146,** 1359-60.

24. van den Hende, C., Lister, D., Muylle, E., Ooms, L. and Oyaert, W. (1976) Malignant hyperthermia in Belgian Landrace pigs rested or exercised before exposure to halothane. *Br. J. Anaesth.*, **48,** 821-9.

25. Denborough, M., Hopkinson, K.C., O'Brien, R.O. and Foster, P.S. (1996) Overheating alone can trigger malignant hyperthermia in piglets. *Anaesth. Intensive Care,* **24,** 348-54.

26. Denborough, M.A. (1982) Heat stroke and malignant hyperpyrexia. *Med. J. Aust.*, **1,** 204-5.

27. Hopkins, P.M., Ellis, F.R. and Halsall, P.J. (1991) Evidence for Related Myopathies in Exertional Heat-Stroke and Malignant Hyperthermia. *Lancet,* **338,**

1491-1492.

28. Wappler, F., Fiege, M., Antz, M. and Esch, J.S.A. (2000) Hemodynamic and metabolic alterations in response to graded exercise in a patient susceptible to malignant hyperthermia. *Anesthesiology,* **92,** 268-272.

29. Wappler, F., Fiege, M., Steinfath, M., Agarwal, K., Scholz, J., Singh, S., Matschke, J. and Esch, J.S.A. (2001) Evidence for susceptibility to malignant hyperthermia in patients with exercise-induced rhabdomyolysis. *Anesthesiology,* **94,** 95-100.

30. Mogensen, J.V., Misfeldt, B.B. and Hanel, H.K. (1974) Letter: Preoperative excitement and malignant hyperthermia. *Lancet,* **1,** 461.

31. Fletcher, R., Ranklev, E., Olsson, A.K. and Leander, S. (1981) Malignant hyperthermia syndrome in an anxious patient. *Br. J. Anaesth.,* **53,** 993-5.

32. Wingard, D.W. (1974) Malignant hyperthermia: A human stress syndrome? *Lancet,* **2,** 1450-1451.

33. Denborough, M.A., McLean, A., Morgan, G. and Hopkinson, K.C. (1994) Fatal inherited rhabdomyolysis and malignant hyperthermia. *Lancet,* **343,** 236-7.

34. Cain, P.A. and Ellis, F.R. (1977) Anaesthesia for patients susceptible to malignant hyperpyrexia. A study of pancuronium and methylprednisolone. *Br. J. Anaesth.,* **49,** 941-4.

35. Denborough, M. and Hopkinson, K.C. (1988) Propofol and malignant hyperpyrexia. *Lancet,* **1,** 191.

36. Carrier, L., Villaz, M. and Dupont, Y. (1991) Abnormal rapid Ca^{2+} release from sarcoplasmic reticulum of malignant hyperthermia susceptible pigs. *Biochim. Biophys. Acta.,* **1064,** 175-83.

37. Lopez, J., R, Alamo, L., Caputo, C., Wikinski, J. and Ledezma, D. (1985) Intercellular ionized calsium concentration in muscles from humans with malignant hyperthermia. *Muscle Nerve,* **8,** 355-358.

38. Mickelson, J.R., Gallant, E.M., Litterer, L.A., Johnson, K.M., Rempel, W.E. and Louis, C.F. (1988) Abnormal sarcoplasmic reticulum ryanodine receptor in malignant hyperthermia. *J. Biol. Chem.,* **263,** 9310-5.

39. Melzer, W. and Dietze, B. (2001) Malignant hyperthermia and excitation-contraction coupling. *Acta Physiol Scand,* **171,** 367-78.

40. Nelson, T.E. and Sweo, T. (1988) Ca^{2+} uptake and Ca^{2+} release by skeletal muscle sarcoplasmic reticulum: differing sensitivity to inhalational anesthetics. *Anesthesiology,* **69,** 571-7.

41. Wolf, M., Eberhart, A., Glossmann, H., Striessnig, J. and Grigorieff, N. (2003)

Visualization of the domain structure of an L-type Ca^{2+} channel using electron cryo-microscopy. *J. Mol. Biol.*, **332,** 171-82.

42. Catterall, W.A. (1991) Functional subunit structure of voltage-gated calcium channels. *Science,* **253,** 1499-500.

43. Tanabe, T., Beam, K.G., Adams, B.A., Niidome, T. and Numa, S. (1990) Regions of the skeletal muscle dihydropyridine receptor critical for excitation-contraction coupling. *Nature,* **346,** 567-9.

44. Grabner, M., Dirksen, R.T., Suda, N. and Beam, K.G. (1999) The II-III loop of the skeletal muscle dihydropyridine receptor is responsible for the Bi-directional coupling with the ryanodine receptor. *J. Biol. Chem.,* **274,** 21913-9.

45. Pessah, I.N., Lynch, C., 3rd and Gronert, G.A. (1996) Complex pharmacology of malignant hyperthermia. *Anesthesiology,* **84,** 1275-9.

46. Walker, D. and De Waard, M. (1998) Subunit interaction sites in voltage-dependent Ca^{2+} channels: role in channel function. *Trends. Neurosci.,* **21,** 148-54.

47. Coronado, R., Morrissette, J., Sukhareva, M. and Vaughan, D.M. (1994) Structure and function of ryanodine receptors. *Am. J. Physiol.,* **266,** C1485-504.

48. Lai, F.A., Erickson, H.P., Rousseau, E., Liu, Q.Y. and Meissner, G. (1988) Purification and reconstitution of the calcium release channel from skeletal muscle. *Nature,* **331,** 315-9.

49. Wagenknecht, T., Grassucci, R., Frank, J., Saito, A., Inui, M. and Fleischer, S. (1989) Three-dimensional architecture of the calcium channel/foot structure of sarcoplasmic reticulum. *Nature,* **338,** 167-70.

50. Takeshima, H., Nishimura, S., Matsumoto, T., Ishida, H., Kangawa, K., Minamino, N., Matsuo, H., Ueda, M., Hanaoka, M., Hirose, T. *et al.* (1989) Primary structure and expression from complementary DNA of skeletal muscle ryanodine receptor. *Nature,* **339,** 439-45.

51. McPherson, P.S. and Campbell, K.P. (1993) The ryanodine receptor/Ca^{2+} release channel. *J. Biol. Chem.,* **268,** 13765-8.

52. Marks, A.R., Tempst, P., Hwang, K.S., Taubman, M.B., Inui, M., Chadwick, C., Fleischer, S. and Nadal-Ginard, B. (1989) Molecular cloning and characterization of the ryanodine receptor/junctional channel complex cDNA from skeletal muscle sarcoplasmic reticulum. *Proc. Natl. Acad. Sci. U .S.A.,* **86,** 8683-7.

53. Otsu, K., Willard, H.F., Khanna, V.K., Zorzato, F., Green, N.M. and MacLennan, D.H. (1990) Molecular cloning of cDNA encoding the Ca^{2+} release channel (ryanodine receptor) of rabbit cardiac muscle sarcoplasmic reticulum. *J. Biol. Chem.,* **265,** 13472-83.

54. Hakamata, Y., Nakai, J., Takeshima, H. and Imoto, K. (1992) Primary structure and distribution of a novel ryanodine receptor/calcium release channel from rabbit brain. *FEBS Lett.*, **312,** 229-35.

55. Fill, M., Coronado, R., Mickelson, J.R., Vilven, J., Ma, J.J., Jacobson, B.A. and Louis, C.F. (1990) Abnormal ryanodine receptor channels in malignant hyperthermia. *Biophys. J.*, **57,** 471-5.

56. Fill, M., Stefani, E. and Nelson, T.E. (1991) Abnormal human sarcoplasmic reticulum Ca^{2+} release channels in malignant hyperthermic skeletal muscle. *Biophys. J.*, **59,** 1085-90.

57. Ording, H. (1988) Diagnosis of susceptibility to malignant hyperthermia in man. *Br. J. Anaesth.*, **60,** 287-302.

58. Fletcher, J.E., Rosenberg, H. and Aggarwal, M. (1999) Comparison of European and North American malignant hyperthermia diagnostic protocol outcomes for use in genetic studies. *Anesthesiology,* **90,** 654-661.

59. Allen, G.C., Larach, M.G. and Kunselman, A.R. (1998) The sensitivity and specificity of the caffeine-halothane contracture test: a report from the North American Malignant Hyperthermia Registry. The North American Malignant Hyperthermia Registry of MHAUS. *Anesthesiology,* **88,** 579-88.

60. Isaacs, H. and Badenhorst, M. (1993) False-negative results with muscle caffeine halothane contracture testing for malignant hyperthermia. *Anesthesiology,* **79,** 5-9.

61. Larach, M.G. (1993) Should we use muscle biopsy to diagnose malignant hyperthermia susceptibility? *Anesthesiology,* **79,** 1-4.

62. Wappler, F., Roewer, N., Lenzen, C., Kochling, A., Scholz, J., Steinfath, M. and Schulte am Esch, J. (1994) High-purity ryanodine and 9,21-dehydroryanodine for in vitro diagnosis of malignant hyperthermia in man. *Br. J. Anaesth.*, **72,** 240-2.

63. Herrmann-Frank, A., Richter, M. and Lehmann-Horn, F. (1996) 4-Chloro-m-cresol: a specific tool to distinguish between malignant hyperthermia-susceptible and normal muscle. *Biochem. Pharmacol.*, **52,** 149-55.

64. Fiege, M., Wappler, F., Weisshorn, R., Gerbershagen, M.U., Kolodzie, K. and Schulte Am Esch, J. (2003) In vitro and in vivo effects of the phosphodiesterase-III inhibitor enoximone on malignant hyperthermia-susceptible swine. *Anesthesiology,* **98,** 944-9.

65. Wappler, F., Anetseder, M., Baur, C.P., Censier, K., Doetsch, S., Felleiter, P., Fiege, M., Fricker, R., Halsall, P.J., Hartung, E. *et al.* (2003) Multicentre evaluation of in vitro contracture testing with bolus administration of 4-chloro-m-cresol for diagnosis of malignant hyperthermia susceptibility. *Eur. J. Anaesthesiol.*, **20,** 528-36.

66. Galloway, G.J. and Denborough, M.A. (1984) Phosphorus-31 nuclear magnetic resonance studies of muscle metabolism in malignant hyperpyrexia. *Br. J. Anaesth.*, **56,** 663-4.

67. Olgin, J., Argov, Z., Rosenberg, H., Tuchler, M. and Chance, B. (1988) Non-invasive evaluation of malignant hyperthermia susceptibility with phosphorus nuclear magnetic resonance spectroscopy. *Anesthesiology,* **68,** 507-13.

68. Argov, Z., Lofberg, M. and Arnold, D.L. (2000) Insights into muscle diseases gained by phosphorus magnetic resonance spectroscopy. *Muscle Nerve,* **23,** 1316-34.

69. Censier, K., Urwyler, A., Zorzato, F. and Treves, S. (1998) Intracellular calcium homeostasis in human primary muscle cells from malignant hyperthermia-susceptible and normal individuals. Effect Of overexpression of recombinant wild-type and Arg163Cys mutated ryanodine receptors. *J. Clin. Invest.*, **101,** 1233-42.

70. Snoeck, M.M., Oosterhof, A., Tangerman, A., Veerkamp, J.H., van Engelen, B.G. and Gielen, M.J. (2002) Halothane-induced calcium release in cultured human skeletal muscle cells from a family susceptible to malignant hyperthermia with an unidentified mutation in chromosome 19. *Anesthesiology,* **97,** 272-4.

71. Girard, T., Treves, S., Censier, K., Mueller, C.R., Zorzato, F. and Urwyler, A. (2002) Phenotyping malignant hyperthermia susceptibility by measuring halothane-induced changes in myoplasmic calcium concentration in cultured human skeletal muscle cells. *Br. J. Anaesth.*, **89,** 571-9.

72. Klingler, W., Baur, C., Georgieff, M., Lehmann-Horn, F. and Melzer, W. (2002) Detection of proton release from cultured human myotubes to identify malignant hyperthermia susceptibility. *Anesthesiology,* **97,** 1059-66.

73. Anetseder, M., Hager, M., Muller, C.R. and Roewer, N. (2002) Diagnosis of susceptibility to malignant hyperthermia by use of a metabolic test. *Lancet,* **359,** 1579-80.

74. Sei, Y., Gallagher, K.L. and Basile, A.S. (1999) Skeletal muscle type ryanodine receptor is involved in calcium signaling in human B lymphocytes. *J. Biol. Chem.*, **274,** 5995-6002.

75. Girard, T., Cavagna, D., Padovan, E., Spagnoli, G., Urwyler, A., Zorzato, F. and Treves, S. (2001) B-lymphocytes from malignant hyperthermia-susceptible patients have an increased sensitivity to skeletal muscle ryanodine receptor activators. *J. Biol. Chem.*, **276,** 48077-82.

76. Sei, Y., Brandom, B.W., Bina, S., Hosoi, E., Gallagher, K.L., Wyre, H.W., Pudimat, P.A., Holman, S.J., Venzon, D.J., Daly, J.W. *et al.* (2002) Patients with malignant hyperthermia demonstrate an altered calcium control mechanism in B lymphocytes. *Anesthesiology,* **97,** 1052-8.

77. Denborough, M.A., Dennett, X. and Anderson, R.M. (1973) Central-core disease and malignant hyperpyrexia. *Br. Med. J.*, **1,** 272-3.

78. King, J.O. and Denborough, M.A. (1973) Anesthetic-induced malignant hyperpyrexia in children. *J. Pediatr.*, **83,** 37-40.

79. Chitayat, D., Hodgkinson, K.A., Ginsburg, O., Dimmick, J. and Watters, G.V. (1992) King syndrome: a genetically heterogenous phenotype due to congenital myopathies. *Am. J. Med. Genet.*, **43,** 954-6.

80. Brownell, A.K. (1988) Malignant hyperthermia: relationship to other diseases. *Br. J. Anaesth.*, **60,** 303-8.

81. Denborough, M.A., Galloway, G.J. and Hopkinson, K.C. (1982) Malignant hyperpyrexia and sudden infant death. *Lancet,* **2,** 1068-9.

82. Peterson, D.R. and Davis, N. (1986) Sudden infant death syndrome and malignant hyperthermia diathesis. *Aust. Paediatr. J.*, **22,** 33-5.

83. Stanton, A.N., Scott, D.J. and Downham, M.A. (1980) Is overheating a factor in some unexpected infant deaths? *Lancet,* **1,** 1054-7.

84. Nelson, E.A., Taylor, B.J. and Weatherall, I.L. (1989) Sleeping position and infant bedding may predispose to hyperthermia and the sudden infant death syndrome. *Lancet,* **1,** 199-201.

85. Hall, L.W., Woolf, N., Bradley, J.W. and Jolly, D.W. (1966) Unusual reaction to suxamethonium chloride. *Br. Med. J.*, **2,** 1305.

86. Davies, W., Harbitz, I., Fries, R., Stranzinger, G. and Hauge, J.G. (1988) Porcine malignant hyperthermia carrier detection and chromosomal assignment using a linked probe. *Anim. Genet.*, **19**.

87. Topel, D.G., Bicknell, E.J., Preston, K.S., Christian, L.L. and Matsushima, C.Y. (1968) Porcine stress syndrome. *Mod. Vet. Pract.*, **49,** 40-41,59-60.

88. Nelson, T.E. (1983) Abnormality in calcium release from skeletal sarcoplasmic reticulum of pigs susceptible to malignant hyperthermia. *J. Clin. Invest.*, **72,** 862-70.

89. Kim, D.H., Sreter, F.A., Ohnishi, S.T., Ryan, J.F., Roberts, J., Allen, P.D., Meszaros, L.G., Antoniu, B. and Ikemoto, N. (1984) Kinetic studies of Ca^{2+} release from sarcoplasmic reticulum of normal and malignant hyperthermia susceptible pig muscles. *Biochim. Biophys. Acta.*, **775,** 320-7.

90. Harbitz, I., Chowdhary, B., Thomsen, P.D., Davies, W., Kaufmann, U., Kran, S., Gustavsson, I., Christensen, K. and Hauge, J.G. (1990) Assignment of the porcine calcium release channel gene, a candidate for the malignant hyperthermia locus, to the 6p11----q21 segment of chromosome 6. *Genomics,* **8,** 243-8.

91. Mickelson, J.R., Knudson, C.M., Kennedy, C.F., Yang, D.I., Litterer, L.A., Rempel, W.E., Campbell, K.P. and Louis, C.F. (1992) Structural and functional correlates of a mutation in the malignant hyperthermia-susceptible pig ryanodine receptor. *FEBS Lett.*, **301,** 49-52.

92. Fletcher, J.E., Calvo, P.A. and Rosenberg, H. (1993) Phenotypes associated with malignant hyperthermia susceptibility in swine genotyped as homozygous or heterozygous for the ryanodine receptor mutation. *Br. J. Anaesth.*, **71,** 410-7.

93. Rempel, W.E., Lu, M., el Kandelgy, S., Kennedy, C.F., Irvin, L.R., Mickelson, J.R. and Louis, C.F. (1993) Relative accuracy of the halothane challenge test and a molecular genetic test in detecting the gene for porcine stress syndrome. *J Anim. Sci.*, **71,** 1395-9.

94. Short, C.E. and Paddleford, R.R. (1973) Letter: Malignant hyperthermia in the dog. *Anesthesiology*, **39,** 462-3.

95. Roberts, M.C., Mickelson, J.R., Patterson, E.E., Nelson, T.E., Armstrong, P.J., Brunson, D.B. and Hogan, K. (2001) Autosomal dominant canine malignant hyperthermia is caused by a mutation in the gene encoding the skeletal muscle calcium release channel (*RYR1*). *Anesthesiology*, **95,** 716-25.

96. de Jong, R.H., Heavner, J.E. and Amory, D.W. (1974) Malignant hyperpyrexia in the cat. *Anesthesiology*, **41,** 608-9.

97. Bellah, J.R., Robertson, S.A., Buergelt, C.D. and McGavin, A.D. (1989) Suspected malignant hyperthermia after halothane anesthesia in a cat. *Vet. Surg.*, **18,** 483-8.

98. Waldron-Mease, E., Klein, L.V., Rosenberg, H. and Leitch, M. (1981) Malignant hyperthermia in a halothane-anesthetized horse. *J. Am. Vet. Med. Assoc.*, **179,** 896-8.

99. Manley, S.V., Kelly, A.B. and Hodgson, D. (1983) Malignant hyperthermia-like reactions in three anesthetized horses. *J. Am. Vet. Med. Assoc.*, **183,** 85-9.

100. MacLennan, D.H., Duff, C., Zorzato, F., Fujii, J., Phillips, M., Korneluk, R.G., Frodis, W., Britt, B.A. and Worton, R.G. (1990) Ryanodine Receptor Gene Is a Candidate for Predisposition to Malignant Hyperthermia. *Nature*, **343,** 559-561.

101. McCarthy, T.V., Healy, J.M.S., Heffron, J.J.A., Lehane, M., Deufel, T., Lehmannhorn, F., Farrall, M. and Johnson, K. (1990) Localization of the Malignant Hyperthermia Susceptibility Locus to Human-Chromosome 19q12-13.2. *Nature*, **343,** 562-564.

102. Rueffert, H., Olthoff, D., Deutrich, C., Thamm, B. and Froster, U.G. (2001) Homozygous and heterozygous Arg614Cys mutations (1840C-->T) in the ryanodine receptor gene co-segregate with malignant hyperthermia susceptibility in a German family. *Br. J. Anaesth.*, **87,** 240-5.

103. Sambuughin, N., McWilliams, S., de Bantel, A., Sivakumar, K. and Nelson, T.E. (2001) Single-amino-acid deletion in the *RYR1* gene, associated with malignant hyperthermia susceptibility and unusual contraction phenotype. *Am. J. Hum. Genet.*, **69,** 204-8.

104. Tong, J., Oyamada, H., Demaurex, N., Grinstein, S., McCarthy, T.V. and MacLennan, D.H. (1997) Caffeine and halothane sensitivity of intracellular Ca^{2+} release is altered by 15 calcium release channel (ryanodine receptor) mutations associated with malignant hyperthermia and/or central core disease. *J. Biol. Chem.*, **272,** 26332-9.

105. Yang, T., Ta, T.A., Pessah, I.N. and Allen, P.D. (2003) Functional defects in six ryanodine receptor isoform-1 (*RyR1*) mutations associated with malignant hyperthermia and their impact on skeletal excitation-contraction coupling. *J. Biol. Chem.*, **278,** 25722-30.

106. Tong, J., McCarthy, T.V. and MacLennan, D.H. (1999) Measurement of resting cytosolic Ca^{2+} concentrations and Ca^{2+} store size in HEK-293 cells transfected with malignant hyperthermia or central core disease mutant Ca^{2+} release channels. *J. Biol. Chem.*, **274,** 693-702.

107. Fiege, M., Wappler, F., Weisshorn, R., Ulrich Gerbershagen, M., Steinfath, M. and Schulte Am Esch, J. (2002) Results of contracture tests with halothane, caffeine, and ryanodine depend on different malignant hyperthermia-associated ryanodine receptor gene mutations. *Anesthesiology,* **97,** 345-50.

108. Quane, K.A., Healy, J.M., Keating, K.E., Manning, B.M., Couch, F.J., Palmucci, L.M., Doriguzzi, C., Fagerlund, T.H., Berg, K., Ording, H. *et al.* (1993) Mutations in the ryanodine receptor gene in central core disease and malignant hyperthermia. *Nat. Genet.*, **5,** 51-5.

109. Gillard, E.F., Otsu, K., Fujii, J., Duff, C., de Leon, S., Khanna, V.K., Britt, B.A., Worton, R.G. and MacLennan, D.H. (1992) Polymorphisms and deduced amino acid substitutions in the coding sequence of the ryanodine receptor (*RYR1*) gene in individuals with malignant hyperthermia. *Genomics,* **13,** 1247-54.

110. Quane, K.A., Keating, K.E., Manning, B.M., Healy, J.M., Monsieurs, K., Heffron, J.J., Lehane, M., Heytens, L., Krivosic-Horber, R., Adnet, P. *et al.* (1994) Detection of a novel common mutation in the ryanodine receptor gene in malignant hyperthermia: implications for diagnosis and heterogeneity studies. *Hum. Mol. Genet.*, **3,** 471-6.

111. Manning, B.M., Quane, K.A., Ording, H., Urwyler, A., Tegazzin, V., Lehane, M., O'Halloran, J., Hartung, E., Giblin, L.M., Lynch, P.J. *et al.* (1998) Identification of novel mutations in the ryanodine-receptor gene (*RYR1*) in malignant hyperthermia: genotype-phenotype correlation. *Am. J. Hum. Genet.*, **62,** 599-609.

112. Keating, K.E., Quane, K.A., Manning, B.M., Lehane, M., Hartung, E., Censier, K., Urwyler, A., Klausnitzer, M., Muller, C.R., Heffron, J.J. *et al.* (1994)

Detection of a novel *RYR1* mutation in four malignant hyperthermia pedigrees. *Hum. Mol. Genet.*, **3,** 1855-8.

113. Brown, R.L., Pollock, A.N., Couchman, K.G., Hodges, M., Hutchinson, D.O., Waaka, R., Lynch, P., McCarthy, T.V. and Stowell, K.M. (2000) A novel ryanodine receptor mutation and genotype-phenotype correlation in a large malignant hyperthermia New Zealand Maori pedigree. *Hum. Mol. Genet.*, **9,** 1515-1524.

114. Lynch, P.J., Tong, J., Lehane, M., Mallet, A., Giblin, L., Heffron, J.J., Vaughan, P., Zafra, G., MacLennan, D.H. and McCarthy, T.V. (1999) A mutation in the transmembrane/luminal domain of the ryanodine receptor is associated with abnormal Ca^{2+} release channel function and severe central core disease. *Proc. Natl. Acad. Sci. USA*, **96,** 4164-9.

115. Jurkat-Rott, K., Hang, C. and Sipos, I. (2000) III-IV loop of cardiac L-type calcium channel contributes to fast inactivation as implied by a naturally occuring disease-causing mutation. *The EMHG Meeting*. p. 40.

116. Monnier, N., Procaccio, V., Stieglitz, P. and Lunardi, J. (1997) Malignant-hyperthermia susceptibility is associated with a mutation of the alpha(1)-subunit of the human dihydropyridine-sensitive L-type voltage-dependent calcium-channel receptor in skeletal muscle. *Am. J. Hum. Genet.*, **60,** 1316-1325.

117. Fletcher, J.E., Tripolitis, L., Hubert, M., Vita, G.M., Levitt, R.C. and Rosenberg, H. (1995) Genotype and phenotype relationships for mutations in the ryanodine receptor in patients referred for diagnosis of malignant hyperthermia. *Br. J. Anaesth.*, **75,** 307-10.

118. Healy, J.M., Quane, K.A., Keating, K.E., Lehane, M., Heffron, J.J. and McCarthy, T.V. (1996) Diagnosis of malignant hyperthermia: a comparison of the in vitro contracture test with the molecular genetic diagnosis in a large pedigree. *J. Med. Genet.*, **33,** 18-24.

119. Rueffert, H., Olthoff, D., Deutrich, C. and Froster, U.G. (2001) Determination of a positive malignant hyperthermia (MH) disposition without the in vitro contracture test in families carrying the *RYR1* Arg614Cys mutation. *Clin. Genet.*, **60,** 117-24.

120. Deufel, T., Golla, A., Iles, D., Meindl, A., Meitinger, T., Schindelhauer, D., DeVries, A., Pongratz, D., MacLennan, D.H., Johnson, K.J. *et al.* (1992) Evidence for genetic heterogeneity of malignant hyperthermia susceptibility. *Am. J. Hum. Genet.*, **50,** 1151-61.

121. Fagerlund, T.H., Ording, H., Bendixen, D., Islander, G., Ranklev Twetman, E. and Berg, K. (1997) Discordance between malignant hyperthermia susceptibility and *RYR1* mutation C1840T in two Scandinavian MH families exhibiting this mutation. *Clin. Genet.*, **52,** 416-21.

122. Serfas, K.D., Bose, D., Patel, L., Wrogemann, K., Phillips, M.S., MacLennan, D.H. and Greenberg, C.R. (1996) Comparison of the segregation of the *RYR1* C1840T mutation with segregation of the caffeine/halothane contracture test results for malignant hyperthermia susceptibility in a large Manitoba Mennonite family. *Anesthesiology,* **84,** 322-9.

123. Urwyler, A., Deufel, T., McCarthy, T. and West, S. (2001) Guidelines for molecular genetic detection of susceptibility to malignant hyperthermia. *Br. J. Anaesth.,* **86,** 283-287.

124. Robinson, R.L., Monnier, N., Wolz, W., Jung, M., Reis, A., Nuernberg, G., Curran, J.L., Monsieurs, K., Stieglitz, P., Heytens, L. *et al.* (1997) A genome wide search for susceptibility loci in three European malignant hyperthermia pedigrees. *Hum. Mol. Genet.,* **6,** 953-961.

125. Sudbrak, R., Procaccio, V., Klausnitzer, M., Curran, J.L., Monsieurs, K., van Broeckhoven, C., Ellis, R., Heyetens, L., Hartung, E.J., Kozak-Ribbens, G. *et al.* (1995) Mapping of a further malignant hyperthermia susceptibility locus to chromosome 3q13.1. *Am. J. Hum. Genet.,* **56,** 684-91.

126. Iles, D.E., Lehmann-Horn, F., Scherer, S.W., Tsui, L.C., Olde Weghuis, D., Suijkerbuijk, R.F., Heytens, L., Mikala, G., Schwartz, A., Ellis, F.R. *et al.* (1994) Localization of the gene encoding the alpha 2/delta-subunits of the L-type voltage-dependent calcium channel to chromosome 7q and analysis of the segregation of flanking markers in malignant hyperthermia susceptible families. *Hum. Mol. Genet.,* **3,** 969-75.

127. Iles, D.E., Segers, B., Sengers, R.C., Monsieurs, K., Heytens, L., Halsall, P.J., Hopkins, P.M., Ellis, F.R., Hall-Curran, J.L., Stewart, A.D. *et al.* (1993) Genetic mapping of the beta 1- and gamma-subunits of the human skeletal muscle L-type voltage-dependent calcium channel on chromosome 17q and exclusion as candidate genes for malignant hyperthermia susceptibility. *Hum. Mol. Genet.,* **2,** 863-8.

128. Davis, M., Brown, R.L., Dickson, A., Horton, H., James, D., Laing, N., Marston, R., Norgate, M., Perlman, D. and Stowell, K.M. (2002) Malignant hyperthermia associated with exercise-induced rhabdmyolysis or congenital abnormalities and a novel *RYR1* mutation in New Zealand and Australian pedigrees. *Br. J. Anaesth.,* **88,** 508-515.

129. Brown, R.L. (2000) A genetic test for malignant hyperthermia. *Institute of Molecular Biosciences.* Massey University, Palmerston North, p. 223.

130. Chomczynski, P. and Sacchi, N. (1987) Single-step method of RNA isolation by acid guanidinium thiocyanate-phenol-chloroform extraction. *Anal. Biochem.,* **162,** 156-9.

131. Miller, S.A., Dykes, D.D. and Polesky, H.F. (1988) A simple salting out procedure for extracting DNA from human nucleated cells. *Nucl. Acids Res.,* **1,** 1215.

132. Saiki, R.K., Scharf, S., Faloona, F., Mullis, K.B., Horn, G.T., Erlich, H.A. and Arnheim, N. (1985) Enzymatic amplification of beta-globin genomic sequences and restriction site analysis for diagnosis of sickle cell anemia. *Science,* **230,** 1350-1354.

133. Innis, M.A., Gelfand, D.H., Sinsky, J.J. and White, T.J. (1990) *PCR protocols, a guide to methods and applications*. Academic Press, San Diego, California.

134. Rychlik, W., Spencer, W.J. and Rhoads, R.E. (1990) Optimization of the annealing temperature for DNA amplification in vitro. *Nucleic Acids Res.,* **18,** 6409-6412.

135. Don, R.H., Cox, P.T., Wainwright, B.J., Baker, K. and Mattick, J.S. (1991) "Touchdown" PCR to circumvent spurious priming during gene amplification. *Nucleic Acids Res.,* **19,** 4008.

136. Li, H., Cui, X. and Arnheim, N. (1990) Direct electrophoretic detection of the allelic state of single DNA molecules in human sperm by using the polymerase chain reaction. *Proc. Natl. Acad. Sci. USA,* **87,** 4580-4584.

137. Varadaraj, K. and Skinner, D.M. (1994) Denaturants or cosolvents improve the specificity of PCR amplification of a G+C-rich DNA using genetically engineered DNA polymerases. *Gene,* **140,** 1-5.

138. Morrison, T.B., Weis, J.J. and Wittwer, C.T. (1998) Quantification of low-copy transcripts by continous SYBR Green I monitoring during amplification. *Biotechniques,* **24,** 954-962.

139. Thompson, J.D., Higgins, D.G. and Gibson, T.J. (1994) CLUSTAL W: improving the sensitivity of progressive multiple sequence alignment through sequence weighting, positions-specific gap penalties and weight matrix choice. *Nucleic Acids Res.,* **22,** 4673-4680.

140. Stewart, S.L., Hogan, K., Rosenberg, H. and Fletcher, J.E. (2001) Identification of the Arg1086His mutation in the alpha subunit of the voltage-dependent calcium channel (*CACNA1S*) in a North American family with malignant hyperthermia. *Clin. Genet.,* **59,** 178-84.

141. Gyapay, G., Morissette, J., Vignal, A., Dib, C., Fizames, C., Millasseau, P., Marc, S., Bernardi, G., Lathrop, M. and Weissenbach, J. (1994) The 1993-94 Genethon human genetic linkage map. *Nat. Genet.,* **7,** 246-339.

142. Weissenbach, J., Gyapay, G., Dib, C., Vignal, A., Morissette, J., Millasseau, P., Vaysseix, G. and Lathrop, M. (1992) A second-generation linkage map of the human genome. *Nature,* **359,** 794-801.

143. Weber, J.L. and May, P.E. (1989) Abundant class of human DNA polymorphisms which can be typed using the polymerase chain reaction. *Am. J. Hum. Genet.,* **44,** 388-396.

144. Kruglyak, L., Daly, M.J., Reeve-Daly, M.P. and Lander, E.S. (1996) Parametric and Nonparametric Linkage Analysis: A Unified Multipoint Approach. *Am. J. Hum. Genet.*, **58,** 1347-1367.

145. Kong, A. and Cox, N.J. (1997) Allele-sharing models: LOD scores and accurate linkage tests. *Am. J. Hum. Genet.*, **61,** 1179-1188.

146. Cottingham, R.W., Idury, R.M. and Schaffer, A.A. (1993) Faster Sequential Genetic-Linkage Computations. *Am. J. Hum. Genet.*, **53,** 252-263.

147. Chamley, D., Pollock, N.A., Stowell, K.M. and Brown, R.L. (2000) Malignant hyperthermia in infancy and identification of novel *RYR1* mutation. *Br. J. Anaesth.*, **84,** 500-504.

148. Orita, M., Iwahana, H., Kanezawa, H., Hayashi, K. and Sekiya, T. (1989) Detection of polymorphisms of human DNA by gel electrophoresis as single-strand conformation polymorphisms. *Proc. Natl. Acad. Sci. USA,* **86,** 2766-2770.

149. Sheffield, V.C., Beck, J.S., Kwitek, A.E. and Sandstram, D.W. (1993) The sensitivity of single-strand conformation polymorphism analysis for the detection of single base substitutions. *Genomics,* **16,** 325-332.

150. Monnier, N., Romero, N.B., Lerale, J., Nivoche, Y., Qi, D., MacLennan, D.H., Fardeau, M. and Lunardi, J. (2000) An autosomal dominant congenital myopathy with cores and rods is associated with a neomutation in the *RYR1* gene encoding the skeletal muscle ryanodine receptor. *Hum. Mol. Genet.*, **9,** 2599-608.

151. Altmuller, J., Palmer, L.J., Fischer, G., Scherb, H. and Wjst, M. (2001) Genomewide scans of complex human diseases: True linkage is hard to find. *Am. J. Hum. Genet.*, **69,** 936-950.

152. Terwilliger, J.D. and Ott, J. (1994) *Handbook of Human Genetic Linkage*. John Hopkins University Press.

153. Norgate, M. (1999) The genetic basis of malignant hyperthermia in New Zealand families. *Institute of molecular biosciences.* Massey University, Palmerston North, p. 63.

154. Burgess, D.L., Gefrides, L.A., Foreman, P.J. and Noebels, J.L. (2001) A cluster of three novel Ca^{2+} channel gamma subunit genes on chromosome 19q13.4: evolution and expression profile of the gamma subunit gene family. *Genomics,* **71,** 339-350.

155. Scriver, C.R. and Waters, P.J. (1999) Monogenic traits are not simple: lessons from phenylketonuria. *Trends. Genet.*, **15,** 267-272.

156. Burgess, D.L., Davis, C.F., Gefrides, L.A. and Noebels, J.L. (1999) Identification of three novel Ca(2+) channel gamma subunit genes reveals

molecular diversification by tandem and chromosome duplication. *Genome Res.*, **9,** 1204-1213.

157. Lio, P. and Morton, N.E. (1997) Comparison of parametric and nonparametric methods to map oligogenes by linkage. *Proc. Natl. Acad. Sci. USA*, **94,** 5344-5348.

158. Sham, P.C., Lin, M.W., Zhao, J.H. and Curtis, D. (2000) Power comparison of parametric and nonparametric linkage tests in small pedigrees. *Am. J. Hum. Genet.*, **66,** 1661-1668.

159. Thomson, G. (2001) An overview of the genetic analysis of complex diseases, with reference to type 1 diabetes. *Best Pract. Res. Clin. Endocrinol. Metab.*, **15,** 265-277.

APPENDICES

Appendix 1 Primers for PCR and sequencing of *RYR1* cDNA

Primers are listed according to position on *RYR1* sequence (from 5' terminus)

Primer	Forward/Reverse	Sequence 5'-3'	Reaction
-7	F	TTCCGACCTCGACATCATGGGTGACG	PCR
163F-bio	F	TCCAAGCAGAGGTCTGAAGGAGAA	PCR, Sequencing
163R	R	AGCGCTCGGAGGAGACACTGACAA	PCR
163R-seq	R	GGAGACACTGACAAGGAT	Sequencing
248F-bio	F	TGCTGACAGTGATGACCAGCGCAG	PCR
248R-seq	R	GTGGCTCCAGCCTCCAGA	Sequencing
952	F	TCCAAGGAGAAGCTGGATGT	PCR
341R	R	TCTGGAGCGGCATAGGTGAG	PCR
1204	R	GCCATTGGTGCTGTGGATCAT	Sequencing
403R-bio	R	GTTGTATAGGCCATTGGTGCT	PCR
522Fwt	F	GGAAAGAGATTGTGAATCTTGTCT	PCR, Sequencing
522R-bio	R	ACCAGCCAGTCCAAGTTTGTGGAG	Sequencing
1755	R	TGCTTGTCCAGGAGGGAAGATG	PCR
1927	F	CATCCGCCCCAACATCTTTGTG	PCR, Sequencing
1993	R	AGTCACCTCGTCCACCATCAC	PCR
2447	F	CTCGAGAGCGACTCCATCTTG	Sequencing
2536	R	GGGCACGAACTCGGTGTGTGA	Sequencing
2859	F	ATGAGCAATGGGTACAAGCC	PCR, Sequencing
3065	R	CTTCATCCAGCAGGCGGTAGG	PCR
3277	F	GCAGTCACCACAGGCGAGATG	Sequencing
3880	F	GTCCAGTTCCACCAGCACTTC	Sequencing
4262	F	ACCCCGAGATCATCCTCAACA	PCR
4296	R	GCAAAGACCCTCACGGAGTAA	PCR, Sequencing
4520	F	TCAGCCACACGGACCTTGTCA	PCR
4766	F	GCCCACCGCGGCTGGAGATG	Sequencing
4800	R	GGCATGCGGCTCCAGGACACT	PCR, Sequencing
5137	R	CACTTTCGAGGTGGATGCTGATGAG	Sequencing
5285	F	CGGGAGTTGGAGTCACCACTT	PCR, Sequencing
5430	R	GCCTCCCCCAGCATCCTCAGT	Sequencing
5555	R	TCACATCCTCATCGCCAAAGA	PCR
5880	F	TGCGGAGCGCTATGTGGACAA	Sequencing
6376	F	CAGTACGACGGGCTGGGTGAG	PCR

6763	R	GCCACTGTTCTCCAGCAGGTA	PCR
7039	R	CACCACCACATTGGCGTTCTC	Sequencing
7361	F	CCATCCTCCGCTCCCTTGTG	PCR
7393	R	GAGGCTGATGATGCCCACAAG	PCR, Sequencing
7699	R	GTGTTCTGTGCCCGCAAAGAG	Sequencing
8025	R	AAAGATGCCCCAGAAGAGTTTC	Sequencing
8525	F	CACAAAGTGCCCAGACCTATG	PCR
8582	R	GGGACAGGGTAACAGCACTAA	Sequencing
8789	R	TAACCGCGTAGCCATTCATCT	PCR
9022	R	GAGGCAGTGGTGGTGAAGTA	Sequencing
9442	F	CAGCACCAGTTCGGAGATGA	PCR
9485	R	CAGCGTTCGGTAGCAAGAGA	PCR, Sequencing
9696	F	CAACAGTGTGGAGGAGATGTGTC	Sequencing
9769	R	TGTGTAGCGGGCACCTGACTC	Sequencing
10052	F	AGCTCCTGCAGTCCCACTTCA	PCR
10109	R	CTCCTCCTCGGACACCACCT	PCR
10809	F	CGAGCACCCTTACAAGTCTAA	PCR, Sequencing
10884	R	AGGGGCGTCATACGGAAACAG	Sequencing
11213	R	AGACCTCAACCTCCTCTTCAG	PCR
11307	F	CGAGATGGTGCTGCAGATGAT	PCR, Sequencing
11725	F	TCATTTGCACTGTGGACTACCTC	PCR, Sequencing
11787	R	ATGACATCCTTGCCCGAGTAG	PCR
11924	R	TGCGTCCCATAGGCGACTGT	PCR
12337	F	CGAAATGATCAACTGCGAAGAGTTC	PCR
12418	R	ATGCTCCGACAGGTTGGTCAG	PCR
12575	F	GAGACCAACCGCGCCCAGTG	PCR
12753	R	CCCTCGTCCTCGTCGGTCTCC	PCR, Sequencing
13285	F	GACGGGGCGGTGGCCGTGAC	PCR
13356	R	GGTTCCGCAGGCGTCGTGTCC	PCR, Sequencing
13377	F	GCCCACACCCGAGGGCTCTC	PCR, Sequencing
13731	R	TCCCCTGGTGGAGAGTCTGAG	PCR, Sequencing
13903	F	GAACCCGCCCTGCGGTGTCTG	PCR
13973	R	TTACCAGGGGCACCTTGAGAC	PCR
14462	F	ACCTGGGCTGGTATATGGTG	PCR
14512	R	GTAGACGACCACCGCCAGAAG	PCR, Sequencing
15137	R	GGGCTTGCTGTGAGAATAAGG	PCR, Sequencing

All primers were diluted to 1 or 10μg/μL in TE, and stored at -20°C until use. Primers were donated by Professor Tommie McCarthy, University of Cork, Ireland, or purchased from Sigma-Aldrich Pty. Ltd., Castle Hill, Australia.

Appendix 2 *RYR1* cDNA sequence

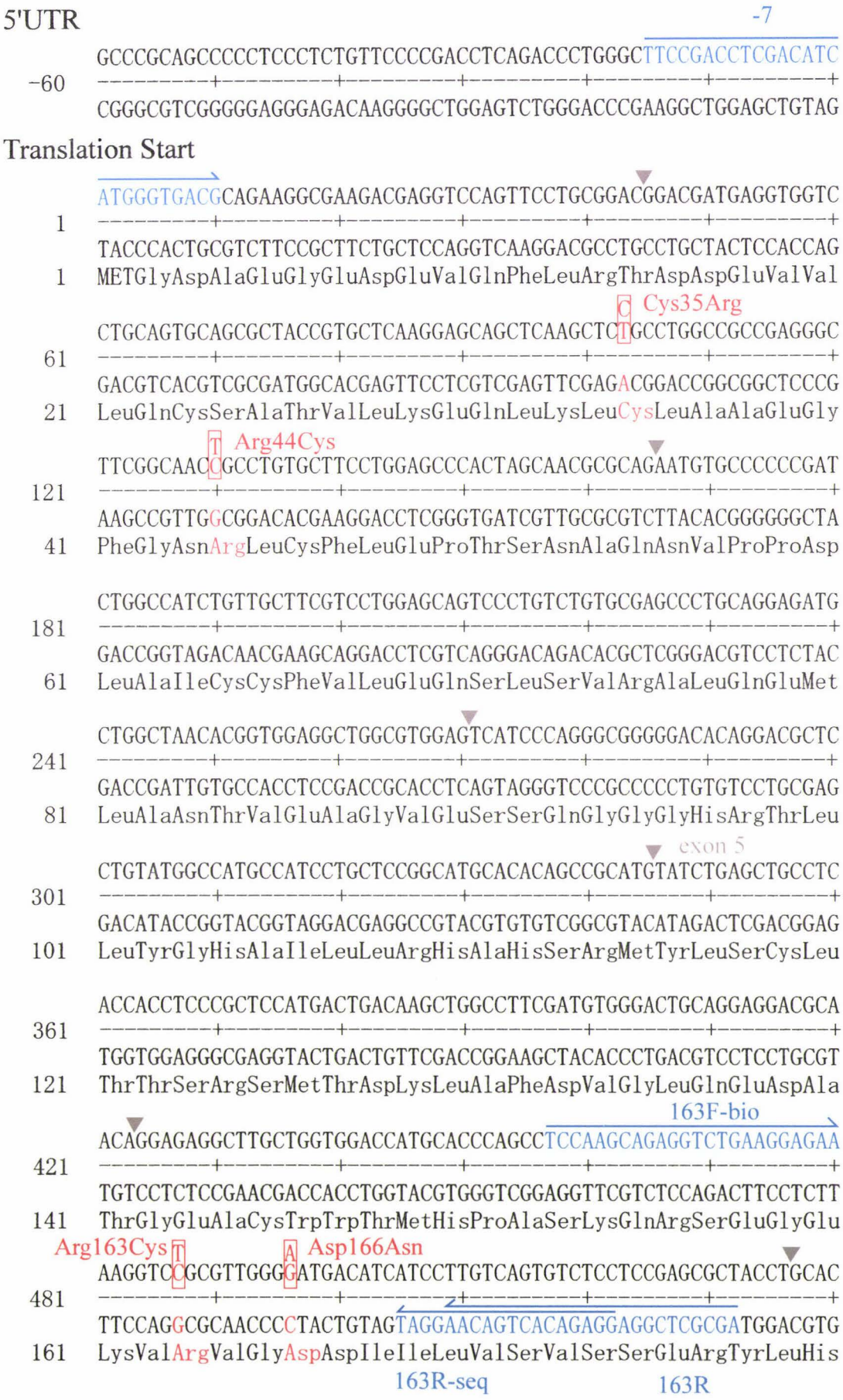


Leu198
Gly216
248F-bio
Gly248Arg
exon 10
952
Arg328Trp
Gly341Arg
Ala359
341R


Arg401His
Arg401Cys
Ile403Met
1204
403R-bio
522Fwt
Tyr522Ser
exon 15
Arg533Cys
Arg533His
Arg552Trp
Ser556
522R-bio
1755
Arg614Cys
Arg614Leu

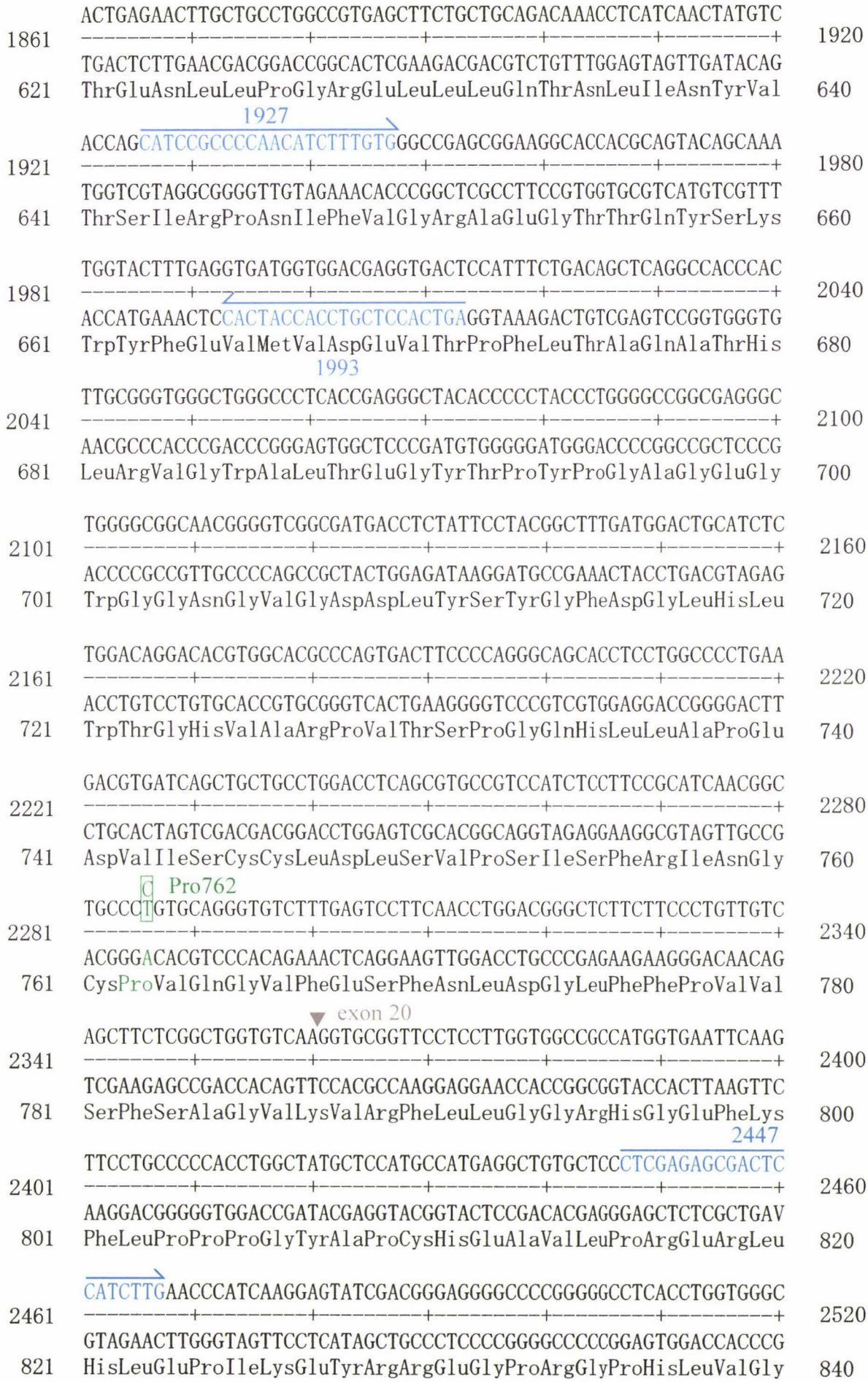
1927
1993
C Pro762
exon 20
2447


2536
2859
G Thr981
T Tyr1006
3065


exon 25
3277


3880
AGCCTGGTGGAGATGCTTTTCCTGCGGCTGAGCCTCCCAGTCCAGTTCCACCAGCACTTC
3841
3900
TCGGACCACCTCTACGAAAAGGACGCCGACTCGGAGGGTCAGGTCAAGGTGGTCGTGAAG
1281
SerLeuValGluMetLeuPheLeuArgLeuSerLeuProValGlnPheHisGlnHisPhe
1300
CGCTGCACTGCAGGGGCCACCCCGCTGGCACCTCCTGGCCTGCAGCCCCCCGCCGAGGAC
3901
3960
GCGACGTGACGTCCCCGGTGGGGCGACCGTGGAGGACCGGACGTCGGGGGGCGGCTCCTG
1301
ArgCysThrAlaGlyAlaThrProLeuAlaProProGlyLeuGlnProProAlaGluAsp
1320
GAGGCCCGGGCGGCGGAACCCGACCCTGACTACGAAAACCTGCGCCGCTCAGCTGGGGGC
3961
4020
CTCCGGGCCCGCCGCCTTGGGCTGGGACTGATGCTTTTGGACGCGGCGAGTCGACCCCCG
1321
GluAlaArgAlaAlaGluProAspProAspTyrGluAsnLeuArgArgSerAlaGlyGly
1340
TGGAGCGAGGCAGAGAACGGCAAAGAAGGGACTGCGAAGGAGGGCGCCCCCGGGGGCACC
4021
4080
ACCTCGCTCCGTCTCTTGCCGTTTCTTCCCTGACGCTTCCTCCCGCGGGGGCCCCCGTGG
1341
TrpSerGluAlaGluAsnGlyLysGluGlyThrAlaLysGluGlyAlaProGlyGlyThr
1360
CCGCAGGCGGGGGGAGAGGCGCAGCCCGCCAGGGCGGAGAATGAGAAGGATGCCACCACC
4081
4140
GGCGTCCGCCCCCCTCTCCGCGTCGGGCGGTCCCGCCTCTTACTCTTCCTACGGTGGTGG
1361
ProGlnAlaGlyGlyGluAlaGlnProAlaArgAlaGluAsnGluLysAspAlaThrThr
1380
GAGAAGAACAAGAAGAGAGGCTTCTTATTCAAGGCCAAGAAGGTCGCCATGATGACCCAG
4141
4200
CTCTTCTTGTTCTTCTCTCCGAAGAATAAGTTCCGGTTCTTCCAGCGGTACTACTGGGTC
1381
GluLysAsnLysLysArgGlyPheLeuPheLysAlaLysLysValAlaMetMetThrGln
1400
CCACCGGCCACCCCCACGCTGCCCCGACTCCCTCACGACGTGGTGCCTGCAGACAACCGC
4201
4260
GGTGGCCGGTGGGGGTGCGACGGGGCTGAGGGAGTGCTGCACCACGGACGTCTGTTGGCG
1401
ProProAlaThrProThrLeuProArgLeuProHisAspValValProAlaAspAsnArg
1420
4262
exon 30
GATGACCCCGAGATCATCCTCAACACCACCACGTACTATTACTCCGTGAGGGTCTTTGCT
4261
4320
CTACTGGGGCTCTAGTAGGAGTTGTGGTGGTGCATGATAATGAGGCACTCCCAGAAACGA
1421
AspAspProGluIleIleLeuAsnThrThrThrTyrTyrTyrSerValArgValPheAla
1440
4296
GGACAGGAGCCCAGCTGCGTGTGGGCGGGCTGGGTCACCCCTGACTACCATCAGCACGAC
4321
4380
CCTGTCCTCGGGTCGACGCACACCCGCCCGACCCAGTGGGGACTGATGGTAGTCGTGCTG
1441
GlyGlnGluProSerCysValTrpAlaGlyTrpValThrProAspTyrHisGlnHisAsp
1460
ATGAGCTTCGACCTCAGCAAGGTCCGGGTCGTGACGGTGACCATGGGGGATGAACAAGGC
4380
4440
TACTCGAAGCTGGAGTCGTTCCAGGCCCAGCACTGCCACTGGTACCCCCTACTTGTTCCG
1461
MetSerPheAspLeuSerLysValArgValValThrValThrMetGlyAspGluGlnGly
1480
AACGTCCACAGCAGCCTCAAGTGTAGCAACTGCTACATGGTGTGGGGCGGAGACTTTGTG
4441
4500
TTGCAGGTGTCGTCGGAGTTCACATCGTTGACGATGTACCACACCCCGCCTCTGAAACAC
1481
AsnValHisSerSerLeuLysCysSerAsnCysTyrMetValTrpGlyGlyAspPheVal
1500

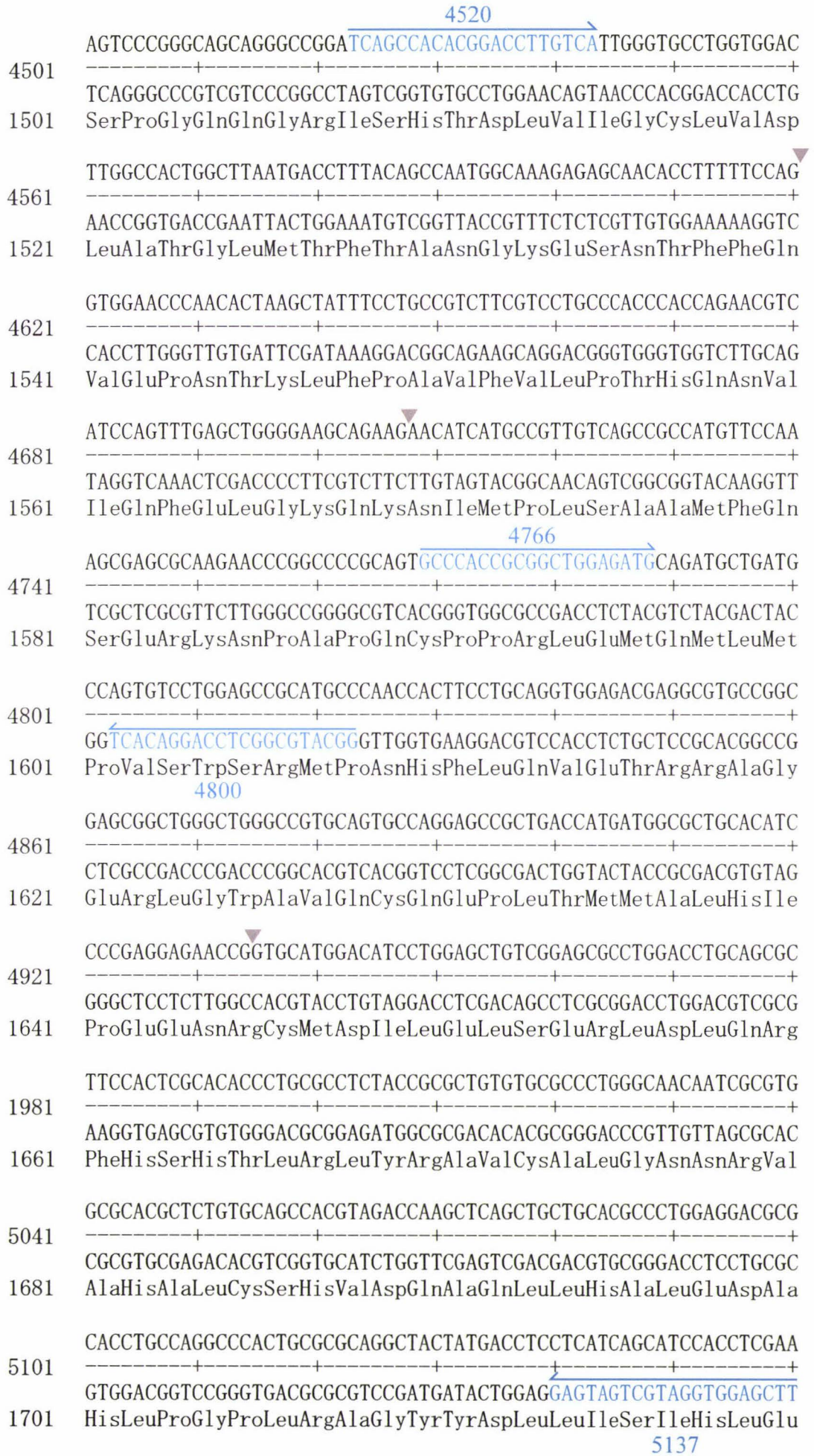
4520
AGTCCCGGGCAGCAGGGCCGGATCAGCCACACGGACCTTGTCATTGGGTGCCTGGTGGAC
4501 4560
TCAGGGCCCGTCGTCCCGGCCTAGTCGGTGTGCCTGGAACAGTAACCCACGGACCACCTG
SerProGlyGlnGlnGlyArgIleSerHisThrAspLeuValIleGlyCysLeuValAsp
1501 1520
TTGGCCACTGGCTTAATGACCTTTACAGCCAATGGCAAAGAGAGCAACACCTTTTTCCAG
4561 4620
AACCGGTGACCGAATTACTGGAAATGTCGGTTACCGTTTCTCTCGTTGTGGAAAAAGGTC
LeuAlaThrGlyLeuMetThrPheThrAlaAsnGlyLysGluSerAsnThrPhePheGln
1521 1540
GTGGAACCCAACACTAAGCTATTTCCTGCCGTCTTCGTCCTGCCCACCCACCAGAACGTC
4621 4680
CACCTTGGGTTGTGATTCGATAAAGGACGGCAGAAGCAGGACGGGTGGGTGGTCTTGCAG
ValGluProAsnThrLysLeuPheProAlaValPheValLeuProThrHisGlnAsnVal
1541 1560
ATCCAGTTTGAGCTGGGGAAGCAGAAGAACATCATGCCGTTGTCAGCCGCCATGTTCCAA
4681 4740
TAGGTCAAACTCGACCCCTTCGTCTTCTTGTAGTACGGCAACAGTCGGCGGTACAAGGTT
IleGlnPheGluLeuGlyLysGlnLysAsnIleMetProLeuSerAlaAlaMetPheGln
1561 1580
4766
AGCGAGCGCAAGAACCCGGCCCCGCAGTGCCCACCGCGGCTGGAGATGCAGATGCTGATG
4741 4800
TCGCTCGCGTTCTTGGGCCGGGGCGTCACGGGTGGCGCCGACCTCTACGTCTACGACTAC
SerGluArgLysAsnProAlaProGlnCysProProArgLeuGluMetGlnMetLeuMet
1581 1600
CCAGTGTCCTGGAGCCGCATGCCCAACCACTTCCTGCAGGTGGAGACGAGGCGTGCCGGC
4801 4860
GGTCACAGGACCTCGGCGTACGGGTTGGTGAAGGACGTCCACCTCTGCTCCGCACGGCCG
ProValSerTrpSerArgMetProAsnHisPheLeuGlnValGluThrArgArgAlaGly
1601 1620
4800
GAGCGGCTGGGCTGGGCCGTGCAGTGCCAGGAGCCGCTGACCATGATGGCGCTGCACATC
4861 4920
CTCGCCGACCCGACCCGGCACGTCACGGTCCTCGGCGACTGGTACTACCGCGACGTGTAG
GluArgLeuGlyTrpAlaValGlnCysGlnGluProLeuThrMetMetAlaLeuHisIle
1621 1640
CCCGAGGAGAACCGGTGCATGGACATCCTGGAGCTGTCGGAGCGCCTGGACCTGCAGCGC
4921 4980
GGGCTCCTCTTGGCCACGTACCTGTAGGACCTCGACAGCCTCGCGGACCTGGACGTCGCG
ProGluGluAsnArgCysMetAspIleLeuGluLeuSerGluArgLeuAspLeuGlnArg
1641 1660
TTCCACTCGCACACCCTGCGCCTCTACCGCGCTGTGTGCGCCCTGGGCAACAATCGCGTG
1981 5040
AAGGTGAGCGTGTGGGACGCGGAGATGGCGCGACACACGCGGGACCCGTTGTTAGCGCAC
PheHisSerHisThrLeuArgLeuTyrArgAlaValCysAlaLeuGlyAsnAsnArgVal
1661 1680
GCGCACGCTCTGTGCAGCCACGTAGACCAAGCTCAGCTGCTGCACGCCCTGGAGGACGCG
5041 5100
CGCGTGCGAGACACGTCGGTGCATCTGGTTCGAGTCGACGACGTGCGGGACCTCCTGCGC
AlaHisAlaLeuCysSerHisValAspGlnAlaGlnLeuLeuHisAlaLeuGluAspAla
1681 1700
CACCTGCCAGGCCCACTGCGCGCAGGCTACTATGACCTCCTCATCAGCATCCACCTCGAA
5101 5160
GTGGACGGTCCGGGTGACGCGCGTCCGATGATACTGGAGGAGTAGTCGTAGGTGGAGCTT
HisLeuProGlyProLeuArgAlaGlyTyrTyrAspLeuLeuIleSerIleHisLeuGlu
1701 1720
5137


5285
Ala1832Gly (seq. error)
5430
exon 35
5555


5880
6376
Val2117Leu
Asp2129Glu
Leu2155


Arg2163His/Pro
Arg2163Cys
TA/C
A
Val2168Met
CAGATCCGCTCGCTGCTCATCGTGCAGATGGGCCCCCAGGAGGAGAACCTCATGATCCAG
6481 6540
GTCTAGGCGAGCGACGAGTAGCACGTCTACCCGGGGGTCCTCCTCTTGGAGTACTAGGTC
2161 GlnIleArgSerLeuLeuIleValGlnMetGlyProGlnGluGluAsnLeuMetIleGln 2180
exon 40
AGCATCGGGAACATCATGAACAACAAAGTCTTCTACCAACACCCGAACCTGATGAGGGCG
6541 6600
TCGTAGCCCTTGTAGTACTTGTTGTTTCAGAAGATGGTTGTGGGCTTGGACTACTCCCGC
2181 SerIleGlyAsnIleMetAsnAsnLysValPheTyrGlnHisProAsnLeuMetArgAla 2200
T/G
Thr2206Met/Arg
A
Val2214Ile
CTGGGCATGCACGAGACGGTCATGGAGGTCATGGTCAACGTCCTCGGGGGCGGCGAGTCC
6601 6660
GACCCGTACGTGCTCTGCCAGTACCTCCAGTACCAGTTGCAGGAGCCCCCGCCGCTCAGG
2201 LeuGlyMetHisGluThrValMetGluValMetValAsnValLeuGlyGlyGlyGluSer 2220
AAGGAGATCCGCTTCCCCAAGATGGTGACAAGCTGCTGCCGCTTCCTCTGCTATTTCTGC
6661 6720
TTCCTCTAGGCGAAGGGGTTCTACCACTGTTCGACGACGGCGAAGGAGACGATAAAGACG
2221 LysGluIleArgPheProLysMetValThrSerCysCysArgPheLeuCysTyrPheCys 2240
CGAATCAGCCGGCAGAACCAGCGCTCCATGTTTGACCACCTGAGCTACCTGCTGGAGAAC
6721 6780
GCTTAGTCGGCCGTCTTGGTCGCGAGGTACAAACTGGTGGACTCGATGGACGACCTCTTG
2241 ArgIleSerArgGlnAsnGlnArgSerMetPheAspHisLeuSerTyrLeuLeuGluAsn 2260
6763
AGTGGCATCGGCCTGGGCATGCAGGGCTCCACGCCCCTGGACGTGGCTGCTGCCTCCGTC
6781 6840
TCACCGTAGCCGGACCCGTACGTCCCGAGGTGCGGGGACCTGCACCGACGACGGAGGCAG
2261 SerGlyIleGlyLeuGlyMetGlnGlySerThrProLeuAspValAlaAlaAlaSerVal 2280
ATTGACAACAATGAGCTGGCCTTGGCATTGCAGGAGCAGGACCTGGAAAAGGTTGTGTCC
6841 6900
TAACTGTTGTTACTCGACCGGAACCGTAACGTCCTCGTCCTGGACCTTTTCCAACACAGG
2281 IleAspAsnAsnGluLeuAlaLeuAlaLeuGlnGluGlnAspLeuGluLysValValSer 2300
TACCTGGCAGGCTGTGGCCTCCAGAGCTGCCCCATGCTTGTGGCCAAAGGGTACCCAGAC
6901 6960
ATGGACCGTCCGACACCGGAGGTCTCGACGGGGTACGAACACCGGTTTCCCATGGGTCTG
2301 TyrLeuAlaGlyCysGlyLeuGlnSerCysProMetLeuValAlaLysGlyTyrProAsp 2320
ATTGGCTGGAACCCCTGTGGTGGAGAGCGCTACCTGGACTTCCTGCGCTTTGCTGTCTTC
6961 7020
TAACCGACCTTGGGGACACCACCTCTCGCGATGGACCTGAAGGACGCGAAACGACAGAAG
2321 IleGlyTrpAsnProCysGlyGlyGluArgTyrLeuAspPheLeuArgPheAlaValPhe 2340
T
Arg2355Cys
GTCAACGGCGAGAGCGTGGAGGAGAACGCCAATGTGGTGGTGCGGCTGCTCATCCGGAAG
7021 7080
CAGTTGCCGCTCTCGCACCTCCTCTTGCGGTTACACCACCACGCCGACGAGTAGGCCTTC
2341 ValAsnGlyGluSerValGluGluAsnAlaAsnValValValArgLeuLeuIleArgLys 2360
7039
Ala2367Thr
A
CCTGAGTGCTTCGGACCCGCCCTGCGGGGTGAGGGTGGCTCAGGGCTGCTGGCTGCCATC
7081 7140
GGACTCACGAAGCCTGGGCGGGACGCCCCACTCCCACCGAGTCCCGACGACCGACGGTAG
2361 ProGluCysPheGlyProAlaLeuArgGlyGluGlyGlySerGlyLeuLeuAlaAlaIle 2380


exon 45
Asp2431Asn Gly2434Arg
Arg2435His/Leu
Ile2453Thr Arg2454Cys/His
Arg2452Trp
Arg2458Cys/His
7361
7393
7699


exon 50
8025


8525
exon 55
8582
8789
exon 60
9022

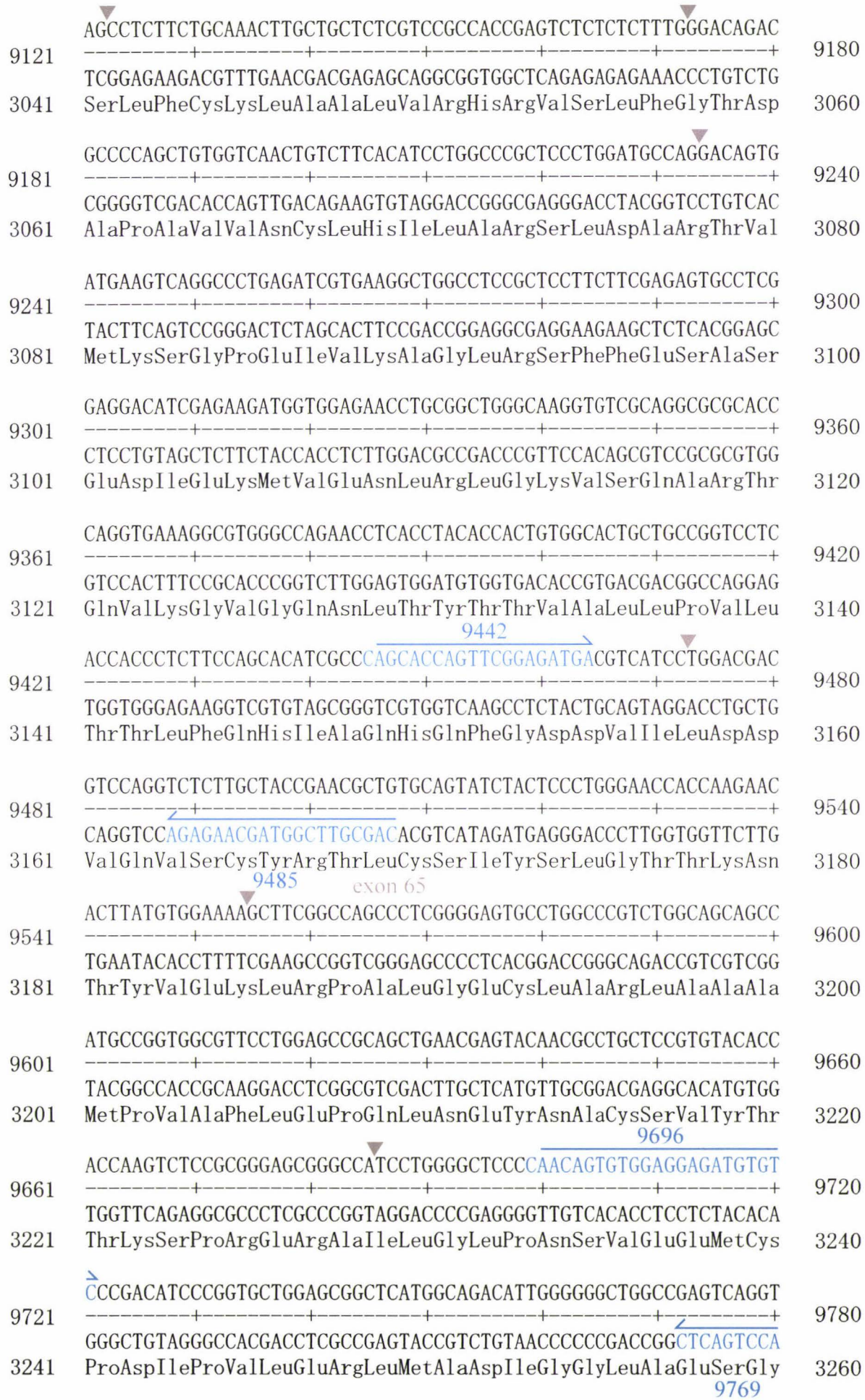
AGCCTCTTCTGCAAACTTGCTGCTCTCGTCCGCCACCGAGTCTCTCTCTTTGGGACAGAC
9121
9180
TCGGAGAAGACGTTTGAACGACGAGAGCAGGCGGTGGCTCAGAGAGAGAAACCCTGTCTG
3041
SerLeuPheCysLysLeuAlaAlaLeuValArgHisArgValSerLeuPheGlyThrAsp
3060
GCCCCAGCTGTGGTCAACTGTCTTCACATCCTGGCCCGCTCCCTGGATGCCAGGACAGTG
9181
9240
CGGGGTCGACACCAGTTGACAGAAGTGTAGGACCGGGCGAGGGACCTACGGTCCTGTCAC
3061
AlaProAlaValValAsnCysLeuHisIleLeuAlaArgSerLeuAspAlaArgThrVal
3080
ATGAAGTCAGGCCCTGAGATCGTGAAGGCTGGCCTCCGCTCCTTCTTCGAGAGTGCCTCG
9241
9300
TACTTCAGTCCGGGACTCTAGCACTTCCGACCGGAGGCGAGGAAGAAGCTCTCACGGAGC
3081
MetLysSerGlyProGluIleValLysAlaGlyLeuArgSerPhePheGluSerAlaSer
3100
GAGGACATCGAGAAGATGGTGGAGAACCTGCGGCTGGGCAAGGTGTCGCAGGCGCGCACC
9301
9360
CTCCTGTAGCTCTTCTACCACCTCTTGGACGCCGACCCGTTCCACAGCGTCCGCGCGTGG
3101
GluAspIleGluLysMetValGluAsnLeuArgLeuGlyLysValSerGlnAlaArgThr
3120
CAGGTGAAAGGCGTGGGCCAGAACCTCACCTACACCACTGTGGCACTGCTGCCGGTCCTC
9361
9420
GTCCACTTTCCGCACCCGGTCTTGGAGTGGATGTGGTGACACCGTGACGACGGCCAGGAG
3121
GlnValLysGlyValGlyGlnAsnLeuThrTyrThrThrValAlaLeuLeuProValLeu
3140
9442
ACCACCCTCTTCCAGCACATCGCCCAGCACCAGTTCGGAGATGACGTCATCCTGGACGAC
9421
9480
TGGTGGGAGAAGGTCGTGTAGCGGGTCGTGGTCAAGCCTCTACTGCAGTAGGACCTGCTG
3141
ThrThrLeuPheGlnHisIleAlaGlnHisGlnPheGlyAspAspValIleLeuAspAsp
3160
GTCCAGGTCTCTTGCTACCGAACGCTGTGCAGTATCTACTCCCTGGGAACCACCAAGAAC
9481
9540
CAGGTCCAGAGAACGATGGCTTGCGACACGTCATAGATGAGGGACCCTTGGTGGTTCTTG
3161
ValGlnValSerCysTyrArgThrLeuCysSerIleTyrSerLeuGlyThrThrLysAsn
3180
9485
exon 65
ACTTATGTGGAAAAGCTTCGGCCAGCCCTCGGGGAGTGCCTGGCCCGTCTGGCAGCAGCC
9541
9600
TGAATACACCTTTTCGAAGCCGGTCGGGAGCCCCTCACGGACCGGGCAGACCGTCGTCGG
3181
ThrTyrValGluLysLeuArgProAlaLeuGlyGluCysLeuAlaArgLeuAlaAlaAla
3200
ATGCCGGTGGCGTTCCTGGAGCCGCAGCTGAACGAGTACAACGCCTGCTCCGTGTACACC
9601
9660
TACGGCCACCGCAAGGACCTCGGCGTCGACTTGCTCATGTTGCGGACGAGGCACATGTGG
3201
MetProValAlaPheLeuGluProGlnLeuAsnGluTyrAsnAlaCysSerValTyrThr
3220
9696
ACCAAGTCTCCGCGGGAGCGGGCCATCCTGGGGCTCCCCAACAGTGTGGAGGAGATGTGT
9661
9720
TGGTTCAGAGGCGCCCTCGCCCGGTAGGACCCCGAGGGGTTGTCACACCTCCTCTACACA
3221
ThrLysSerProArgGluArgAlaIleLeuGlyLeuProAsnSerValGluGluMetCys
3240
CCCGACATCCCGGTGCTGGAGCGGCTCATGGCAGACATTGGGGGGCTGGCCGAGTCAGGT
9721
9780
GGGCTGTAGGGCCACGACCTCGCCGAGTACCGTCTGTAACCCCCCGACCGGCTCAGTCCA
3241
ProAspIleProValLeuGluArgLeuMetAlaAspIleGlyGlyLeuAlaGluSerGly
3260
9769


GCCCGCTACACAGAGATGCCGCATGTCATCGAGATCACGCTGCCCATGCTATGCAGCTAC
9781
9840
CGGGCGATGTGTCTCTACGGCGTACAGTAGCTCTAGTGCGACGGGTACGATACGTCGATG
3261
AlaArgTyrThrGluMetProHisValIleGluIleThrLeuProMetLeuCysSerTyr
3280
CTGCCCCGATGGTGGGAGCGCGGGCCCGAGGCACCCCCTTCCGCCCTGCCCGCCGGCGCC
9841
9900
GACGGGGCTACCACCCTCGCGCCCGGGCTCCGTGGGGGAAGGCGGGACGGGCGGCCGCGG
3281
LeuProArgTrpTrpGluArgGlyProGluAlaProProSerAlaLeuProAlaGlyAla
3300
CCCCCACCCTGCACAGCTGTCACCTCTGACCACCTCAACTCCCTGCTGGGGAATATCCTG
9901
9960
GGGGGTGGGACGTGTCGACAGTGGAGACTGGTGGAGTTGAGGGACGACCCCTTATAGGAC
3301
ProProProCysThrAlaValThrSerAspHisLeuAsnSerLeuLeuGlyAsnIleLeu
3320
AGAATCATCGTCAACAACCTGGGCATTGACGAGGCCTCCTGGATGAAGCGGCTGGCTGTG
9961
10020
TCTTAGTAGCAGTTGTTGGACCCGTAACTGCTCCGGAGGACCTACTTCGCCGACCGACAC
3321
ArgIleIleValAsnAsnLeuGlyIleAspGluAlaSerTrpMetLysArgLeuAlaVal
3340
10052
TTCGCACAGCCCATTGTGAGCCGTGCACGGCCGGAGCTCCTGCAGTCCCACTTCATCCCA
10021
10080
AAGCGTGTCGGGTAACACTCGGCACGTGCCGGCCTCGAGGACGTCAGGGTGAAGTAGGGT
3341
PheAlaGlnProIleValSerArgAlaArgProGluLeuLeuGlnSerHisPheIlePro
3360
ACTATCGGGCGGCTGCGCAAGAGGGCAGGGAAGGTGGTGTCCGAGGAGGAGCAGCTGCGC
10081
10140
TGATAGCCCGCCGACGCGTTCTCCCGTCCCTTCCACCACAGGCTCCTCCTCGTCGACGCG
3361
ThrIleGlyArgLeuArgLysArgAlaGlyLysValValSerGluGluGluGlnLeuArg
3380
10109
CTGGAGGCCAAGGCGGAGGCCCAGGAGGGCGAGCTGCTGGTGCGGGACGAGTTCTCTGTG
10141
10200
GACCTCCGGTTCCGCCTCCGGGTCCTCCCGCTCGACGACCACGCCCTGCTCAAGAGACAC
3381
LeuGluAlaLysAlaGluAlaGlnGluGlyGluLeuLeuValArgAspGluPheSerVal
3400
CTCTGCCGGGACCTCTACGCCCTGTATCCGCTGCTCATCCGCTACGTGGACAACAACAGG
10201
10260
GAGACGGCCCTGGAGATGCGGGACATAGGCGACGAGTAGGCGATGCACCTGTTGTTGTCC
3401
LeuCysArgAspLeuTyrAlaLeuTyrProLeuLeuIleArgTyrValAspAsnAsnArg
3420
GCGCAGTGGCTGACGGAGCCGAATCCCAGCGCGGAGGAGCTGTTCAGGATGGTGGGCGAG
10261
10320
CGCGTCACCGACTGCCTCGGCTTAGGGTCGCGCCTCCTCGACAAGTCCTACCACCCGCTC
3421
AlaGlnTrpLeuThrGluProAsnProSerAlaGluGluLeuPheArgMetValGlyGlu
3440
ATCTTCATCTACTGGTCCAAGTCCCACAACTTCAAGCGCGAGGAGCAGAACTTTGTGGTC
10321
10380
TAGAAGTAGATGACCAGGTTCAGGGTGTTGAAGTTCGCGCTCCTCGTCTTGAAACACCAG
3441
IlePheIleTyrTrpSerLysSerHisAsnPheLysArgGluGluGlnAsnPheValVal
3460
CAGAATGAGATCAACAACATGTCCTTCCTGACTGCTGACAACAAAAGCAAAATGGCTAAG
10381
10440
GTCTTACTCTAGTTGTTGTACAGGAAGGACTGACGACTGTTGTTTTCGTTTTACCGATTC
3461
GlnAsnGluIleAsnAsnMetSerPheLeuThrAlaAspAsnLysSerLysMetAlaLys
3480


exon 70
10809
exon 75
10884


11213
11307
exon 80
exon 85
11725

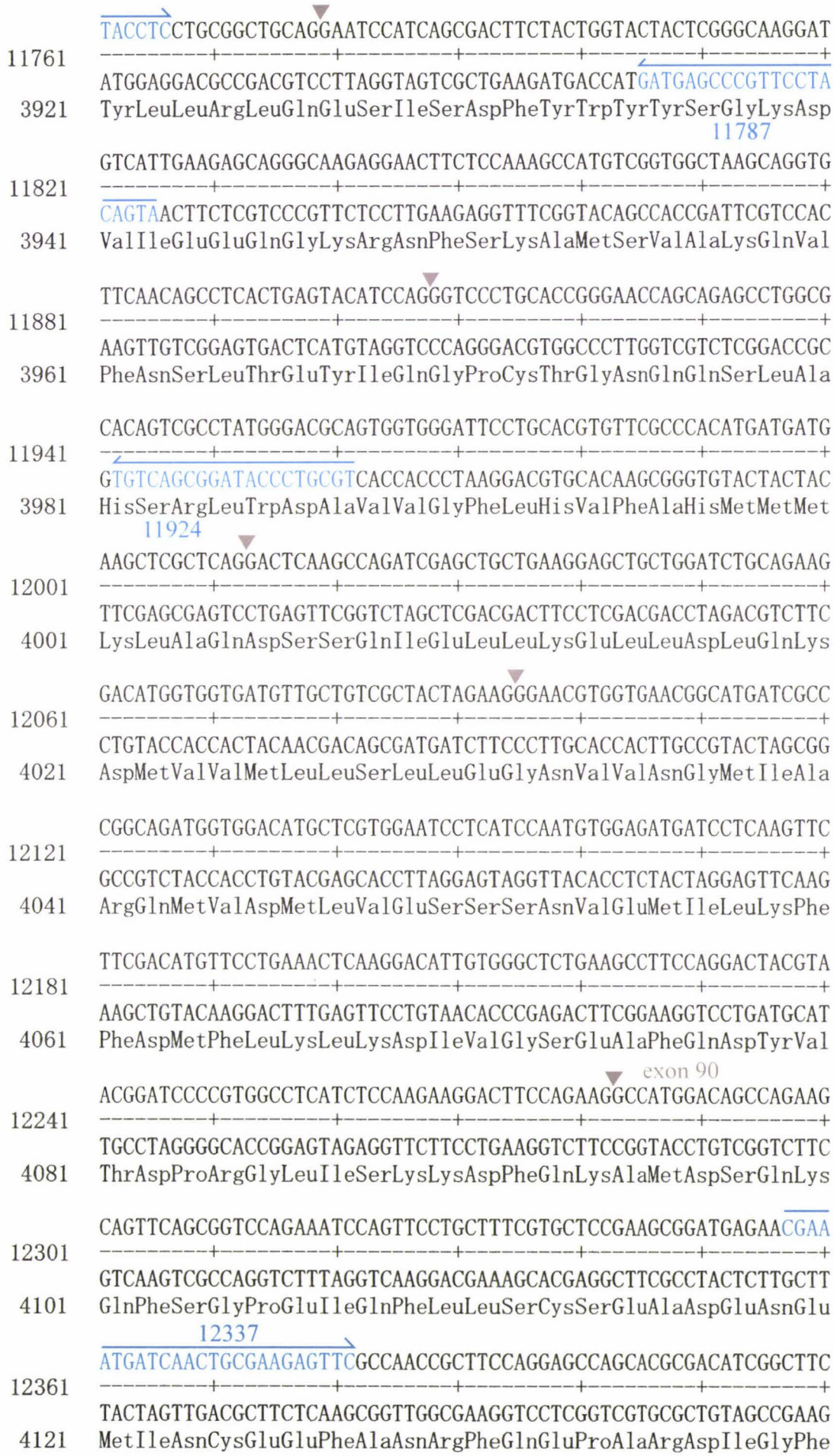
TACCTCCTGCGGCTGCAGGAATCCATCAGCGACTTCTACTGGTACTACTCGGGCAAGGAT
11761
11820
ATGGAGGACGCCGACGTCCTTAGGTAGTCGCTGAAGATGACCATGATGAGCCCGTTCCTA
3921
TyrLeuLeuArgLeuGlnGluSerIleSerAspPheTyrTrpTyrTyrSerGlyLysAsp
3940
11787
GTCATTGAAGAGCAGGGCAAGAGGAACTTCTCCAAAGCCATGTCGGTGGCTAAGCAGGTG
11821
11880
CAGTAACTTCTCGTCCCGTTCTCCTTGAAGAGGTTTCGGTACAGCCACCGATTCGTCCAC
3941
ValIleGluGluGlnGlyLysArgAsnPheSerLysAlaMetSerValAlaLysGlnVal
3960
TTCAACAGCCTCACTGAGTACATCCAGGGTCCCTGCACCGGGAACCAGCAGAGCCTGGCG
11881
11940
AAGTTGTCGGAGTGACTCATGTAGGTCCCAGGGACGTGGCCCTTGGTCGTCTCGGACCGC
3961
PheAsnSerLeuThrGluTyrIleGlnGlyProCysThrGlyAsnGlnGlnSerLeuAla
3980
CACAGTCGCCTATGGGACGCAGTGGTGGGATTCCTGCACGTGTTCGCCCACATGATGATG
11941
12000
GTGTCAGCGGATACCCTGCGTCACCACCCTAAGGACGTGCACAAGCGGGTGTACTACTAC
3981
HisSerArgLeuTrpAspAlaValValGlyPheLeuHisValPheAlaHisMetMetMet
4000
11924
AAGCTCGCTCAGGACTCAAGCCAGATCGAGCTGCTGAAGGAGCTGCTGGATCTGCAGAAG
12001
12060
TTCGAGCGAGTCCTGAGTTCGGTCTAGCTCGACGACTTCCTCGACGACCTAGACGTCTTC
4001
LysLeuAlaGlnAspSerSerGlnIleGluLeuLeuLysGluLeuLeuAspLeuGlnLys
4020
GACATGGTGGTGATGTTGCTGTCGCTACTAGAAGGGAACGTGGTGAACGGCATGATCGCC
12061
12120
CTGTACCACCACTACAACGACAGCGATGATCTTCCCTTGCACCACTTGCCGTACTAGCGG
4021
AspMetValValMetLeuLeuSerLeuLeuGluGlyAsnValValAsnGlyMetIleAla
4040
CGGCAGATGGTGGACATGCTCGTGGAATCCTCATCCAATGTGGAGATGATCCTCAAGTTC
12121
12180
GCCGTCTACCACCTGTACGAGCACCTTAGGAGTAGGTTACACCTCTACTAGGAGTTCAAG
4041
ArgGlnMetValAspMetLeuValGluSerSerSerAsnValGluMetIleLeuLysPhe
4060
TTCGACATGTTCCTGAAACTCAAGGACATTGTGGGCTCTGAAGCCTTCCAGGACTACGTA
12181
12240
AAGCTGTACAAGGACTTTGAGTTCCTGTAACACCCGAGACTTCGGAAGGTCCTGATGCAT
4061
PheAspMetPheLeuLysLeuLysAspIleValGlySerGluAlaPheGlnAspTyrVal
4080
exon 90
ACGGATCCCCGTGGCCTCATCTCCAAGAAGGACTTCCAGAAGGCCATGGACAGCCAGAAG
12241
12300
TGCCTAGGGGCACCGGAGTAGAGGTTCTTCCTGAAGGTCTTCCGGTACCTGTCGGTCTTC
4081
ThrAspProArgGlyLeuIleSerLysLysAspPheGlnLysAlaMetAspSerGlnLys
4100
CAGTTCAGCGGTCCAGAAATCCAGTTCCTGCTTTCGTGCTCCGAAGCGGATGAGAACGAA
12301
12360
GTCAAGTCGCCAGGTCTTTAGGTCAAGGACGAAAGCACGAGGCTTCGCCTACTCTTGCTT
4101
GlnPheSerGlyProGluIleGlnPheLeuLeuSerCysSerGluAlaAspGluAsnGlu
4120
12337
ATGATCAACTGCGAAGAGTTCGCCAACCGCTTCCAGGAGCCAGCACGCGACATCGGCTTC
12361
12420
TACTAGTTGACGCTTCTCAAGCGGTTGGCGAAGGTCCTCGGTCGTGCGCTGTAGCCGAAG
4121
MetIleAsnCysGluGluPheAlaAsnArgPheGlnGluProAlaArgAspIleGlyPhe
4140

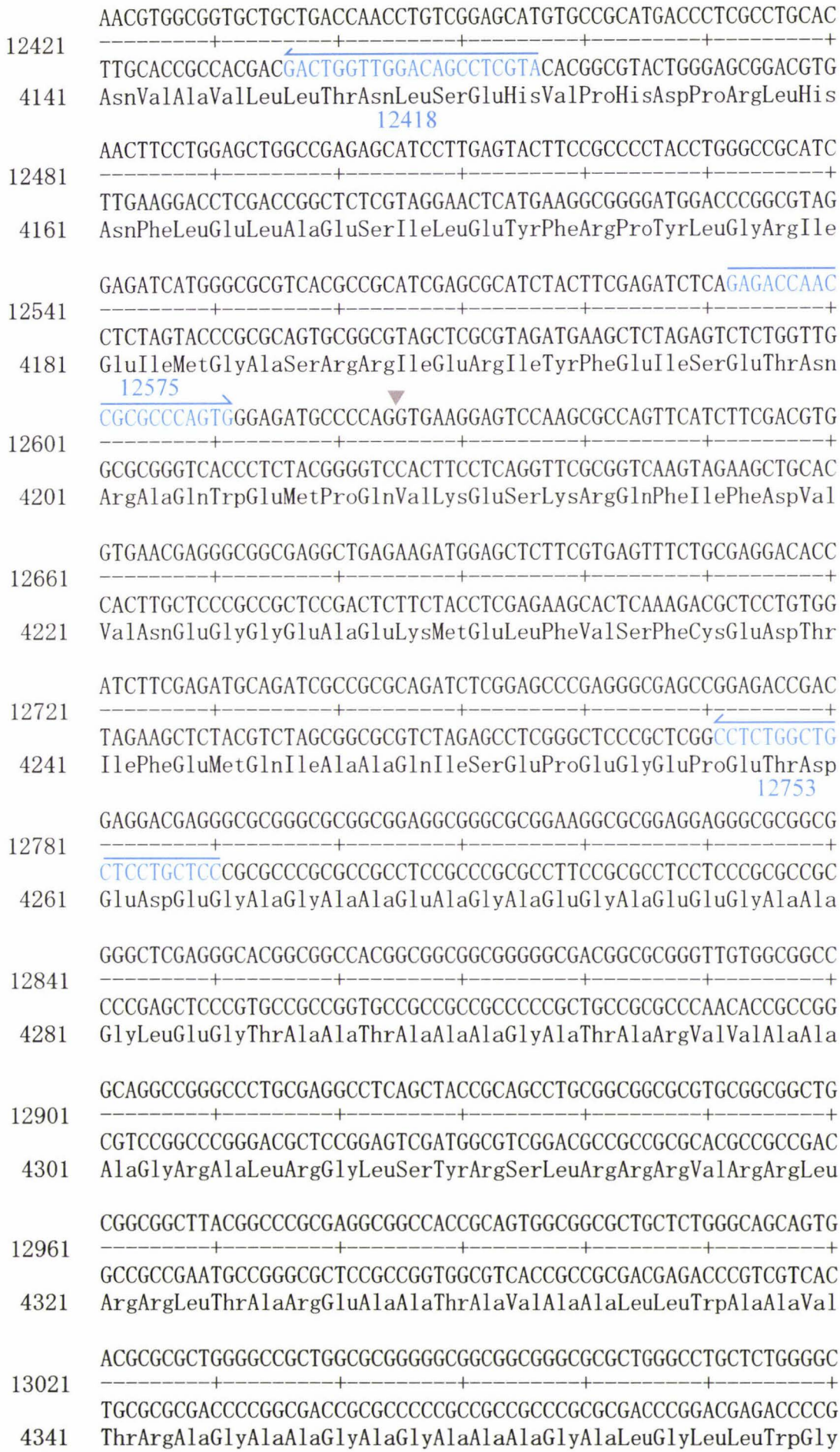
AACGTGGCGGTGCTGCTGACCAACCTGTCGGAGCATGTGCCGCATGACCCTCGCCTGCAC
12421
12480
TTGCACCGCCACGACGACTGGTTGGACAGCCTCGTACACGGCGTACTGGGAGCGGACGTG
4141
AsnValAlaValLeuLeuThrAsnLeuSerGluHisValProHisAspProArgLeuHis
4160
12418
AACTTCCTGGAGCTGGCCGAGAGCATCCTTGAGTACTTCCGCCCCTACCTGGGCCGCATC
12481
12540
TTGAAGGACCTCGACCGGCTCTCGTAGGAACTCATGAAGGCGGGGATGGACCCGGCGTAG
4161
AsnPheLeuGluLeuAlaGluSerIleLeuGluTyrPheArgProTyrLeuGlyArgIle
4180
GAGATCATGGGCGCGTCACGCCGCATCGAGCGCATCTACTTCGAGATCTCAGAGACCAAC
12541
12600
CTCTAGTACCCGCGCAGTGCGGCGTAGCTCGCGTAGATGAAGCTCTAGAGTCTCTGGTTG
4181
GluIleMetGlyAlaSerArgArgIleGluArgIleTyrPheGluIleSerGluThrAsn
4200
12575
CGCGCCCAGTGGGAGATGCCCCAGGTGAAGGAGTCCAAGCGCCAGTTCATCTTCGACGTG
12601
12660
GCGCGGGTCACCCTCTACGGGGTCCACTTCCTCAGGTTCGCGGTCAAGTAGAAGCTGCAC
4201
ArgAlaGlnTrpGluMetProGlnValLysGluSerLysArgGlnPheIlePheAspVal
4220
GTGAACGAGGGCGGCGAGGCTGAGAAGATGGAGCTCTTCGTGAGTTTCTGCGAGGACACC
12661
12720
CACTTGCTCCCGCCGCTCCGACTCTTCTACCTCGAGAAGCACTCAAAGACGCTCCTGTGG
4221
ValAsnGluGlyGlyGluAlaGluLysMetGluLeuPheValSerPheCysGluAspThr
4240
ATCTTCGAGATGCAGATCGCCGCGCAGATCTCGGAGCCCGAGGGCGAGCCGGAGACCGAC
12721
12780
TAGAAGCTCTACGTCTAGCGGCGCGTCTAGAGCCTCGGGCTCCCGCTCGGCCTCTGGCTG
4241
IlePheGluMetGlnIleAlaAlaGlnIleSerGluProGluGlyGluProGluThrAsp
4260
12753
GAGGACGAGGGCGCGGGCGCGGCGGAGGCGGGCGCGGAAGGCGCGGAGGAGGGCGCGGCG
12781
12840
CTCCTGCTCCCGCGCCCGCGCCGCCTCCGCCCGCGCCTTCCGCGCCTCCTCCCGCGCCGC
4261
GluAspGluGlyAlaGlyAlaAlaGluAlaGlyAlaGluGlyAlaGluGluGlyAlaAla
4280
GGGCTCGAGGGCACGGCGGCCACGGCGGCGGCGGGGGCGACGGCGCGGGTTGTGGCGGCC
12841
12900
CCCGAGCTCCCGTGCCGCCGGTGCCGCCGCCGCCCCCGCTGCCGCGCCCAACACCGCCGG
4281
GlyLeuGluGlyThrAlaAlaThrAlaAlaAlaGlyAlaThrAlaArgValValAlaAla
4300
GCAGGCCGGGCCCTGCGAGGCCTCAGCTACCGCAGCCTGCGGCGGCGCGTGCGGCGGCTG
12901
12960
CGTCCGGCCCGGGACGCTCCGGAGTCGATGGCGTCGGACGCCGCCGCGCACGCCGCCGAC
4301
AlaGlyArgAlaLeuArgGlyLeuSerTyrArgSerLeuArgArgArgValArgArgLeu
4320
CGGCGGCTTACGGCCCGCGAGGCGGCCACCGCAGTGGCGGCGCTGCTCTGGGCAGCAGTG
12961
13020
GCCGCCGAATGCCGGGCGCTCCGCCGGTGGCGTCACCGCCGCGACGAGACCCGTCGTCAC
4321
ArgArgLeuThrAlaArgGluAlaAlaThrAlaValAlaAlaLeuLeuTrpAlaAlaVal
4340
ACGCGCGCTGGGGCCGCTGGCGCGGGGGCGGCGGCGGGCGCGCTGGGCCTGCTCTGGGGC
13021
13080
TGCGCGCGACCCCGGCGACCGCGCCCCCGCCGCCGCCCGCGCGACCCGGACGAGACCCCG
4341
ThrArgAlaGlyAlaAlaGlyAlaGlyAlaAlaAlaGlyAlaLeuGlyLeuLeuTrpGly
4360


TCGCTGTTCGGCGGCGGCCTGGTGGAGGGCGCCAAGAAGGTGACGGTGACCGAGCTCCTG
13081
13140
AGCGACAAGCCGCCGCCGGACCACCTCCCGCGGTTCTTCCACTGCCACTGGCTCGAGGAC
4361 SerLeuPheGlyGlyGlyLeuValGluGlyAlaLysLysValThrValThrGluLeuLeu 4380
GCAGGCATGCCCGACCCCACCAGCGACGAGGTGCACGGCGAGCAGCCGGCCGGGCCGGGC
13141
13200
CGTCCGTACGGGCTGGGGTGGTCGCTGCTCCACGTGCCGCTCGTCGGCCGGCCCGGCCCG
4381 AlaGlyMetProAspProThrSerAspGluValHisGlyGluGlnProAlaGlyProGly 4400
GGAGACGCAGACGGCGAGGGTGCCAGCGAGGGCGCTGGAGACGCCGCGGAGGGCGCTGGA
13201
13260
CCTCTGCGTCTGCCGCTCCCACGGTCGCTCCCGCGACCTCTGCGGCGCCTCCCGCGACCT
4401 GlyAspAlaAspGlyGluGlyAlaSerGluGlyAlaGlyAspAlaAlaGluGlyAlaGly 4420
13285
GACGAGGAGGAGGCGGTGCACGAGGCCGGGCCGGGCGGTGCCGACGGGGCGGTGGCCGTG
13261
13320
CTGCTCCTCCTCCGCCACGTGCTCCGGCCCGGCCCGCCACGGCTGCCCCGCCACCGGCAC
4421 AspGluGluGluAlaValHisGluAlaGlyProGlyGlyAlaAspGlyAlaValAlaVal 4440
ACCGATGGGGGCCCCTTCCGGCCCGAAGGGGCTGGCGGTCTCGGGGACATGGGGGACACG
13321
13380
TGGCTACCCCCGGGGAAGGCCGGGCTTCCCCGACCGCCAGAGCCCCTGTACCCCCTGTGC
4441 ThrAspGlyGlyProPheArgProGluGlyAlaGlyGlyLeuGlyAspMetGlyAspThr 4460
13377
ACGCCTGCGGAACCGCCCACACCCGAGGGCTCTCCCATCCTCAAGAGGAAATTGGGGGTG
13381
13440
TGCGGACGCCTTGGCGGGTGTGGGCTCCCGAGAGGGTAGGAGTTCTCCTTTAACCCCCAC
4461 ThrProAlaGluProProThrProGluGlySerProIleLeuLysArgLysLeuGlyVal 4480
13356
GATGGAGTGGAGGAGGAGCTCCCGCCAGAGCCAGAGCCCGAGCCGGAACCAGAGCTGGAG
13441
13500
CTACCTCACCTCCTCCTCGAGGGCGGTCTCGGTCTCGGGCTCGGCCTTGGTCTCGACCTC
4481 AspGlyValGluGluGluLeuProProGluProGluProGluProGluProGluLeuGlu 4500
CCGGAGAAAGCCGATGCCGAGAATGGGGAGAAGGAAGAAGTTCCCGAGCCCACACCAGAG
13501
13560
GGCCTCTTTCGGCTACGGCTCTTACCCCTCTTCCTTCTTCAAGGGCTCGGGTGTGGTCTC
4501 ProGluLysAlaAspAlaGluAsnGlyGluLysGluGluValProGluProThrProGlu 4520
CCCCCCAAGAAGCAAGCACCTCCCTCACCCCCTCCAAAGAAGGAGGAAGCTGGAGGCGAA
13561
13620
GGGGGGTTCTTCGTTCGTGGAGGGAGTGGGGGAGGTTTCTTCCTCCTTCGACCTCCGCTT
4521 ProProLysLysGlnAlaProProSerProProProLysLysGluGluAlaGlyGlyGlu 4540
TTCTGGGGAGAACTGGAGGTGCAGAGGGTGAAGTTCCTGAACTACCTGTCCCGGAACTTT
13621
13680
AAGACCCCTCTTGACCTCCACGTCTCCCACTTCAAGGACTTGATGGACAGGGCCTTGAAA
4541 PheTrpGlyGluLeuGluValGlnArgValLysPheLeuAsnTyrLeuSerArgAsnPhe 4560
TACACCCTGCGGTTCCTTGCCCTCTTCTTGGCATTTGCCATCAACTTCATCTTGCTGTTT
13681
13740
ATGTGGGACGCCAAGGAACGGGAGAAGAACCGTAAACGGTAGTTGAAGTAGAACGACAAA
4561 TyrThrLeuArgPheLeuAlaLeuPheLeuAlaPheAlaIleAsnPheIleLeuLeuPhe 4580


exon 95
13731
13903
Thr4637Ala
13973
exon 100
Tyr4796Cys
14462

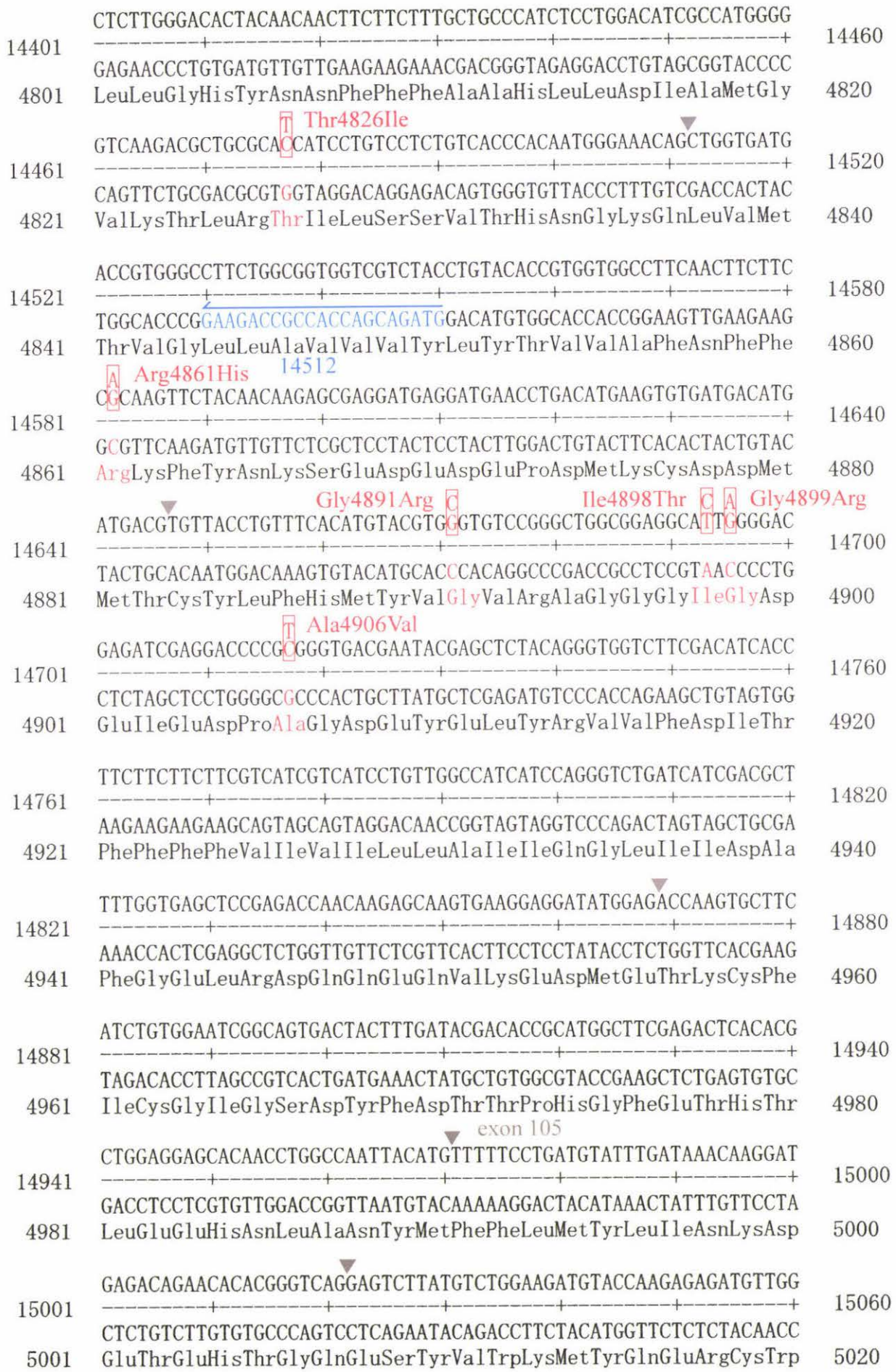
Thr4826Ile
Arg4861His
14512
Gly4891Arg
Ile4898Thr
Gly4899Arg
Ala4906Val
exon 105

The *RYR1* mRNA consists of 15,117 bp coding 5,038 amino acids. Primers used for PCR and sequencing in this project are described in blue arrows. Currently reported *RYR1* mutations are shown in red, and polymorphisms identified from the M818 patient are highlighted in green. The splice sites are indicated by the grey marks.

Appendix 3 Microsatellite markers for a genome-wide scan

Chromosome 1

Marker	Location (cM)	Fragment range	Heterozygosity	Dye label
D1S468	6.2	173-195	76	HEX
D1S214	16.4	122-152	78	NED
D1S450	22.9	316-340	81	FAM
D1S2667	26.9	128-156	82	HEX
D1S2697	39.9	273-281	69	HEX
D1S199	47.7	94-116	84	FAM
D1S234	56.6	226-238	82	FAM
D1S255	66.6	91-111	75	HEX
D1S2797	77.6	102-138	74	FAM
D1S2890	87.7	214-238	76	HEX
D1S230	97.4	154-166	78	HEX
D1S2841	108.8	234-254	78	HEX
D1S207	117.6	149-179	84	FAM
D1S2868	129.9	210-224	76	FAM
D1S206	137.6	208-226	82	NED
D1S2726	149.0	284-296	81	NED
D1S252	155.1	90-115	81	HEX
D1S498	160.7	190-212	82	NED
D1S484	173.9	276-290	64	HEX
D1S2878	181.7	152-178	84	NED
D1S196	186.4	322-338	74	HEX
D1S218	196.5	271-295	83	NED
D1S238	206.7	296-330	86	FAM
D1S413	216.5	254-270	76	FAM
D1S425	235.3	336-360	81	NED
D1S213	246.2	107-133	86	NED
D1S249	255.1	163-193	87	FAM
D1S2800	256.1	210-224	63	FAM
D1S2785	269.7	173-187	76	HEX
D1S2842	277.3	338-358	76	NED
D1S2836	290.1	246-260	79	NED

Chromosome 2

Marker	Location (cM)	Fragment range	Heterozygosity	Dye label
D2S319	6.0	132-144	73	HEX
D2S2211	14.0	241-261	74	FAM
D2S162	21.3	124-152	75	FAM
D2S168	28.6	159-183	94	HEX
D2S305	40.7	316-338	72	NED
D2S165	50.7	145-177	85	FAM
D2S367	58.3	309-341	86	FAM
D2S2259	67.4	322-342	79	FAM
D2S391	73.8	147-161	79	NED
D2S337	84.1	295-319	88	NED
D2S2368	89.2	97-121	83	NED
D2S286	98.4	85-127	66	FAM
D2S2333	107.7	84-106	82	NED
D2S2216	115.3	213-227	76	FAM
D2S160	127.4	211-227	78	FAM
D2S347	135.7	271-301	80	FAM
D2S112	145.8	76-94	71	FAM
D2S151	156.4	228-256	82	HEX
D2S142	166.3	239-259	76	HEX
D2S2330	175.5	171-189	81	FAM
D2S335	182.5	189-209	79	NED
D2S364	192.9	234-260	80	NED
D2S117	201.4	193-221	82	HEX
D2S325	210.9	158-186	82	NED
D2S2382	220.7	299-337	81	HEX
D2S126	228.8	119-149	82	NED
D2S396	240.2	236-254	83	NED
D2S206	248.3	128-166	80	HEX
D2S338	258.7	270-294	81	NED
D2S125	269.5	92-112	82	HEX

Chromosome 3

Marker	Location (cM)	Fragment range	Heterozygosity	Dye label
D3S1297	2.5	352-370	82	HEX
D3S1304	16.5	258-280	80	HEX
D3S1263	30.4	194-214	86	NED

D3S2338	36.3	94-118	86	HEX
D3S1266	46.9	292-308	73	HEX
D3S1277	56.1	292-314	83	NED
D3S1289	69.1	204-226	81	NED
D3S1300	79.0	235-267	82	FAM
D3S1285	91.0	238-256	73	NED
D3S1566	97.2	158-180	84	NED
D3S3681	108.8	124-164	83	HEX
D3S1271	117.7	88-108	73	HEX
D3S1278	131.8	236-264	87	HEX
D3S1267	141.1	96-136	88	NED
D3S1292	148.7	115-149	85	NED
D3S1569	162.0	154-178	80	FAM
D3S1279	173.0	272-290	85	FAM
D3S1614	183.1	107-131	83	NED
D3S1565	193.0	182-198	64	FAM
D3S1262	207.2	115-137	80	FAM
D3S1580	213.7	220-240	84	FAM
D3S1601	220.4	299-331	85	HEX
D3S1311	230.7	137-164	83	FAM

Chromosome 4

Marker	Location (cM)	Fragment range	Heterozygosity	Dye label
D4S412	3.7	161-179	77	HEX
D4S2935	12.2	90-110	62	HEX
D4S403	24.9	173-189	77	FAM
D4S419	32.6	229-249	77	NED
D4S391	43.2	153-173	85	HEX
D4S405	56.7	284-312	86	HEX
D4S1592	68.4	115-145	72	HEX
D4S392	77.9	84-114	82	FAM
D4S2964	87.1	124-148	76	HEX
D4S1534	93.5	150-172	77	NED
D4S414	99.2	235-253	89	HEX
D4S1572	106.3	195-217	84	FAM
D4S406	115.8	246-272	87	FAM
D4S402	123.5	112-158	91	FAM
D4S1575	131.9	292-310	65	FAM
D4S424	143.8	197-215	83	HEX

D4S413	157.9	286-338	85	FAM
D4S1597	169.1	278-304	76	NED
D4S1539	181.2	319-327	68	FAM
D4S415	185.0	268-304	80	NED
D4S1535	198.5	254-268	77	NED
D4S426	211.0	163-183	76	NED

Chromosome 5

Marker	Location (cM)	Fragment range	Heterozygosity	Dye label
D5S1981	0.6	121-131	73	NED
D5S406	10.7	168-196	79	NED
D5S2095	18.6	151-181	66	FAM
D5S416	27.9	289-301	77	NED
D5S419	39.5	258-290	81	HEX
D5S426	51.6	279-303	80	HEX
D5S418	58.1	212-232	80	HEX
D5S407	65.0	87-115	86	FAM
D5S647	74.7	328-368	82	NED
D5S424	82.8	215-237	76	HEX
D5S641	92.3	301-341	77	NED
D5S428	95.4	248-266	76	HEX
D5S644	104.5	86-116	85	HEX
D5S433	112.2	190-220	85	NED
D5S2027	118.9	184-206	78	FAM
D5S471	129.6	241-261	76	NED
D5S2115	138.6	146-172	76	HEX
D5S436	147.2	242-262	83	FAM
D5S410	156.0	332-354	79	FAM
D5S422	163.9	118-140	84	NED
D5S400	174.3	200-243	82	NED
D5S408	195.8	253-289	73	FAM

Chromosome 6

Marker	Location (cM)	Fragment range	Heterozygosity	Dye label
D6S1574	8.7	150-176	84	FAM
D6S309	13.6	307-333	83	NED
D6S470	17.7	125-145	80	NED
D6S289	29.6	215-235	79	FAM

D6S422	35.7	300-322	77	FAM
D6S276	44.9	205-237	83	FAM
D6S1610	53.9	204-218	84	FAM
D6S257	80.0	170-198	87	NED
D6S460	90.0	283-307	81	FAM
D6S462	99.0	108-124	80	HEX
D6S434	109.2	206-250	86	HEX
D6S287	122.0	110-144	85	HEX
D6S262	129.8	171-191	82	HEX
D6S292	138.2	158-180	83	HEX
D6S308	145.5	328-356	75	FAM
D6S441	155.3	166-200	86	NED
D6S1581	165.0	261-275	72	FAM
D6S264	179.1	111-135	70	FAM
D6S446	188.4	222-234	62	NED
D6S281	201.1	136-164	68	HEX

Chromosome 7

Marker	Location (cM)	Fragment range	Heterozygosity	Dye label
D7S531	4.8	281-299	77	NED
D7S517	7.8	247-265	83	FAM
D7S507	29.1	86-114	89	FAM
D7S493	35.0	207-239	88	HEX
D7S516	42.1	308-328	76	NED
D7S484	55.6	102-120	74	FAM
D7S510	60.5	85-101	77	NED
D7S519	70.5	260-288	81	FAM
D7S502	79.6	291-311	84	HEX
D7S669	90.9	176-198	80	HEX
D7S630	98.7	328-356	73	HEX
D7S657	105.2	248-274	81	NED
D7S515	112.9	140-206	82	FAM
D7S486	FAM	226-240	81	FAM
D7S530	136.4	109-127	78	HEX
D7S640	139.7	111-155	85	NED
D7S684	149.6	344-366	81	HEX
D7S661	157.5	307-339	75	FAM
D7S636	165.0	141-177	90	NED
D7S798	171.3	76-98	84	HEX

D7S2465	182.1	321-345	83	FAM

Chromosome 8

Marker	Location (cM)	Fragment range	Heterozygosity	Dye label
D8S264	0.7	140-164	83	FAM
D8S277	8.4	154-188	73	HEX
D8S550	20.4	191-221	87	NED
D8S549	30.7	78-88	63	HEX
D8S258	40.3	146-160	70	HEX
D8S1771	49.6	345-369	75	NED
D8S505	60.0	114-128	79	HEX
D8S285	70.6	317-333	78	NED
D8S260	78.8	195-221	81	FAM
D8S270	102.1	107-123	79	NED
D8S1784	116.8	280-298	67	FAM
D8S514	128.9	216-236	77	NED
D8S284	142.7	275-309	83	HEX
D8S272	152.5	215-265	81	HEX

Chromosome 9

Marker	Location (cM)	Fragment range	Heterozygosity	Dye label
D9S288	8.8	138-158	84	NED
D9S286	16.8	139-173	88	FAM
D9S285	27.9	85-113	78	NED
D9S157	31.8	229-253	84	NED
D9S171	42.0	164-188	79	NED
D9S161	50.3	126-144	78	FAM
D9S1817	57.9	283-317	88	FAM
D9S273	64.5	206-226	77	NED
D9S175	68.8	259-291	85	FAM
D9S167	82.4	307-341	87	NED
D9S283	93.2	94-120	80	NED
D9S287	103.3	299-317	67	HEX
D9S1690	106.5	230-244	78	FAM
D9S1677	117.8	234-258	81	FAM
D9S1776	124.2	176-214	84	HEX
D9S1682	132.9	152-162	68	HEX

D9S290	141.1	246-268	83	FAM
D9S164	148.1	90-106	80	FAM
D9S1826	160.2	219-233	69	FAM
D9S158	163.0	333-357	69	FAM

Chromosome 10

Marker	Location (cM)	Fragment range	Heterozygosity	Dye label
D10S249	0.0	122-144	74	NED
D10S591	12.3	312-340	71	HEX
D10S189	17.3	180-200	72	NED
D10S547	28.1	238-260	74	HEX
D10S1653	38.8	122-136	77	HEX
D10S548	43.4	186-202	70	FAM
D10S197	50.2	161-180	75	FAM
D10S208	60.2	177-197	79	NED
D10S196	72.5	109-119	77	HEX
D10S1652	83.3	273-299	78	NED
D10S537	93.8	143-169	83	NED
D10S1686	109.2	247-285	86	HEX
D10S185	123.3	206-230	77	FAM
D10S192	131.2	242-268	77	NED
D10S597	137.6	278-298	64	HEX
D10S1693	146.1	202-231	80	HEX
D10S587	156.6	96-118	80	NED
D10S217	167.2	100-124	81	FAM
D10S1651	178.3	210-232	80	NED
D10S212	180.7	193-209	71	HEX

Chromosome 11

Marker	Location (cM)	Fragment range	Heterozygosity	Dye label
D11S4046	3.9	105-129	86	NED
D11S1338	14.9	259-277	74	HEX
D11S902	24.7	152-172	80	HEX
D11S904	37.0	182-210	82	HEX
D11S935	49.6	200-222	73	FAM
D11S905	55.7	272-298	75	HEX

D11S4191	63.4	94-124	87	HEX
D11S987	71.5	100-138	82	FAM
D11S1314	77.5	97-123	78	HEX
D11S937	84.6	142-183	88	FAM
D11S901	89.8	314-330	82	FAM
D11S4175	96.3	290-342	89	NED
D11S898	103.1	144-166	85	FAM
D11S908	112.5	175-191	76	HEX
D11S925	123.5	265-293	84	NED
D11S4151	132.9	335-347	79	FAM
D11S1320	147.2	264-280	68	FAM
D11S968	152.8	144-164	81	HEX

Chromosome 12

Marker	Location (cM)	Fragment range	Heterozygosity	Dye label
D12S352	0.0	156-176	73	HEX
D12S99	13.9	268-300	83	NED
D12S336	21.3	117-135	82	NED
D12S364	31.7	300-328	87	FAM
D12S310	36.1	248-260	69	HEX
D12S1617	45.1	250-290	80	NED
D12S345	54.4	215-251	87	NED
D12S85	62.7	104-136	67	FAM
D12S368	67.3	206-226	81	FAM
D12S83	76.5	107-127	81	FAM
D12S326	87.6	210-236	80	HEX
D12S351	97.0	149-173	75	FAM
D12S346	106.1	191-217	84	NED
D12S78	113.3	177-215	91	FAM
D12S79	126.1	163-189	87	NED
D12S86	135.1	132-172	89	HEX
D12S324	148.3	238-260	69	NED
D12S1659	157.2	294-326	78	FAM
D12S1723	165.7	201-219	67	HEX

Chromosome 13

Marker	Location (cM)	Fragment range	Heterozygosity	Dye label
D13S175	7.4	101-125	75	NED
D13S217	19.1	246-266	68	FAM
D13S171	27.3	173-207	73	NED
D13S218	35.3	145-157	66	FAM
D13S263	40.4	150-178	84	NED
D13S153	47.6	90-126	81	NED
D13S156	57.3	280-300	80	HEX
D13S170	65.4	146-176	90	HEX
D13S265	70.6	93-131	70	HEX
D13S159	81.5	157-199	90	FAM
D13S158	86.9	121-139	82	FAM
D13S173	95.9	237-257	82	FAM
D13S1265	101.7	280-310	80	FAM
D13S285	112.8	93-119	81	HEX

Chromosome 14

Marker	Location (cM)	Fragment range	Heterozygosity	Dye label
D14S261	0.0	276-308	75	NED
D14S283	7.5	132-162	81	HEX
D14S275	21.9	150-164	70	FAM
D14S70	32.9	103-119	75	HEX
D14S288	39.1	196-220	83	NED
D14S276	47.0	241-253	76	NED
D14S63	59.0	180-198	76	HEX
D14S258	65.8	198-218	79	FAM
D14S74	76.2	301-325	79	HEX
D14S48	84.3	257-281	76	NED
D14S280	95.5	243-263	68	FAM
D14S65	108.1	129-161	79	NED
D14S985	117.1	244-258	76	HEX
D14S292	124.2	88-104	73	FAM

Chromosome 15

Marker	Location (cM)	Fragment range	Heterozygosity	Dye label
D15S128	6.1	201-219	78	NED
D15S1002	14.5	110-138	78	HEX
D15S165	20.2	185-217	79	HEX
D15S1007	25.9	89-113	86	NED
D15S1012	35.3	104-118	72	HEX
D15S994	40.0	306-318	73	NED
D15S978	45.5	187-215	83	HEX
D15S117	50.8	324-342	78	NED
D15S153	62.1	244-278	87	NED
D15S131	70.7	244-284	83	HEX
D15S205	77.4	130-170	88	FAM
D15S127	84.8	119-157	86	NED
D15S130	98.0	388-302	66	FAM
D15S120	109.6	158-186	73	NED

Chromosome 16

Marker	Location (cM)	Fragment range	Heterozygosity	Dye label
D16S423	8.4	140-166	73	HEX
D16S404	16.7	265-285	80	HEX
D16S3075	21.8	81-99	79	FAM
D16S3013	31.1	316-344	81	HEX
D16S3046	39.3	85-113	74	FAM
D16S3068	46.6	223-239	77	FAM
D16S3136	60.0	176-188	69	FAM
D16S415	65.6	216-244	72	FAM
D16S503	81.8	300-320	81	HEX
D16S515	90.2	327-359	80	FAM
D16S516	98.3	248-270	73	NED
D16S3091	109.1	170-192	73	NED
D16S520	123.3	152-170	84	HEX

Chromosome 17

Marker	Location (cM)	Fragment range	Heterozygosity	Dye label
D17S849	0.6	257-271	67	NED

D17S831	6.6	112-134	82	HEX
D17S938	14.8	242-262	76	FAM
D17S1852	23.2	283-311	87	FAM
D17S799	32.8	189-211	68	HEX
D17S921	37.3	196-214	72	HEX
D17S1857	44.1	167-177	64	HEX
D17S798	53.9	300-324	80	HEX
D17S1868	65.1	258-272	73	HEX
D17S787	75.7	142-178	81	NED
D17S944	84.2	333-347	75	NED
D17S949	94.9	214-232	80	FAM
D17S785	104.7	169-197	73	NED
D17S784	117.7	233-247	77	HEX
D17S928	128.7	74-108	76	NED

Chromosome 18

Marker	Location (cM)	Fragment range	Heterozygosity	Dye label
D18S59	0.1	154-176	81	HEX
D18S63	7.9	80-106	79	HEX
D18S452	17.7	131-149	83	NED
D18S464	32.4	303-319	64	FAM
D18S53	40.4	156-186	79	FAM
D18S478	52.3	247-261	94	FAM
D18S1102	61.7	96-108	79	NED
D18S474	71.3	126-148	82	FAM
D18S64	83.0	319-345	74	HEX
D18S68	94.4	273-299	68	NED
D18S61	102.8	213-243	87	NED
D18S1161	112.0	215-241	82	NED
D18S462	118.0	300-322	70	NED
D18S70	123.8	115-135	83	FAM

Chromosome 19

Marker	Location (cM)	Fragment range	Heterozygosity	Dye label
D19S209	10.8	243-259	77	FAM
D19S216	19.1	258-276	76	HEX

D19S884	26.0	97-117	86	NED
D19S221	35.5	91-115	86	HEX
D19S226	41.7	241-273	85	NED
D19S414	53.2	168-198	78	NED
D19S220	61.4	271-295	84	FAM
D19S420	66.0	101-121	79	NED
D19S902	76.2	241-277	79	FAM
D19S571	87.7	290-322	83	NED
D19S418	97.5	90-110	66	HEX
D19S210	104.9	175-195	74	HEX

Chromosome 20

Marker	Location (cM)	Fragment range	Heterozygosity	Dye label
D20S117	2.9	150-190	84	FAM
D20S889	11.0	93-129	83	FAM
D20S115	20.9	238-250	66	NED
D20S186	33.2	121-143	88	HEX
D20S112	39.3	217-241	81	FAM
D20S195	50.2	133-159	81	FAM
D20S107	54.9	200-224	80	FAM
D20S119	61.0	109-129	82	FAM
D20S178	65.5	244-260	84	NED
D20S196	74.5	263-299	81	NED
D20S100	83.4	213-239	76	HEX
D20S171	94.4	130-158	78	HEX
D20S173	96.5	131-185	67	HEX

Chromosome 21

Marker	Location (cM)	Fragment range	Heterozygosity	Dye label
D21S1256	8.6	101-121	65	NED
D21S1914	23.0	262-284	86	HEX
D21S263	31.4	198-232	75	HEX
D21S1252	38.7	156-180	80	NED
D21S266	49.9	159-181	59	FAM

Chromosome 22

Marker	Location (cM)	Fragment range	Heterozygosity	Dye label
D22S420	0.0	156-172	77	HEX
D22S539	13.7	203-221	58	NED
D22S315	16.2	181-214	78	FAM
D22S280	25.9	216-228	82	HEX
D22S283	33.4	132-160	89	NED
D22S423	40.2	290-312	82	HEX
D22S274	45.5	202-220	77	NED

Chromosome X

Marker	Location (cM)	Fragment range	Heterozygosity	Dye label
DXS1060	10.1	249-271	84	NED
DXS8051	15.7	110-140	88	NED
DXS987	25.5	210-232	83	FAM
DXS1226	36.8	284-306	84	NED
DXS1214	46.2	287-301	79	HEX
DXS1068	56.2	248-268	79	HEX
DXS993	66.1	271-297	79	FAM
DXS991	86.9	316-344	80	NED
DXS986	95.9	156-184	77	FAM
DXS990	104.9	128-138	74	FAM
DXS1106	115.1	128-142	67	HEX
DXS8055	126.8	314-326	65	HEX
DXS1001	139.4	194-214	82	HEX
DXS1047	150.3	160-174	81	HEX
DXS1227	164.7	84-104	73	FAM
DXS8043	176.7	150-184	80	NED
DXS8091	186.3	84-106	78	HEX
DXS1073	196.5	310-336	80	FAM

400 microsatellite markers in total were used for a genome-wide scan. Markers are listed according to the location on each chromosome. Each marker was labelled with FAM (blue), HEX (green) or NED (yellow). Amplification of marker loci and genotyping was carried out at the Australian Genome Research Facility, Parkville

Victoria, Australia. Data were obtained from several on-line resources including:

Genetic Analysis of Multiple sclerosis in EuropeanS (GAMES)
(http://www-gene.cimr.cam.ac.uk/MSgenetics/GAMES/GAMES.html)

Genomics Core Facility human marker search page
(http://www.cores.utah.edu/GENOMICS/markerSearch.php)

An STS-Based Map of the Human Genome
(http://www.broad.mit.edu/cgi-bin/contig/phys_map)

CGAP-GAI Marker Maps
(http://lpgws.nci.nih.gov/html-chlc/CGAPMarkerMaps.html)

The Genome Database
(http://gdb.wehi.edu.au/gdb/)

and the marker list provided by ABI
(genetics.med.harvard.edu/~depalma/misc/all-ABI-markers.xls)

Appendix 4 The output data of a genome-wide scan

The EA branch

Chromosome 1

position	LOD score	NPL score	p-value	information
-10.00	-0.114055	0.032280	0.250000	0.078725
-8.00	-0.130391	0.035335	0.250000	0.091834
-6.00	-0.148896	0.038617	0.250000	0.107016
-4.00	-0.169908	0.042120	0.250000	0.124595
-2.00	-0.193839	0.045835	0.250000	0.144975
0.00	-0.221207	0.049744	0.250000	0.168692
2.33	-0.319311	-0.031047	0.437500	0.189127
4.66	-0.431348	-0.111347	0.437500	0.218920
7.00	-0.557603	-0.190405	0.500000	0.260247
9.33	-0.694416	-0.267451	0.500000	0.317415
11.66	-0.827529	-0.341730	0.500000	0.408818
13.01	-0.827329	-0.368105	0.500000	0.404628
14.35	-0.833182	-0.396116	0.500000	0.408726
15.70	-0.843582	-0.425641	0.500000	0.419994
17.05	-0.856768	-0.456540	0.500000	0.439703
18.39	-0.870599	-0.488659	0.812500	0.475515
19.23	-0.873063	-0.491809	0.812500	0.464162
20.06	-0.876552	-0.495796	0.812500	0.456403
20.89	-0.881138	-0.500626	0.812500	0.451331
21.73	-0.886856	-0.506307	0.812500	0.448884
22.56	-0.893702	-0.512844	0.812500	0.450019
25.57	-0.805047	-0.435968	0.500000	0.279491
28.58	-0.687767	-0.361452	0.500000	0.191828
31.60	-0.595205	-0.294132	0.500000	0.146658
34.61	-0.551309	-0.239352	0.500000	0.136343
37.62	-0.583102	-0.202387	0.500000	0.157645
39.31	-0.528679	-0.166803	0.500000	0.171970
41.01	-0.498075	-0.137286	0.500000	0.199026
42.71	-0.493720	-0.115229	0.500000	0.240569
44.40	-0.523091	-0.102012	0.437500	0.301106
46.10	-0.605071	-0.098945	0.437500	0.403764
48.06	-0.012616	0.043046	0.250000	0.329115
50.02	0.245516	0.200433	0.187500	0.302998
51.98	0.420904	0.375461	0.187500	0.313203
53.94	0.559051	0.570230	0.187500	0.361677
55.90	0.676450	0.786457	0.093750	0.475269
58.13	0.685239	0.869717	0.093750	0.384646
60.36	0.697760	0.965325	0.093750	0.339727
62.59	0.713990	1.072673	0.062500	0.318424
64.82	0.733780	1.191187	0.062500	0.317365
67.06	0.756859	1.320454	0.062500	0.338860
69.54	0.725077	1.218352	0.062500	0.312597
72.03	0.692754	1.131488	0.062500	0.302455
74.51	0.659951	1.058524	0.093750	0.302453
76.99	0.626727	0.998230	0.093750	0.312073
79.48	0.593145	0.949500	0.093750	0.334821
81.74	0.491037	0.709568	0.093750	0.315757
83.99	0.364862	0.483308	0.187500	0.313538
86.25	0.198414	0.270462	0.187500	0.323986
88.50	-0.051821	0.070708	0.250000	0.348323
90.76	-0.614023	-0.116368	0.500000	0.397390
92.92	-0.500606	-0.114711	0.500000	0.356894
95.07	-0.457281	-0.124010	0.500000	0.334251
97.23	-0.464379	-0.143872	0.500000	0.322982
99.39	-0.523108	-0.173959	0.500000	0.322339
101.54	-0.657534	-0.214005	0.500000	0.335902
104.13	-0.514374	-0.238326	0.500000	0.315404
106.72	-0.466285	-0.277882	0.500000	0.318003
109.31	-0.485805	-0.331682	0.500000	0.341073

111.90	-0.586049	-0.398873	0.500000	0.388134
114.48	-0.861599	-0.478883	0.812500	0.481619
116.42	-0.648726	-0.380536	0.500000	0.388891
118.36	-0.548864	-0.286259	0.500000	0.357133
120.29	-0.508416	-0.199204	0.500000	0.361727
122.23	-0.516941	-0.122797	0.500000	0.401982
124.16	-0.585825	-0.060348	0.437500	0.490763
126.99	0.139150	0.249144	0.187500	0.403852
129.81	0.413267	0.589972	0.187500	0.368912
132.63	0.589640	0.959699	0.093750	0.362387
135.46	0.720724	1.354837	0.062500	0.381766
138.28	0.824896	1.771498	0.062500	0.432933
139.95	0.849706	1.881099	0.062500	0.428955
141.63	0.874101	2.001164	0.062500	0.434697
143.30	0.897960	2.132059	0.062500	0.447706
144.97	0.921167	2.274116	0.062500	0.468432
146.64	0.943621	2.427617	0.062500	0.500487
149.23	0.933969	2.308484	0.062500	0.469330
151.82	0.923229	2.213660	0.062500	0.456373
154.41	0.911458	2.142256	0.062500	0.456469
156.99	0.898764	2.093420	0.062500	0.469776
159.58	0.885302	2.066360	0.062500	0.503109
160.88	0.785227	1.626968	0.062500	0.468862
162.18	0.658903	1.192697	0.062500	0.453307
163.48	0.487101	0.768777	0.093750	0.455185
164.79	0.214144	0.360357	0.187500	0.477089
166.09	-0.570254	-0.027847	0.437500	0.536868
167.27	-0.347941	0.014071	0.250000	0.493793
168.46	-0.211283	0.053357	0.250000	0.463130
169.65	-0.115291	0.090186	0.250000	0.438320
170.84	-0.043317	0.124723	0.250000	0.417706
172.03	0.012675	0.157134	0.250000	0.400422
175.09	-0.052118	0.047009	0.250000	0.321117
178.16	-0.155053	-0.079791	0.437500	0.279061
181.22	-0.304357	-0.215777	0.500000	0.270783
184.29	-0.520804	-0.353619	0.500000	0.301980
187.35	-0.869488	-0.487463	0.812500	0.406612
189.05	-0.631862	-0.360136	0.500000	0.303150
190.74	-0.492149	-0.248134	0.500000	0.262713
192.44	-0.401972	-0.155899	0.500000	0.253455
194.14	-0.344559	-0.086674	0.437500	0.269327
195.83	-0.312691	-0.042171	0.437500	0.308845
196.82	-0.348464	-0.056135	0.437500	0.327013
197.81	-0.393756	-0.073579	0.437500	0.350608
198.79	-0.451685	-0.094568	0.437500	0.379757
199.78	-0.527405	-0.119127	0.500000	0.415983
200.77	-0.630418	-0.147236	0.500000	0.467346
203.02	-0.573876	-0.195864	0.500000	0.450308
205.28	-0.568127	-0.255139	0.500000	0.460153
207.54	-0.605213	-0.323012	0.500000	0.495483
209.79	-0.692005	-0.397449	0.500000	0.560342
212.05	-0.860680	-0.476678	0.500000	0.678974
214.33	-0.761064	-0.462694	0.500000	0.655538
216.61	-0.718852	-0.455951	0.500000	0.649116
218.89	-0.720458	-0.456348	0.500000	0.654682
221.18	-0.764730	-0.463927	0.500000	0.672658
223.46	-0.861599	-0.478883	0.812500	0.708837
225.64	-0.531475	-0.325290	0.500000	0.581738
227.82	-0.401126	-0.185464	0.500000	0.531481
230.00	-0.362822	-0.064008	0.437500	0.531224
232.18	-0.405205	0.035516	0.250000	0.581117
234.37	-0.571365	0.111147	0.250000	0.708827
239.08	-0.324911	0.090323	0.250000	0.549336
243.80	-0.238715	0.069518	0.250000	0.468067
248.51	-0.221634	0.049960	0.250000	0.425108
253.23	-0.250599	0.031084	0.250000	0.412065
257.95	-0.322060	0.011045	0.250000	0.435951
260.41	-0.294771	-0.018969	0.250000	0.409934
262.86	-0.285146	-0.050204	0.437500	0.401281
265.32	-0.290219	-0.082550	0.437500	0.404026
267.78	-0.308672	-0.115984	0.500000	0.418662
270.24	-0.340431	-0.150562	0.500000	0.454061

272.20	-0.418566	-0.140585	0.500000	0.358789
274.16	-0.498889	-0.125659	0.500000	0.323549
276.12	-0.579158	-0.108524	0.437500	0.326439
278.08	-0.655756	-0.092189	0.437500	0.368479
280.04	-0.722810	-0.079479	0.437500	0.468494
280.24	-0.709464	-0.105350	0.437500	0.437862
280.45	-0.706947	-0.130973	0.500000	0.425754
280.65	-0.714966	-0.156297	0.500000	0.424654
280.85	-0.734017	-0.181271	0.500000	0.435151
281.05	-0.765515	-0.205847	0.500000	0.468069
284.23	-0.677359	-0.140749	0.500000	0.402530
287.40	-0.614473	-0.081891	0.437500	0.373077
290.58	-0.567697	-0.029539	0.437500	0.366882
293.75	-0.608405	0.016147	0.250000	0.381993
296.92	-0.698502	0.055010	0.250000	0.424545
298.57	-0.684253	0.030392	0.250000	0.409056
300.22	-0.682866	0.005092	0.250000	0.400311
301.87	-0.692317	-0.020779	0.250000	0.396784
303.52	-0.711168	-0.047128	0.437500	0.398554
305.17	-0.738276	-0.073875	0.437500	0.407843
308.13	-0.689997	-0.149774	0.500000	0.365818
311.18	-0.701078	-0.232186	0.500000	0.352419
314.04	-0.750546	-0.319303	0.500000	0.362169
317.00	-0.812928	-0.408750	0.500000	0.398034
319.96	-0.879987	-0.498642	0.812500	0.481121
321.95	-0.778523	-0.456568	0.500000	0.379350
323.95	-0.764937	-0.413921	0.500000	0.311558
325.95	-0.677358	-0.374016	0.500000	0.258592
327.95	-0.574152	-0.336111	0.500000	0.215727
329.95	-0.510022	-0.300408	0.500000	0.180476

Chromosome 10

position	LOD score	NPL score	p-value	information
-10.00	-0.145612	-0.105889	0.437500	0.108046
-8.00	-0.194095	-0.123452	0.500000	0.132231
-6.00	-0.288187	-0.146014	0.500000	0.157574
-4.00	-0.380110	-0.170551	0.500000	0.191613
-2.00	-0.467193	-0.261233	0.500000	0.235776
0.00	-0.590023	-0.234470	0.500000	0.304691
2.82	-0.586164	-0.263475	0.500000	0.276547
5.65	-0.559735	-0.303506	0.500000	0.280116
8.47	-0.585400	-0.354285	0.500000	0.307573
11.29	-0.670741	-0.413398	0.500000	0.361883
14.12	-0.862649	-0.480208	0.812500	0.496339
15.17	-0.826155	-0.467405	0.500000	0.443744
16.23	-0.804887	-0.456071	0.500000	0.429002
17.28	-0.797008	-0.446206	0.500000	0.418719
18.33	-0.801782	-0.437815	0.500000	0.412209
19.39	-0.819543	-0.430905	0.500000	0.410051
21.82	-0.683738	-0.414773	0.500000	0.390561
24.25	-0.628203	-0.406590	0.500000	0.388873
26.69	-0.629593	-0.406342	0.500000	0.399985
29.12	-0.690112	-0.414067	0.500000	0.425379
31.55	-0.841629	-0.429862	0.500000	0.476968
33.96	-0.712698	-0.432321	0.500000	0.407518
36.37	-0.671647	-0.443489	0.500000	0.369519
38.78	-0.688057	-0.462808	0.500000	0.347037
41.19	-0.759027	-0.489777	0.812500	0.337420
43.59	-0.904338	-0.523959	0.812500	0.343908
44.56	-0.899445	-0.536520	0.812500	0.347045
45.52	-0.905023	-0.550390	0.812500	0.353577
46.49	-0.921063	-0.565537	0.812500	0.363348
47.45	-0.948292	-0.581929	0.875000	0.377175
48.42	-0.988363	-0.599536	0.875000	0.399407
49.88	-0.773816	-0.580352	0.875000	0.375012
51.34	-0.638834	-0.563646	0.812500	0.360563
52.80	-0.542507	-0.549272	0.812500	0.351757
54.27	-0.469209	-0.537086	0.812500	0.348004

55.73	-0.411256	-0.526943	0.812500	0.350737
57.96	-0.438961	-0.444627	0.500000	0.238559
60.19	-0.473328	-0.361614	0.500000	0.190239
62.42	-0.517614	-0.281008	0.500000	0.177622
64.65	-0.577809	-0.206105	0.500000	0.198419
66.89	-0.665424	-0.139903	0.500000	0.260768
69.71	-0.509765	-0.114772	0.500000	0.243648
72.53	-0.415860	-0.093336	0.437500	0.238672
75.36	-0.356308	-0.075138	0.437500	0.241632
78.18	-0.319231	-0.059685	0.437500	0.252530
81.00	-0.298251	-0.046471	0.437500	0.274358
83.44	-0.339199	-0.086006	0.437500	0.269835
85.87	-0.393598	-0.127176	0.500000	0.274533
88.30	-0.465505	-0.170028	0.500000	0.288021
90.74	-0.561881	-0.214559	0.500000	0.312324
93.17	-0.696506	-0.260720	0.500000	0.357903
95.53	-0.657951	-0.262141	0.500000	0.326837
97.89	-0.643594	-0.268450	0.500000	0.310115
100.24	-0.650880	-0.279528	0.500000	0.302621
102.60	-0.679703	-0.295279	0.500000	0.303732
104.96	-0.732365	-0.315626	0.500000	0.316960
108.64	-0.643821	-0.331442	0.500000	0.210487
112.32	-0.627002	-0.366723	0.500000	0.165257
116.00	-0.671214	-0.419193	0.500000	0.162447
119.68	-0.799474	-0.485653	0.812500	0.203015
123.37	-1.142678	-0.562736	0.812500	0.314520
126.68	-0.837902	-0.571758	0.875000	0.269664
129.99	-0.759779	-0.601306	0.875000	0.259826
133.30	-0.793499	-0.651511	0.875000	0.273385
136.62	-0.945355	-0.721744	0.875000	0.311563
139.93	-1.378916	-0.810671	0.875000	0.394863
141.65	-1.218240	-0.811758	0.875000	0.381199
143.37	-1.169063	-0.817559	0.875000	0.383157
145.09	-1.195560	-0.827817	0.875000	0.396633
146.81	-1.309370	-0.842241	0.875000	0.423072
148.53	-1.609087	-0.860514	0.875000	0.474007
149.90	-1.550740	-0.859335	0.875000	0.452747
151.27	-1.535815	-0.860389	0.875000	0.443149
152.64	-1.558050	-0.863718	0.875000	0.440660
154.01	-1.620628	-0.869354	0.875000	0.445016
155.38	-1.739388	-0.877322	0.875000	0.459678
157.24	-1.589261	-0.862084	0.875000	0.435889
159.10	-1.514421	-0.852054	0.875000	0.427827
160.97	-1.494060	-0.847398	0.875000	0.429811
162.83	-1.526148	-0.848233	0.875000	0.441947
164.69	-1.624824	-0.854617	0.875000	0.470276
167.05	-1.222519	-0.784782	0.875000	0.416655
169.41	-1.033322	-0.716997	0.875000	0.397767
171.76	-0.937069	-0.652179	0.875000	0.399640
174.12	-0.912762	-0.591323	0.875000	0.422215
176.48	-0.974180	-0.535471	0.812500	0.476603
178.86	0.009566	-0.147482	0.500000	0.295382
181.24	0.358512	0.337961	0.187500	0.226322
183.63	0.599206	0.923210	0.093750	0.220527
186.01	0.792032	1.601880	0.062500	0.273099
188.39	0.957115	2.359279	0.062500	0.401123
190.90	0.955144	2.376358	0.062500	0.397376
193.41	0.954131	2.414055	0.062500	0.410641
195.92	0.954288	2.473593	0.062500	0.438503
198.43	0.955839	2.556351	0.062500	0.483528
200.94	0.959002	2.663835	0.062500	0.557247
201.44	0.957139	2.652478	0.062500	0.555650
201.93	0.955144	2.642013	0.062500	0.554684
202.42	0.953018	2.632434	0.062500	0.554257
202.91	0.950761	2.623735	0.062500	0.554374
203.40	0.948373	2.615910	0.062500	0.555132
205.40	0.901881	2.345788	0.062500	0.451451
207.40	0.855149	2.097975	0.062500	0.376920
209.40	0.808373	1.871633	0.062500	0.316711
211.40	0.761756	1.665773	0.062500	0.266737
213.40	0.715508	1.479289	0.062500	0.224779

Chromosome 16

position	LOD score	NPL score	p-value	information
-10.00	0.002196	-0.184179	0.500000	0.201602
-8.00	-0.047161	-0.228188	0.500000	0.240071
-6.00	-0.118701	-0.279015	0.500000	0.286836
-4.00	-0.227725	-0.337315	0.500000	0.344720
-2.00	-0.413705	-0.403733	0.500000	0.419291
0.00	-0.861599	-0.478883	0.812500	0.534996
1.82	-0.350062	-0.425419	0.500000	0.353574
3.63	-0.178801	-0.386119	0.500000	0.262180
5.45	-0.100856	-0.360759	0.500000	0.215306
7.26	-0.074413	-0.348446	0.500000	0.205013
9.08	-0.089039	-0.347721	0.500000	0.229163
10.15	-0.071619	-0.277605	0.500000	0.241761
11.23	-0.092556	-0.214522	0.500000	0.276450
12.30	-0.159812	-0.159302	0.500000	0.333261
13.38	-0.304136	-0.112528	0.437500	0.417142
14.46	-0.665087	-0.074512	0.437500	0.553543
16.51	0.303564	0.366843	0.187500	0.449323
18.57	0.606652	0.873500	0.093750	0.418783
20.63	0.800549	1.435774	0.062500	0.435666
22.69	0.946496	2.040189	0.062500	0.500796
24.75	1.064872	2.671656	0.062500	0.643860
26.54	1.064437	2.622090	0.062500	0.622659
28.33	1.062722	2.586642	0.062500	0.612788
30.12	1.059716	2.565015	0.062500	0.610769
31.91	1.055433	2.557020	0.062500	0.616503
33.70	1.049914	2.562573	0.062500	0.633314
35.28	1.026762	2.388083	0.062500	0.588583
36.86	1.002742	2.227047	0.062500	0.558099
38.44	0.977923	2.078629	0.062500	0.535756
40.01	0.952385	1.941986	0.062500	0.520331
41.59	0.926211	1.816283	0.062500	0.512811
44.88	0.835617	1.365000	0.062500	0.444330
48.16	0.725070	0.942107	0.093750	0.412512
51.45	0.585327	0.548531	0.187500	0.409387
54.73	0.396154	0.185229	0.187500	0.437414
58.02	0.096495	-0.147466	0.500000	0.515230
59.21	0.036742	-0.199332	0.500000	0.464992
60.39	-0.048579	-0.257436	0.500000	0.437712
61.58	-0.174456	-0.321142	0.500000	0.422522
62.77	-0.380491	-0.389747	0.500000	0.418382
63.96	-0.856336	-0.462499	0.500000	0.429879
67.87	-0.132736	-0.225397	0.500000	0.274257
71.79	0.069124	-0.012639	0.250000	0.203996
75.70	0.170990	0.177347	0.187500	0.181042
79.62	0.228496	0.346260	0.187500	0.199414
83.54	0.259266	0.496127	0.187500	0.262008
85.37	0.232598	0.492501	0.187500	0.276007
87.21	0.203073	0.491179	0.187500	0.297121
89.05	0.169882	0.492160	0.187500	0.325374
90.89	0.131944	0.495414	0.187500	0.362399
92.73	0.087768	0.500885	0.187500	0.413351
94.50	-0.066738	0.347036	0.187500	0.356346
96.27	-0.249712	0.195439	0.187500	0.350513
98.03	-0.465454	0.049109	0.250000	0.378038
99.80	-0.701798	-0.088977	0.437500	0.441120
101.57	-0.877171	-0.216235	0.500000	0.567566
104.00	-0.847925	-0.197019	0.500000	0.519681
106.44	-0.821698	-0.178869	0.500000	0.493936
108.87	-0.804937	-0.161720	0.500000	0.481637
111.30	-0.802018	-0.145544	0.500000	0.481236
113.74	-0.816510	-0.130365	0.500000	0.495394
117.08	-0.692032	-0.163765	0.500000	0.344978
120.42	-0.582190	-0.204434	0.500000	0.266494
123.76	-0.484241	-0.248353	0.500000	0.234110
127.10	-0.394780	-0.290927	0.500000	0.244621
130.44	-0.311463	-0.328037	0.500000	0.317830
132.44	-0.284007	-0.305635	0.500000	0.260511
134.44	-0.259322	-0.284170	0.500000	0.220381
136.44	-0.237068	-0.263676	0.500000	0.187773

138.44	-0.216955	-0.244174	0.500000	0.160466
140.44	-0.198738	-0.225678	0.500000	0.137307

Chromosome 18

position	LOD score	NPL score	p-value	information
-10.00	-0.096774	0.198943	0.187500	0.221419
-8.00	-0.141912	0.213216	0.187500	0.260868
-6.00	-0.202795	0.227823	0.187500	0.307568
-4.00	-0.288109	0.242606	0.187500	0.363490
-2.00	-0.416130	0.257381	0.187500	0.432298
0.00	-0.638100	0.271936	0.187500	0.527933
1.70	-0.605575	0.292662	0.187500	0.520071
3.39	-0.585066	0.314325	0.187500	0.519811
5.09	-0.576871	0.336939	0.187500	0.525170
6.78	-0.582125	0.360483	0.187500	0.535966
8.48	-0.603104	0.384903	0.187500	0.553311
10.66	-0.551448	0.394861	0.187500	0.540497
12.84	-0.523126	0.406695	0.187500	0.538894
15.02	-0.516216	0.420489	0.187500	0.546564
17.21	-0.531767	0.436229	0.187500	0.564305
19.39	-0.574314	0.453799	0.187500	0.598441
22.87	-0.464153	0.335929	0.187500	0.488261
26.35	-0.440750	0.212741	0.187500	0.435074
29.83	-0.471298	0.087292	0.250000	0.424665
33.31	-0.552178	-0.037749	0.437500	0.458024
36.79	-0.702736	-0.160636	0.500000	0.562626
38.54	-0.437740	-0.081835	0.437500	0.405477
40.28	-0.342878	-0.000914	0.250000	0.339507
42.03	-0.332029	0.080405	0.250000	0.327158
43.77	-0.401766	0.160327	0.187500	0.365874
45.51	-0.618122	0.237139	0.187500	0.474315
48.23	-0.520740	0.289707	0.187500	0.468649
50.95	-0.469737	0.341164	0.187500	0.483742
53.67	-0.456907	0.392503	0.187500	0.514094
56.38	-0.484920	0.444342	0.187500	0.561020
59.10	-0.570217	0.496869	0.187500	0.633377
61.19	-0.525748	0.482622	0.187500	0.593097
63.27	-0.503192	0.470434	0.187500	0.568587
65.35	-0.500234	0.460566	0.187500	0.554846
67.43	-0.517399	0.453204	0.187500	0.551251
69.52	-0.558323	0.448450	0.187500	0.560350
71.65	-0.417363	0.392239	0.187500	0.524961
73.78	-0.320461	0.337115	0.187500	0.516154
75.91	-0.246215	0.285153	0.187500	0.531598
78.04	-0.184767	0.238510	0.187500	0.574619
80.18	-0.130829	0.199249	0.187500	0.668760
82.84	0.217327	0.393128	0.187500	0.534741
85.51	0.416602	0.609268	0.187500	0.457318
88.17	0.558545	0.847141	0.093750	0.408058
90.84	0.669510	1.105984	0.062500	0.380591
93.50	0.760775	1.384970	0.062500	0.371739
96.09	0.838825	1.628186	0.062500	0.386628
98.68	0.911740	1.907716	0.062500	0.419218
101.27	0.980029	2.224423	0.062500	0.472307
103.85	1.044058	2.578927	0.062500	0.551513
106.44	1.104097	2.971736	0.062500	0.682282
108.28	1.104666	2.924413	0.062500	0.661636
110.12	1.103921	2.893991	0.062500	0.652890
111.96	1.101831	2.880081	0.062500	0.652233
113.80	1.098393	2.882438	0.062500	0.659426
115.64	1.093630	2.900964	0.062500	0.677152
117.43	1.091700	2.841667	0.062500	0.654153
119.22	1.088382	2.796357	0.062500	0.641834
121.01	1.083672	2.764690	0.062500	0.637094
122.80	1.077587	2.746415	0.062500	0.639841
124.60	1.070170	2.741372	0.062500	0.653189
125.87	1.065620	2.811645	0.062500	0.564265
127.15	1.063863	2.891946	0.062500	0.527609

128.43	1.064981	2.980405	0.062500	0.519611
129.71	1.068957	3.075080	0.062500	0.537921
130.99	1.075682	3.174131	0.031250	0.586474
132.22	1.078886	3.178759	0.031250	0.577847
133.45	1.081842	3.190638	0.031250	0.574415
134.69	1.084539	3.209810	0.031250	0.574500
135.92	1.086973	3.236339	0.031250	0.578167
137.15	1.089141	3.270306	0.031250	0.587042
139.15	1.038983	2.921575	0.062500	0.485124
141.15	0.988469	2.603747	0.062500	0.409970
143.15	0.937803	2.315355	0.062500	0.348294
145.15	0.887199	2.054753	0.062500	0.296450
147.15	0.836877	1.820178	0.062500	0.252431

Chromosome 19

position	LOD score	NPL score	p-value	information
-10.00	0.779779	1.432547	0.062500	0.178735
-8.00	0.829003	1.621109	0.062500	0.209925
-6.00	0.878625	1.831182	0.062500	0.246984
-4.00	0.928415	2.064284	0.062500	0.291609
-2.00	0.978152	2.321833	0.062500	0.346954
0.00	1.027627	2.605104	0.062500	0.425330
1.82	1.018279	2.503721	0.062500	0.418011
3.63	1.010535	2.416090	0.062500	0.424770
5.45	1.004442	2.342215	0.062500	0.444075
7.26	1.000016	2.282210	0.062500	0.478077
9.08	0.997237	2.236264	0.062500	0.540652
10.56	0.983279	2.128721	0.062500	0.523940
12.05	0.968876	2.030123	0.062500	0.516240
13.53	0.954021	1.939858	0.062500	0.515291
15.02	0.938714	1.857356	0.062500	0.521524
16.50	0.922961	1.782088	0.062500	0.539697
18.61	0.809258	1.266988	0.062500	0.463304
20.72	0.667285	0.776346	0.093750	0.423680
22.82	0.476127	0.315898	0.187500	0.410542
24.93	0.172332	-0.109232	0.437500	0.424847
27.04	-0.876701	-0.495172	0.812500	0.485397
28.36	-0.778212	-0.482757	0.812500	0.476147
29.68	-0.735815	-0.475081	0.500000	0.474110
31.01	-0.734548	-0.471973	0.500000	0.477673
32.33	-0.772990	-0.473283	0.500000	0.487267
33.66	-0.861599	-0.478883	0.812500	0.506576
36.27	-0.311958	-0.369099	0.500000	0.391676
38.88	-0.140365	-0.285944	0.500000	0.336056
41.50	-0.064804	-0.227753	0.500000	0.309576
44.11	-0.037428	-0.192192	0.500000	0.306214
46.72	-0.040984	-0.176458	0.500000	0.323844
48.52	-0.122687	-0.233992	0.500000	0.352321
50.31	-0.223770	-0.292857	0.500000	0.387896
52.10	-0.355006	-0.353186	0.500000	0.432513
53.89	-0.540840	-0.415135	0.500000	0.489905
55.68	-0.861599	-0.478883	0.812500	0.575012
56.65	-0.843015	-0.475829	0.500000	0.502627
57.61	-0.835547	-0.474530	0.500000	0.473212
58.58	-0.837093	-0.474768	0.500000	0.468864
59.54	-0.846157	-0.476303	0.500000	0.489694
60.51	-0.861599	-0.478883	0.812500	0.554626
62.79	-0.801112	-0.469349	0.500000	0.528364
65.07	-0.778201	-0.464975	0.500000	0.522014
67.35	-0.782700	-0.465326	0.500000	0.528946
69.63	-0.810598	-0.470054	0.500000	0.549433
71.91	-0.861599	-0.478883	0.812500	0.590690
74.53	-0.756212	-0.444072	0.500000	0.398963
77.14	-0.662259	-0.408673	0.500000	0.313866
79.76	-0.574210	-0.373027	0.500000	0.297661
82.37	-0.490365	-0.337678	0.500000	0.349984
84.98	-0.410964	-0.303303	0.500000	0.513432
87.16	-0.430593	-0.298534	0.500000	0.396974

89.35	-0.467360	-0.294726	0.500000	0.341966
91.53	-0.523060	-0.292000	0.500000	0.318006
93.71	-0.602371	-0.290509	0.500000	0.320123
95.89	-0.715684	-0.290468	0.500000	0.351474
97.49	-0.721344	-0.324571	0.500000	0.353249
99.09	-0.737037	-0.360817	0.500000	0.365694
100.70	-0.763864	-0.398848	0.500000	0.388580
102.30	-0.804032	-0.438312	0.500000	0.424329
103.90	-0.861599	-0.478883	0.812500	0.486340
105.90	-0.700109	-0.437635	0.500000	0.389370
107.90	-0.586383	-0.398946	0.500000	0.324067
109.90	-0.499793	-0.362833	0.500000	0.272117
111.90	-0.430852	-0.329280	0.500000	0.229332
113.90	-0.374384	-0.298242	0.500000	0.193567

The ES branch

Chromosome 6

position	LOD score	NPL score	p-value	information
-10.00	-0.270808	-0.021489	0.309570	0.332813
-8.00	-0.369840	-0.045352	0.321289	0.395765
-6.00	-0.496292	-0.071567	0.335938	0.470488
-4.00	-0.665110	-0.100075	0.363281	0.560268
-2.00	-0.911993	-0.130793	0.370605	0.671478
0.00	-1.379462	-0.163623	0.390625	0.831137
1.03	-1.026914	-0.150512	0.382812	0.732124
2.06	-0.829428	-0.144377	0.381836	0.689667
3.09	-0.689732	-0.145624	0.381836	0.679080
4.13	-0.578703	-0.154361	0.384766	0.699044
5.16	-0.482868	-0.170374	0.395508	0.766946
6.01	-0.415541	-0.145603	0.381836	0.720273
6.87	-0.363112	-0.121898	0.370605	0.693352
7.72	-0.322182	-0.099717	0.363281	0.677150
8.58	-0.290598	-0.079493	0.335938	0.670091
9.43	-0.266920	-0.061616	0.334961	0.672042
12.15	-0.311750	-0.114282	0.365723	0.577559
14.87	-0.303619	-0.161130	0.388672	0.546569
17.59	-0.273913	-0.201420	0.416016	0.563007
20.31	-0.261514	-0.236751	0.447754	0.628935
23.03	-0.315391	-0.271203	0.486328	0.773495
24.33	0.706973	0.253412	0.167969	0.670007
25.63	1.027914	0.864920	0.073242	0.625947
26.93	1.240491	1.564393	0.070312	0.615703
28.23	1.407325	2.350582	0.013672	0.637502
29.53	1.549154	3.219990	0.007812	0.707617
31.56	1.605760	3.631770	0.007812	0.678026
33.60	1.655670	4.067126	0.007812	0.668006
35.63	1.699237	4.527808	0.007812	0.673575
37.66	1.736733	5.015823	0.007812	0.695663
39.70	1.768369	5.533507	0.007812	0.744596
41.68	1.769207	5.493907	0.007812	0.679597
43.67	1.769481	5.483444	0.007812	0.654114
45.65	1.769409	5.502057	0.007812	0.654993
47.64	1.768986	5.549868	0.007812	0.682630
49.62	1.767986	5.627196	0.007812	0.752090
57.00	1.740146	4.696580	0.007812	0.486617
64.38	1.730536	4.328691	0.007812	0.388839
71.76	1.743340	4.467027	0.007812	0.392859
79.15	1.778804	5.157513	0.007812	0.499529
86.53	1.833029	6.563128	0.007812	0.777032
88.76	1.852671	6.638047	0.007812	0.716460
90.99	1.867946	6.767057	0.007812	0.688016
93.22	1.878866	6.952147	0.007812	0.679087
95.45	1.885406	7.195903	0.007812	0.688120
97.68	1.887505	7.501630	0.007812	0.718032
99.67	1.833979	6.797128	0.007812	0.623983
101.65	1.776992	6.136255	0.007812	0.574098

103.64	1.716116	5.518718	0.007812	0.549656
105.62	1.650613	4.944582	0.007812	0.547817
107.61	1.579344	4.413953	0.007812	0.569279
109.89	1.370624	3.229609	0.007812	0.484013
112.17	1.113498	2.184806	0.019531	0.465574
114.45	0.769142	1.312835	0.070801	0.496031
116.73	0.222384	0.630602	0.088379	0.578276
119.02	-1.470026	0.135833	0.215820	0.743711
121.97	-1.297090	0.074339	0.261719	0.598013
124.93	-1.197644	0.005807	0.294922	0.531981
127.89	-1.138753	-0.065371	0.335938	0.517133
130.84	-1.099284	-0.134917	0.374512	0.551700
133.80	-1.066915	-0.199362	0.416016	0.655128
135.50	-1.146438	-0.204791	0.416016	0.609364
137.19	-1.249267	-0.218648	0.433594	0.600001
138.89	-1.385462	-0.241150	0.447754	0.616810
140.58	-1.567918	-0.271660	0.486328	0.661551
142.28	-1.807033	-0.308765	0.527344	0.753413
144.12	-1.778375	-0.312216	0.529297	0.702436
145.96	-1.791569	-0.317541	0.532715	0.682559
147.80	-1.834326	-0.324537	0.547363	0.684139
149.64	-1.894551	-0.332928	0.557129	0.707109
151.48	-1.958408	-0.342393	0.580566	0.760209
153.06	-1.879202	-0.322414	0.536621	0.711610
154.63	-1.814349	-0.303578	0.522949	0.679195
156.21	-1.766685	-0.286016	0.495117	0.656144
157.79	-1.738325	-0.269842	0.486328	0.641184
159.37	-1.731274	-0.255151	0.467285	0.635183
161.55	-1.562225	-0.235801	0.447754	0.585238
163.73	-1.450635	-0.219221	0.433594	0.554371
165.91	-1.378239	-0.205482	0.416016	0.537653
168.09	-1.335672	-0.194600	0.410645	0.534070
170.28	-1.316766	-0.186545	0.404785	0.543975
172.43	-1.374613	-0.203866	0.416016	0.544917
174.59	-1.450623	-0.223155	0.439453	0.565291
176.75	-1.546135	-0.244302	0.450684	0.605638
178.90	-1.663306	-0.267186	0.486328	0.669942
181.06	-1.806644	-0.291671	0.502930	0.779854
184.37	-1.511705	-0.242332	0.447754	0.601833
187.69	-1.209235	-0.181229	0.404297	0.507989
191.00	-1.032296	-0.114451	0.365723	0.465964
194.31	-0.994179	-0.050524	0.322266	0.472818
197.62	-1.150504	0.001683	0.294922	0.542852
199.68	-0.948117	0.039728	0.280273	0.474285
201.74	-0.810676	0.079193	0.258301	0.443803
203.80	-0.714806	0.119350	0.239746	0.441491
205.86	-0.653652	0.159353	0.196289	0.469014
207.91	-0.629221	0.198262	0.191406	0.546043
210.84	-0.330763	0.222642	0.176758	0.425880
213.77	-0.159408	0.243256	0.170898	0.351090
216.70	-0.046125	0.260985	0.167969	0.298754
219.63	0.032173	0.276709	0.164062	0.263218
222.57	0.086540	0.291248	0.150879	0.242314
224.57	0.107969	0.282739	0.153320	0.203827
226.57	0.125159	0.273377	0.164062	0.172980
228.57	0.138693	0.263310	0.167969	0.147048
230.57	0.149059	0.252688	0.167969	0.125010
232.57	0.156670	0.241655	0.170898	0.106210

Chromosome 12

position	LOD score	NPL score	p-value	information
-10.00	-0.122429	0.169937	0.194824	0.246007
-8.00	-0.220422	0.154058	0.208008	0.289201
-6.00	-0.350416	0.133953	0.220215	0.339931
-4.00	-0.528635	0.109402	0.239746	0.400266
-2.00	-0.787605	0.080289	0.258301	0.474248
0.00	-1.206485	0.046621	0.280273	0.579436
3.26	-1.051488	0.005457	0.294922	0.529083

6.51	-1.039537	-0.064444	0.334961	0.536748
9.77	-1.146375	-0.157972	0.386719	0.587114
13.03	-1.372287	-0.266395	0.484375	0.684352
16.29	-1.701514	-0.378897	0.659180	0.864708
17.89	-1.643068	-0.377496	0.645508	0.807193
19.49	-1.605994	-0.377313	0.645508	0.772093
21.09	-1.587518	-0.378328	0.647461	0.748745
22.69	-1.586079	-0.380518	0.659180	0.735395
24.29	-1.600876	-0.383860	0.661133	0.733326
26.63	-1.384508	-0.282463	0.493164	0.619389
28.96	-1.181122	-0.170519	0.395508	0.570461
31.29	-1.015301	-0.051466	0.333008	0.564470
33.62	-0.884174	0.070851	0.261719	0.601936
35.95	-0.782121	0.192796	0.192871	0.705683
36.88	-0.668705	0.223614	0.176758	0.649778
37.80	-0.580044	0.255054	0.167969	0.614244
38.72	-0.507174	0.287154	0.152832	0.588328
39.64	-0.445267	0.319947	0.135254	0.569844
40.56	-0.391461	0.353466	0.123535	0.557988
42.54	-0.297380	0.430608	0.107910	0.496756
44.53	-0.221357	0.513053	0.100586	0.467950
46.51	-0.158373	0.601152	0.089355	0.461915
48.50	-0.106434	0.695203	0.080566	0.478029
50.48	-0.065589	0.795414	0.076172	0.521074
52.54	0.020555	0.928873	0.072754	0.506475
54.60	0.090644	1.068761	0.071777	0.513836
56.66	0.144811	1.215142	0.071289	0.538432
58.71	0.182292	1.368015	0.070312	0.581687
60.77	0.201024	1.527154	0.070312	0.656786
62.59	0.232438	1.529583	0.070312	0.619793
64.40	0.250912	1.536846	0.070312	0.597535
66.22	0.256291	1.548743	0.070312	0.586717
68.03	0.247608	1.565000	0.070312	0.586878
69.85	0.222851	1.585257	0.070312	0.599609
70.81	0.232640	1.587098	0.070312	0.574530
71.78	0.238506	1.589766	0.070312	0.562627
72.74	0.240397	1.593144	0.070312	0.559666
73.71	0.238074	1.597099	0.070312	0.566027
74.67	0.231081	1.601484	0.070312	0.588011
76.71	0.554877	1.726886	0.061523	0.546797
78.74	0.759354	1.886668	0.040039	0.528861
80.77	0.915976	2.087614	0.026855	0.529227
82.81	1.047135	2.337922	0.013672	0.548799
84.84	1.162504	2.647275	0.008789	0.598883
87.35	1.353086	3.220440	0.007812	0.527804
89.86	1.503845	3.920185	0.007812	0.499995
92.37	1.627328	4.733316	0.007812	0.499748
94.88	1.730072	5.641132	0.007812	0.525400
97.39	1.816005	6.623252	0.007812	0.587478
99.48	1.822651	6.599928	0.007812	0.580693
101.56	1.828851	6.608961	0.007812	0.595368
103.64	1.834940	6.654479	0.007812	0.629172
105.72	1.841166	6.741336	0.007812	0.685586
107.81	1.847673	6.875007	0.007812	0.785398
109.81	1.882119	7.052739	0.007812	0.762583
111.82	1.908497	7.265815	0.007812	0.758733
113.83	1.926943	7.520982	0.007812	0.767271
115.84	1.937704	7.825506	0.007812	0.788109
117.85	1.941129	8.187219	0.007812	0.827843
119.41	1.945217	8.166522	0.007812	0.780643
120.96	1.947397	8.180288	0.007812	0.758412
122.51	1.947699	8.227780	0.007812	0.750880
124.07	1.946123	8.308458	0.007812	0.756825
125.62	1.942638	8.422027	0.007812	0.778990
128.58	1.931966	8.165738	0.007812	0.660168
131.54	1.924646	8.044116	0.007812	0.611833
134.50	1.921382	8.049781	0.007812	0.608415
137.45	1.922138	8.179409	0.007812	0.648226
140.41	1.926146	8.433780	0.007812	0.741987
142.39	1.927479	8.208188	0.007812	0.706814
144.38	1.924613	8.041424	0.007812	0.689070
146.36	1.917433	7.929427	0.007812	0.682153

148.35	1.905873	7.868863	0.007812	0.685300
150.33	1.889921	7.857073	0.007812	0.700477
153.40	1.784085	6.536193	0.007812	0.558427
156.46	1.682789	5.436613	0.007812	0.490274
159.53	1.587256	4.526878	0.007812	0.474490
162.59	1.497721	3.778748	0.007812	0.511960
165.66	1.413431	3.167040	0.007812	0.630995
167.62	1.290172	2.501664	0.011719	0.569694
169.58	1.148554	1.923781	0.040039	0.535237
171.54	0.985228	1.431956	0.070312	0.516731
173.50	0.794939	1.022064	0.072266	0.512411
175.46	0.568445	0.687541	0.082031	0.522600
177.32	0.365962	0.468552	0.104980	0.491107
179.19	0.121007	0.281228	0.155762	0.485869
181.05	-0.190725	0.123148	0.234863	0.503335
182.91	-0.619721	-0.008541	0.306641	0.546606
184.78	-1.229299	-0.116996	0.370605	0.637586
186.78	-0.930633	-0.087185	0.336426	0.510947
188.78	-0.715916	-0.060281	0.334961	0.422722
190.78	-0.555757	-0.036296	0.314941	0.351885
192.78	-0.432239	-0.015184	0.306641	0.293338
194.78	-0.334696	0.003144	0.294922	0.244392

A genome-wide scan was performed by GENEHUNTER for autosomes and GENEHUNTER-PLUS for X chromosome. These software produced output data after analysis in a text format. Data are shown here for only some chromosomes where candidate loci were identified (five for the EA branch and two for the ES branch). Data for other loci were omitted. Notable data showing linkage (over two or five for NPL score in the EA or the ES branch, respectively) are highlighted in red. Output data indicate (from left):

- Genetic location from the first marker (cM)
- LOD score from parametric linkage analysis
- NPL score from non-parametric linkage analysis
- Exact computed significance (p-value)
- Information content of the genotype data

Computation was performed from 10 cM before and ahead of the markers.

Appendix 5 The output data of secondary linkage analysis

Disease status 0 (unknown)

position	LOD score	NPL score	p-value	information
-10.00	0.663734	1.170201	0.070312	0.382531
-8.00	0.656908	1.303034	0.070312	0.445216
-6.00	0.631887	1.444611	0.070312	0.517412
-4.00	0.578278	1.593896	0.070312	0.601376
-2.00	0.473256	1.749449	0.063477	0.701425
0.00	0.245568	1.909404	0.051758	0.834431
0.40	0.249436	1.918316	0.051758	0.846176
0.80	0.252412	1.927495	0.051758	0.859144
1.20	0.254499	1.936945	0.051758	0.873492
1.60	0.255698	1.946670	0.051758	0.889727
2.00	0.256006	1.956674	0.051758	0.910317
2.26	0.259399	1.958713	0.051758	0.910499
2.52	0.262292	1.960861	0.051758	0.911024
2.78	0.264691	1.963120	0.051758	0.911785
3.04	0.266600	1.965490	0.051758	0.912764
3.30	0.268022	1.967971	0.051758	0.913971
3.90	0.272226	1.971769	0.051758	0.915809
4.50	0.273844	1.976183	0.051758	0.918834
5.10	0.272869	1.981218	0.051758	0.922960
5.70	0.269279	1.986878	0.051758	0.928285
6.30	0.263035	1.993167	0.051758	0.935244
6.64	0.263580	2.044259	0.039062	0.904091
6.98	0.264192	2.096140	0.034180	0.891737
7.32	0.264872	2.148501	0.034180	0.889179
7.66	0.265613	2.201028	0.034180	0.895327
8.00	0.266398	2.253408	0.020508	0.911228
8.46	0.269367	2.263281	0.020508	0.913216
8.92	0.270929	2.273521	0.020508	0.916702
9.38	0.271087	2.284117	0.020508	0.921622
9.84	0.269839	2.295055	0.020508	0.928163
10.30	0.267176	2.306325	0.020508	0.936888
10.52	0.267826	2.306580	0.020508	0.937495
10.74	0.268106	2.306925	0.020508	0.938327
10.96	0.268019	2.307359	0.020508	0.939361
11.18	0.267563	2.307882	0.020508	0.940609
11.40	0.266739	2.308495	0.020508	0.942126
11.50	0.266700	2.307257	0.020508	0.941832
11.60	0.266583	2.306037	0.020508	0.941597
11.70	0.266389	2.304837	0.020508	0.941406
11.80	0.266116	2.303655	0.020508	0.941256
11.90	0.265766	2.302491	0.020508	0.941154
12.36	0.267520	2.291411	0.020508	0.937972
12.82	0.267632	2.280747	0.020508	0.935592
13.28	0.266110	2.270495	0.020508	0.933888
13.74	0.262954	2.260650	0.020508	0.932849
14.20	0.258161	2.251207	0.020508	0.932621
14.42	0.295714	2.178916	0.034180	0.885186
14.64	0.329587	2.106823	0.034180	0.862238
14.86	0.360537	2.035234	0.051758	0.852164
15.08	0.389139	1.964450	0.051758	0.854697
15.30	0.415838	1.894761	0.051758	0.880112
17.30	0.558413	1.744837	0.063477	0.739103
19.30	0.630846	1.598526	0.070312	0.632748
21.30	0.667553	1.457609	0.070312	0.543889
23.30	0.682521	1.323455	0.070312	0.467770
25.30	0.682943	1.197048	0.070312	0.401887

Disease status 1 (not affected)

position	LOD score	NPL score	p-value	information
-10.00	-1.871356	1.170201	0.070312	0.382531
-8.00	-2.101045	1.303034	0.070312	0.445216
-6.00	-2.385332	1.444611	0.070312	0.517412
-4.00	-2.766393	1.593896	0.070312	0.601376
-2.00	-3.359959	1.749449	0.063477	0.701425
0.00	-5.323007	1.909404	0.051758	0.834431
0.40	-5.386144	1.918316	0.051758	0.846176
0.80	-5.494693	1.927495	0.051758	0.859144
1.20	-5.664969	1.936945	0.051758	0.873492
1.60	-5.947133	1.946670	0.051758	0.889727
2.00	-6.641502	1.956674	0.051758	0.910317
2.26	-6.581219	1.958713	0.051758	0.910499
2.52	-6.538693	1.960861	0.051758	0.911024
2.78	-6.511381	1.963120	0.051758	0.911785
3.04	-6.497789	1.965490	0.051758	0.912764
3.30	-6.497165	1.967971	0.051758	0.913971
3.90	-6.379094	1.971769	0.051758	0.915809
4.50	-6.329994	1.976183	0.051758	0.918834
5.10	-6.339740	1.981218	0.051758	0.922960
5.70	-6.411170	1.986878	0.051758	0.928285
6.30	-6.564427	1.993167	0.051758	0.935244
6.64	-6.598124	2.044259	0.039062	0.904091
6.98	-6.664341	2.096140	0.034180	0.891737
7.32	-6.765049	2.148501	0.034180	0.889179
7.66	-6.906119	2.201028	0.034180	0.895327
8.00	-7.099309	2.253408	0.020508	0.911228
8.46	-7.019179	2.263281	0.020508	0.913216
8.92	-6.990574	2.273521	0.020508	0.916702
9.38	-7.005369	2.284117	0.020508	0.921622
9.84	-7.061484	2.295055	0.020508	0.928163
10.30	-7.161419	2.306325	0.020508	0.936888
10.52	-7.150674	2.306580	0.020508	0.937495
10.74	-7.149576	2.306925	0.020508	0.938327
10.96	-7.158149	2.307359	0.020508	0.939361
11.18	-7.176724	2.307882	0.020508	0.940609
11.40	-7.205976	2.308495	0.020508	0.942126
11.50	-7.184372	2.307257	0.020508	0.941832
11.60	-7.165368	2.306037	0.020508	0.941597
11.70	-7.148852	2.304837	0.020508	0.941406
11.80	-7.134734	2.303655	0.020508	0.941256
11.90	-7.122946	2.302491	0.020508	0.941154
12.36	-6.975053	2.291411	0.020508	0.937972
12.82	-6.880153	2.280747	0.020508	0.935592
13.28	-6.830060	2.270495	0.020508	0.933888
13.74	-6.822557	2.260650	0.020508	0.932849
14.20	-6.860678	2.251207	0.020508	0.932621
14.42	-6.298967	2.178916	0.034180	0.885186
14.64	-6.002045	2.106823	0.034180	0.862238
14.86	-5.799009	2.035234	0.051758	0.852164
15.08	-5.651579	1.964450	0.051758	0.854697
15.30	-5.543946	1.894761	0.051758	0.880112
17.30	-4.117263	1.744837	0.063477	0.739103
19.30	-3.313022	1.598526	0.070312	0.632748
21.30	-2.754456	1.457609	0.070312	0.543889
23.30	-2.334562	1.323455	0.070312	0.467770
25.30	-2.004103	1.197048	0.070312	0.401887

Disease status 2 (affected)

position	LOD score	NPL score	p-value	information
-10.00	1.422358	1.615482	0.012665	0.382531
-8.00	1.441460	1.734149	0.010815	0.445216
-6.00	1.438094	1.811953	0.009933	0.517412
-4.00	1.397292	1.822859	0.009052	0.601376
-2.00	1.281420	1.732522	0.010883	0.701425
0.00	0.923392	1.496876	0.017296	0.834431

0.40	0.929930	1.509618	0.015900	0.846176
0.80	0.934999	1.521841	0.015900	0.859144
1.20	0.938583	1.533513	0.015831	0.873492
1.60	0.940651	1.544599	0.015831	0.889727
2.00	0.941166	1.555062	0.015350	0.910317
2.26	0.948151	1.562089	0.014828	0.910499
2.52	0.954368	1.568908	0.014782	0.911024
2.78	0.959830	1.575515	0.014370	0.911785
3.04	0.964548	1.581906	0.014359	0.912764
3.30	0.968531	1.588077	0.013775	0.913971
3.90	0.976235	1.597744	0.013775	0.915809
4.50	0.979989	1.606032	0.013214	0.918834
5.10	0.979711	1.612863	0.013214	0.922960
5.70	0.975255	1.618152	0.012611	0.928285
6.30	0.966404	1.621801	0.012611	0.935244
6.64	0.969778	1.667235	0.012016	0.904091
6.98	0.972685	1.712865	0.011181	0.891737
7.32	0.975120	1.758458	0.010139	0.889179
7.66	0.977061	1.803770	0.009933	0.895327
8.00	0.978475	1.848558	0.008778	0.911228
8.46	0.983302	1.858473	0.008469	0.913216
8.92	0.985764	1.867531	0.008446	0.916702
9.38	0.985879	1.875729	0.008274	0.921622
9.84	0.983642	1.883062	0.008183	0.928163
10.30	0.979018	1.889521	0.008022	0.936888
10.52	0.980150	1.890285	0.008022	0.937495
10.74	0.980696	1.890862	0.008022	0.938327
10.96	0.980656	1.891252	0.008022	0.939361
11.18	0.980032	1.891456	0.008022	0.940609
11.40	0.978821	1.891474	0.008022	0.942126
11.50	0.978916	1.890719	0.008022	0.941832
11.60	0.978889	1.889926	0.008022	0.941597
11.70	0.978739	1.889095	0.008022	0.941406
11.80	0.978466	1.888226	0.008022	0.941256
11.90	0.978072	1.887318	0.008022	0.941154
12.36	0.982048	1.881157	0.008274	0.937972
12.82	0.983415	1.874184	0.008343	0.935592
13.28	0.982205	1.866412	0.008469	0.933888
13.74	0.978427	1.857850	0.008469	0.932849
14.20	0.972062	1.848505	0.008778	0.932621
14.42	1.051952	1.877681	0.008274	0.885186
14.64	1.117054	1.904517	0.008022	0.862238
14.86	1.171911	1.929187	0.007729	0.852164
15.08	1.219317	1.951861	0.007683	0.854697
15.30	1.261108	1.972708	0.007500	0.880112
17.30	1.449943	2.140502	0.005756	0.739103
19.30	1.519464	2.170105	0.005711	0.632748
21.30	1.538188	2.105820	0.006596	0.543889
23.30	1.528457	1.981825	0.007431	0.467770
25.30	1.500566	1.823709	0.009052	0.401887

Secondary linkage analysis was carried out on chromosome 16p12 using GENEHUNTER. The disease status of five MHE individuals were set as 0 (unknown), 1 (not affected) or 2 (affected), and linkage analysis was performed separately.

Appendix 6 *CACNG3* sequence

5'UTR

gtttgtttgctggggaaccaaattgagacagactctacacagatgtgattgtgacaacac
caaacaaacgacccttggtttaactctgtctgagatgtgtctacactaacactgttgtg

Exon 1

TTTTTGCCCGCCTAAGCGAGCCATAGAGCCGTCTCCAGAGCTGCCGGTGCCTTTAAGAAG
AAAAACGGGCGGATTCGCTCGGTATCTCGGCAGAGGTCTCGACGGCCACGGAAATTCTTC

ACTCGGTCTTTCGGGTCTTCTTTTTCCCCAATGGGCTCCAGTGGTGCCCGCAGCAAAAGG
TGAGCCAGAAAGCCCAGAAGAAAAAGGGGTTACCCGAGGTCACCACGGGCGTCGTTTTCC

CAAACTTGCCTGGCTCATGGGGTGAAAGGGAGGATTGAAGAATGCCGCGTTGGGTGGGTG
GTTTGAACGGACCGAGTACCCCACTTTCCCTCCTAACTTCTTACGGCGCAACCCACCCAC

CTGAGGGAGCGCCAGAGTGCGCTACGGGCTTCGCTCCCCTTCCCCTTTCCTTAACCCTTC
GACTCCCTCGCGGTCTCACGCGATGCCCGAAGCGAGGGGAAGGGGAAAGGAATTGGGAAG

CTAGAGCGGAGGAACCGGGTCGTGCTGCAGCGCCCAGGAGCCAGGGCGCTGACTGTCCTC
GATCTCGCCTCCTTGGCCCAGCACGACGTCGCGGGTCCTCGGTCCCGCGACTGACAGGAG

GGCTCCAGAAACTTTGCGCGGAGAGTGGGCTTGACTGGGCAGAGCCGAGCCGGCTGGCTG
CCGAGGTCTTTGAAACGCGCCTCTCACCCGAACTGACCCGTCTCGGCTCGGCCGACCGAC

ACCCGGGAAGGAACGGGGGAAGGGCGGGGTGAGGGAAGAAAGACCCTTTAGCACCCCGGG
TGGGCCCTTCCTTGCCCCCTTCCCGCCCCACTCCCTTCTTTCTGGGAAATCGTGGGGCCC

TTTCTAGCCCGGGCGGCGGTGTGCAGCTGCATGAGGGAGCTGTCCCTTCGGCACCACGGA
AAAGATCGGGCCCGCCGCCACACGTCGACGTACTCCCTCGACAGGGAAGCCGTGGTGCCT

CCTTAAAGCCTAGGCGTTAAGACGACGGAGGCGGGGCAACAGGCGGGGAGCTGTCCCTTC
GGAATTTCGGATCCGCAATTCTGCTGCCTCCGCCCCGTTGTCCGCCCCTCGACAGGGAAG

AGCACCACGGACCTTGGCGCCCCCAGGGAAACCAGCCGGCCCCCGCCCCAGGACTCTGTC
TCGTGGTGCCTGGAACCGCGGGGGTCCCTTTGGTCGGCCGGGGGCGGGGTCCTGAGACAG

TTTTCTCCAGTTTGAGCGGGGGTGTCGGGAGCAGGCGGAGAGCTTTCCTGCGAGGCTGTG
AAAAGAGGTCAAACTCGCCCCCACAGCCCTCGTCCGCCTCTCGAAAGGACGCTCCGACAC

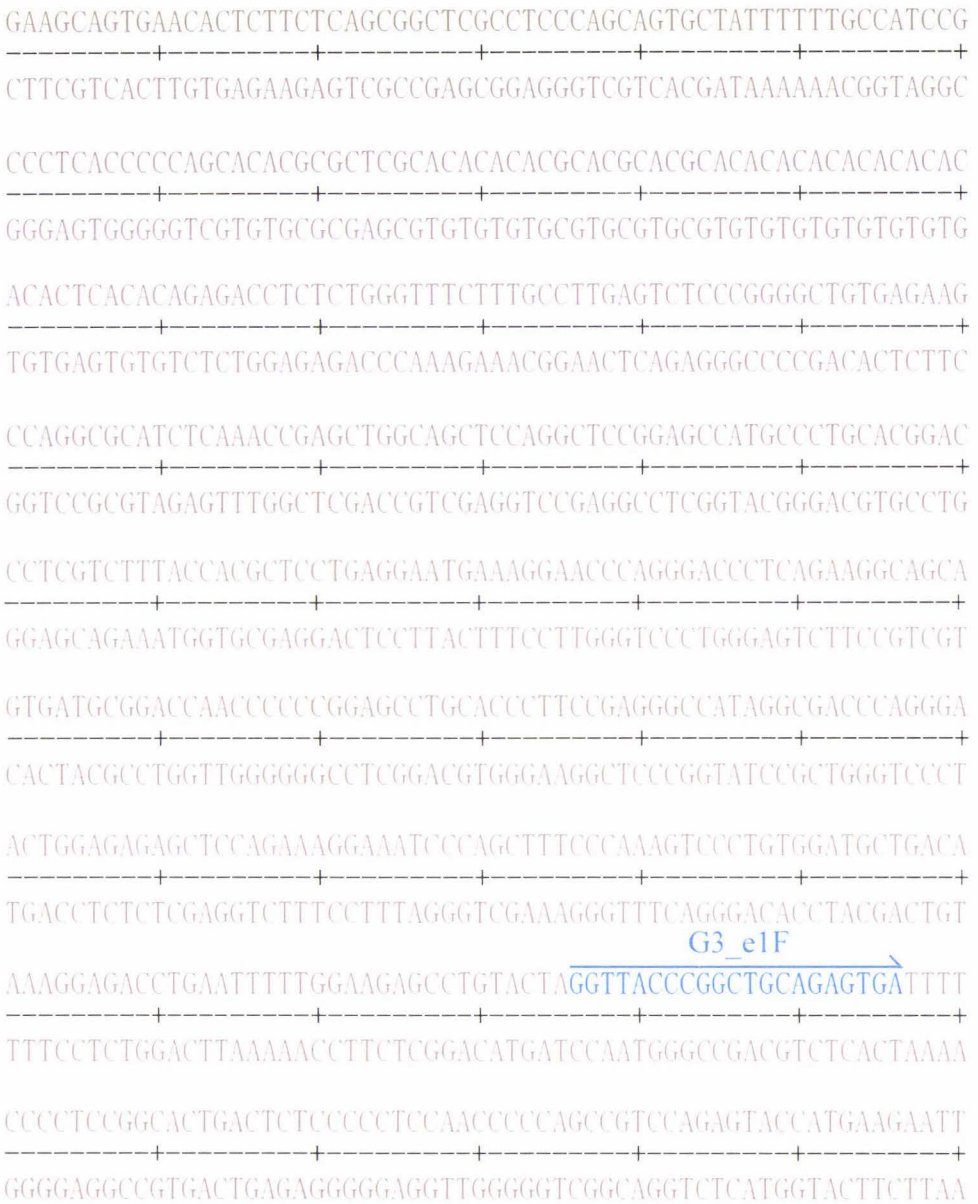

Translation Start

```
       ATGAGGATGTGTGACAGAGGTATCCAGATGTTGATCACCACTGTAGGAGCCTTTGCCGCT
1      ---------+---------+---------+---------+---------+---------+      60
       TACTCCTACACACTGTCTCCATAGGTCTACAACTAGTGGTGACATCCTCGGAAACGGCGA
1      METArgMetCysAspArgGlyIleGlnMetLeuIleThrThrValGlyAlaPheAlaAla      20

       TTTAGTTTAATGACCATTGCAGTGGGCACGGACTACTGGTTATATTCCAGAGGTGTGTGC
61     ---------+---------+---------+---------+---------+---------+     120
       AAATCAAATTACTGGTAACGTCACCCGTGCCTGATGACCAATATAAGGTCTCCACACACG
21     PheSerLeuMetThrIleAlaValGlyThrAspTyrTrpLeuTyrSerArgGlyValCys      40

       AGGACTAAATCTACAAGTGATAATGAAACCAGCAGGAAGAATGAAGAAGTAATGACCCAT
121    ---------+---------+---------+---------+---------+---------+     180
       TCCTGATTTAGATGTTCACTATTACTTTGGTCGTCCTTCTTACTTCTTCATTACTGGGTA
41     ArgThrLysSerThrSerAspAsnGluThrSerArgLysAsnGluGluValMetThrHis      60
```

```
                TCGGGGCTGTGGAGGACCTGCTGCCTAGAAG
181             ---------+---------+---------+---------+---------+---------+  211
                AGCCCCGACACCTCCTGGACGACGGATCTTC
 61             SerGlyLeuTrpArgThrCysCysLeuGlu                                 70
```

Intron 1-2

```
gtatttacaatttcctctcaatagctctgaataatccagttctgatattctggtgggtgt
---------+---------+---------+---------+---------+---------+
cataaatgttaaaggagagttatcgagacttattaggtcaagactataagaccacccaca

ttggaggagatggaaatggtgataaggaaagaagagaagttcaaattattgctgagaatg
---------+---------+---------+---------+---------+---------+
aacctcctctacctttaccactattcctttcttctcttcaagtttaataacgactcttac

tgcaggtgcccagactctgttaacagcaagactgacgccatgtgggttaaaggggtt...
---------+---------+---------+---------+---------+---------+
acgtccacgggtctgagacaattgtcgttctgactgcggtacacccaatttccccaa...
      G3_e1R

                                                    G3_e2F
...caaccctacagcccccaacaaccagagaaaggatctgcacatagcggtgaggaccca
---------+---------+---------+---------+---------+---------+
...gttgggatgtcgggggttgttggtctctttcctagacgtgtatcgccactcctgggt

ggctggcccccagagctctgtctcctcccccaggctcagaacccttatctgtttccacag
---------+---------+---------+---------+---------+---------+
ccgaccgggggtctcgagacagaggaggggtccgagtcttgggaatagacaaaggtgtc
```

Exon 2

```
                                        GGGCTTTCCGAGGCGTGTGCAAGAAAATC
212             ---------+---------+---------+---------+---------+  240
                                        CCCGAAAGGCTCCGCACACGTTCTTTTAG
 71                                     GlyAlaPheArgGlyValCysLysLysIle  80

                GATCACTTCCCTGAAGATGCTGACTACGAACAGGACACAGCCGAATATCTCCTGC
241             ---------+---------+---------+---------+---------+  295
                CTAGTGAAGGGACTTCTACGACTGATGCTTGTCCTGTGTCGGCTTATAGAGGACG
 81             AspHisPheProGluAspAlaAspTyrGluGlnAspThrAlaGluTyrLeuLeu  98
```

Intron 2-3

```
gtaagttccccggcttctcgggtctctctgggaggaagggatgggcctctgccatca...
---------+---------+---------+---------+---------+---------+
cattcaaggggccgaagagcccagagagaccctccttccctacccggagacggtagt...
                 G3_e2R
                                                    G3_e3F
...cacacattcgattataaaatcgttaagactctcagaatggtgactgcagagcatcaa
---------+---------+---------+---------+---------+---------+
...gtgtgtaagctaatattttagcaattctgagagtcttaccactgacgtctcgtagtt

ccccaagtgccaagactccttctaagcacaggccctgagcgcctggtctcatgcccgtgt
---------+---------+---------+---------+---------+---------+
ggggttcacggttctgaggaagattcgtgtccgggactcgcggaccagagtacgggcaca
```

```
tagacatgggctctgttctcttcctgtgctgccttcctctcaggcactcctgcgcttgca
---------+---------+---------+---------+---------+---------+
atctgtacccgagacaagagaaggacacgacggaaggagagtccgtgaggacgcgaacgt

atgggaggaccccaggggctggctgggcacaggcagaagcctctctccttctctccgcag
---------+---------+---------+---------+---------+---------+
taccctcctggggtccccgaccgacccgtgtccgtcttcggagagaggaagagaggcgtc
```

Exon 3

```
                                                          GAGCT
296 ---------+---------+---------+---------+---------+---------+ 300
                                                          CTCGA
 99                                                       ArgAla  100

    GTGAGGGCCTCCAGTGTCTTCCCCATCCTCAGTGTCACGCTGCTGTTCTTCGGCGGGCTC
301 ---------+---------+---------+---------+---------+---------+ 360
    CACTCCCGGAGGTCACAGAAGGGGTAGGAGTCACAGTGCGACGACAAGAAGCCGCCCGAG
101 ValArgAlaSerSerValPheProIleLeuSerValThrLeuLeuPhePheGlyGlyLeu  120

    TGCGTGGCAGCCAGTGAGTTCCACCGCAGCAGACACAACGTCATTCTCAGCGCGGGCATC
361 ---------+---------+---------+---------+---------+---------+ 420
    ACGCACCGTCGGTCACTCAAGGTGGCGTCGTCTGTGTTGCAGTAAGAGTCGCGCCCGTAG
121 CysValAlaAlaSerGluPheHisArgSerArgHisAsnValIleLeuSerAlaGlyIle  140

    TTTTTTGTCTCTGCAG
421 ---------+---------+---------+---------+---------+---------+ 436
    AAAAAACAGAGACGTC
141 PhePheValSerAla                                               145
```

Intron 3-4

```
gtgagtgtctggccccagccctgagatcttcacagataccaaactgaagccagggccaca
---------+---------+---------+---------+---------+---------+
cactcacagaccggggtcgggactctagaagtgtctatggtttgacttcggtcccggtgt

tggaggaagcaatgctactcagggctccctccagggaaggagcaagaaaatgttcca...
---------+---------+---------+---------+---------+---------+
acctccttcgttacgatgagtcccgagggaggtcccttcctcgttcttttacaaggt...
          G3_e3R
                                                  G3_e4F
...cttcatttcctaagtgacagaccatgcaagaagaactaggtggttggatttcccagc
---------+---------+---------+---------+---------+---------+
...gaagtaaaggattcactgtctggtacgttcttcttgatccaccaacctaaagggtcg

tataatccattctcctctctccccattacctccacattttctataaatattttaagatgg
---------+---------+---------+---------+---------+---------+
atattaggtaagaggagagaggggtaatggaggtgtaaaagatatttataaaattctacc

aaagtgacagttctctccgaggtgtataaaggacgtgtttttctttcccccttctcttag
---------+---------+---------+---------+---------+---------+
tttcactgtcaagagaggctccacatatttcctgcacaaaaagaaaaaggggaagagaatc
```

Exon 4


GGTTAAGCAACATCATTGGCATCATAGTTTATATATCAGCCAAC
437
480
CCAATTCGTTGTAGTAACCGTAGTATCAAATATATAGTCGGTTG
146
GlyLeuSerAsnIleIleGlyIleIleValTyrIleSerAlaAsn
160
GCCGGAGACCCCGGGCAGCGTGACTCCAAAAAAAGTTACTCCTATGGTTGGTCCTTTTAT
481
540
CGGCCTCTGGGGCCCGTCGCACTGAGGTTTTTTTCAATGAGGATACCAACCAGGAAAATA
161
AlaGlyAspProGlyGlnArgAspSerLysLysSerTyrSerTyrGlyTrpSerPheTyr
180
TTCGGAGCCTTCTCTTTCATCATCGCAGAAATTGTAGGAGTGGTTGCCGTGCACATCTAT
541
600
AAGCCTCGGAAGAGAAAGTAGTAGCGTCTTTAACATCCTCACCAACGGCACGTGTAGATA
181
PheGlyAlaPheSerPheIleIleAlaGluIleValGlyValValAlaValHisIleTyr
200
ATTGAAAAACATCAGCAGTTACGAGCCAAATCCCACTCGGAGTTCCTGAAGAAATCTACT
601
660
TAACTTTTTGTAGTCGTCAATGCTCGGTTTAGGGTGAGCCTCAAGGACTTCTTTAGATGA
201
IleGluLysHisGlnGlnLeuArgAlaLysSerHisSerGluPheLeuLysLysSerThr
220
TTTGCCCGCCTCCCACCCTACAGGTATCGATTCCGGAGGCGGTCAAGTTCTCGCTCCACC
661
720
AAACGGGCGGAGGGTGGGATGTCCATAGCTAAGGCCTCCGCCAGTTCAAGAGCGAGGTGG
221
PheAlaArgLeuProProTyrArgTyrArgPheArgArgArgSerSerSerArgSerThr
240
GAGCCCAGATCCCGAGACCTGTCCCCCATCAGCAAAGGCTTCCACACCATCCCTTCCACT
721
780
CTCGGGTCTAGGGCTCTGGACAGGGGGTAGTCGTTTCCGAAGGTGTGGTAGGGAAGGTGA
241
GluProArgSerArgAspLeuSerProIleSerLysGlyPheHisThrIleProSerThr
260
GACATCTCGATGTTCACCCTCTCCCGGGACCCCTCAAAGATCACCATGGGGACCCTCCTC
781
840
CTGTAGAGCTACAAGTGGGAGAGGGCCCTGGGGAGTTTCTAGTGGTACCCCTGGGAGGAG
261
AspIleSerMetPheThrLeuSerArgAspProSerLysIleThrMetGlyThrLeuLeu
280
AACTCCGACCGGGACCACGCTTTTCTACAGTTCCACAATTCCACACCCAAAGAGTTCAAA
841
900
TTGAGGCTGGCCCTGGTGCGAAAAGATGTCAAGGTGTTAAGGTGTGGGTTTCTCAAGTTT
281
AsnSerAspArgAspHisAlaPheLeuGlnPheHisAsnSerThrProLysGluPheLys
300
GAGTCACTGCATAATAATCCGGCCAACAGGCGCACCACGCCCGTCTGA
901
948
CTCAGTGACGTATTATTAGGCCGGTTGTCCGCGTGGTGCGGGCAGACT
301
GluSerLeuHisAsnAsnProAlaAsnArgArgThrThrProValEnd
315
ACTGACCTCTGACCTCTGCCCCACGCCCAGCACAGCCTTGGGGGAAGTGTACAGAGATGT
TGACTGGAGACTGGAGACGGGGTGCGGGTCGTGTCGGAACCCCCTTCACATGTCTCTACA

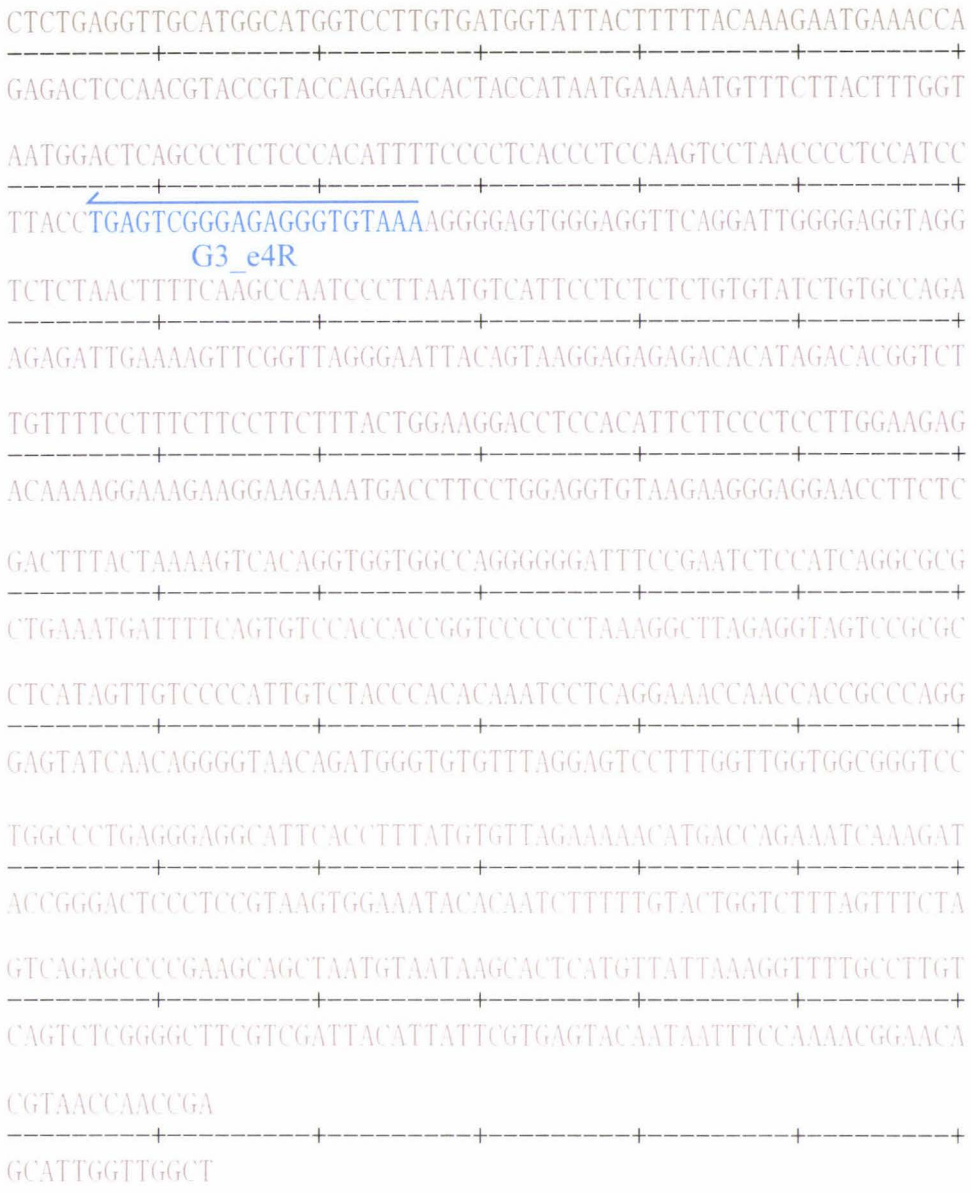

3'UTR

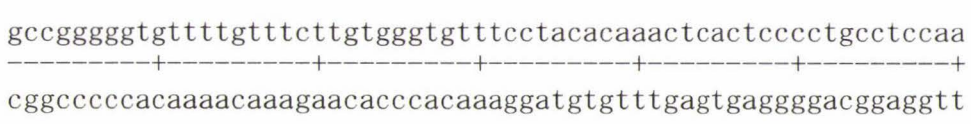

Sequencing was carried out using genomic DNA because any muscle or blood samples were not available to extract RNA for cDNA synthesis. This gene consists of four exons and most regions are the untranslated region (shown in grey). Introns between each exon are described in small letters. Primers used for PCR are highlighted in blue. Sequencing was performed using forward primers for each fragment.